USGS
science for a changing world

In cooperation with the Bureau of Reclamation and the California Department of Fish and Game

Geochemistry of Mercury and other Trace Elements in Fluvial Tailings Upstream of Daguerre Point Dam, Yuba River, California, August 2001

Scientific Investigations Report 2004-5165

U.S. Department of the Interior
U.S. Geological Survey

Cover photo descriptions:

1. (upper left) View from the left bank of the Yuba River at Daguerre Point Dam, looking across from Daguerre Point Dam. M.P. Hunerlach, 2001.
2. (center) View from Daguerre Point looking upstream at the Yuba River flood plain filled with hydraulic mining debris prior to dredging. USGS Archive Photo, G.K. Gilbert, 1906.
3. (lower right) View from the left bank abutment of the Daguerre Point Dam looking upstream at large piles of coarse dredge tailings and eroding training walls. M.P. Hunerlach, August 2001.
4. (upper right) Piston activated sand pump dumping sample of sand and gravel into stainless steel troughduring churn drilling. M. P. Hunerlach, 2001.

Geochemistry of Mercury and other Trace Elements in Fluvial Tailings Upstream of Daguerre Point Dam, Yuba River, California, August 2001

By Michael P. Hunerlach, Charles N. Alpers, Mark Marvin-DiPasquale, Howard E. Taylor, and John F. De Wild

In cooperation with the Bureau of Reclamation and the California Department of Fish and Game

Scientific Investigations Report 2004-5165

U.S. Department of the Interior
U.S. Geological Survey

U.S. Department of the Interior
Gale A. Norton, Secretary

U.S. Geological Survey
Charles G. Groat, Director

U.S. Geological Survey, Reston, Virginia: 2004

For sale by U.S. Geological Survey, Information Services
Box 25286, Denver Federal Center
Denver, CO 80225

For more information about the USGS and its products:
Telephone: 1-888-ASK-USGS
World Wide Web: *http://www.usgs.gov/*

Suggested citation:
Hunerlach, M.P., Alpers, C.N., Marvin-DiPasquale, M., Taylor, H.E., and De Wild, J.F., 2004, Geochemistry of mercury and other trace elements in fluvial tailings upstream of Daguerre Point Dam, Yuba River, California, August 2001: U.S. Geological Survey Scientific Investigations Report 2004-5165, 66 p.

Contents

First time use of glossary terms are in italics and linked to the glossary.

Figures

Tables

Conversion Factors, Spatial Datums, Acronyms and Abbreviations, and Chemical Elements

Multiply	By	To obtain
cubic foot per second (ft^3/s)	0.02832	cubic meter per second (m^3/s)
foot (ft)	0.3048	meter (m)
gallon (gal)	3.785	liter (L)
pound (lb)	0.4536	kilogram (kg)

Temperature in degrees Celsius (°C) may be converted to degrees Fahrenheit (°F) as follows:

$$°F = (1.8 \times °C) + 32$$

Spatial Datums

Vertical coordinate information is referenced to the National Geodetic Vertical Datum of 1929 (NGVD) – a geodetic datum derived from a general adjustment of the first-order level nets of the United States and Canada, formerly called Sea Level Datum of 1929. Horizontal coordinate information is referenced to the North American Datum of 1983 (NAD83) unless otherwise noted.

Acronyms, Abbreviations, and Chemical Elements

Acronyms

AVS	acid volatile sulfur
CVAFS	cold vapor atomic-fluorescence spectrometry
CVO	Cascades Volcanic Observatory
DOC	dissolved organic carbon
DP	demethylation potential
DPD (Used with site numbers)	Daguerre Point Dam
EDX	energy dispersive X-ray
GC	gas chromatography
IAEA	International Atomic Energy Agency
ICP–AES	inductively coupled plasma–Atomic Emission Spectrometry
ICP–MS	inductively coupled plasma–Mass Spectrometry
LOI	loss on ignition
MDL	method detection limit
MP	methylation potential
PEC	probable effects concentration
QA-QC	quality assurance–quality control
RPD	relative percent difference
rpm	revolutions per minute
SEM	scanning electron microscope
SRM	standard reference material
SRWS	standard reference water sample
TEC	threshold effects concentrations
TRS	total reduced sulfur
USGS	U.S. Geological Survey
WDML	Wisconsin District Mercury Laboratory

Abbreviations

cm	centimeter
cm^3	cubic centimeter
g	gram
kg	kilogram
kg/yd^3	kilogram per cubic yard
L	liter
µCi/100 µL	microcurie per 100 microliters
µg	microgram
µg/g	microgram per gram (part per million)
µm	micrometer
µS/cm	microsiemens per centimeter
mCi/mg	millicurie per milligram
mg	milligram
mg/kg	milligram per kilogram (part per million)
mg/L	milligram per liter
mg/yd^3	milligram per cubic yard
mL	milliliter
mm	millimeter
mV	millivolt
nCi/100 µL	nanocurie per 100 microliters
ng	nanogram
ng/g	nanogram per gram (part per billion)
ng/g/d	nanogram per gram (of dry sediment) per day; also ng/g dry sed/d
ng/L	nanogram per liter
nmol/g dry sed	nanomole per gram dry sediment
s	second

~	approximately
>	greater than
<	less than

Chemical Elements

Al	aluminum
As	arsenic
B	boron
Ba	barium
Be	beryllium
Bi	bismuth
B	boron
Ca	calcium
Cd	cadmium
Ce	cerium
Cl	chloride
Co	cobalt
Cr	chromium
Cs	cesium
Cu	copper
Dy	dysprosium
Er	erbium
Eu	europium
Fe	iron
Gd	gadolinium
Hg	mercury
Ho	holmium
K	potassium
Lu	lutetium
Mg	magnesium
Mn	manganese
N_2	nitrogen gas
Na	sodium
Nd	neodymium
Ni	nickel
O_2	oxygen gas
Pb	lead
Pr	praseodymium
Rb	rubidium
S	sulfur
Sb	antimony
Se	selenium
Si	silicon
Tb	terbium
Tl	thallium
Tm	thulium
U	uranium
V	vanadium
Y	yttrium
Yb	ytterbium
Zn	zinc

Chemical Compounds and Isotopes

^{14}C	radio-labeled carbon
$^{14}CH_3HgCl$	methylmercury chloride with radio-labeled carbon
$CH_3{}^{203}Hg^+$	methylmercury ion with radio-labeled mercury
CH_4	methane
$^{14}CH_4$	methane with radio-labeled carbon
CH_2Cl_2	methylene chloride
^{14}C-MeHg	methylmercury with radio-labeled carbon
$^{14}CO_2$	carbon dioxide with radio-labeled carbon
$CuSO_4$	copper sulfate
HCl	hydrochloric acid
HF	hydrofluoric acid
Hg^0	elemental mercury
Hg^{2+}	mercuric ion
Hg(II)	divalent mercury
^{203}Hg(II)	radio-labeled divalent mercury
Hg_T	total mercury
HNO_3	nitric acid
KBr	potassium bromide
MeHg	methylmercury (monomethylmercury)
$NaBEt_4$	sodium tetraethyl borate

Geochemistry of Mercury and other Trace Elements in Fluvial Tailings Upstream of Daguerre Point Dam, Yuba River, California, August 2001

By Michael P. Hunerlach, Charles N. Alpers, Mark Marvin-DiPasquale, Howard E. Taylor, and John F. De Wild

Abstract

This study was designed to characterize the particle-size distribution and the concentrations of total mercury (Hg_T), methylmercury (MeHg), and other constituents in sediments trapped behind Daguerre Point Dam, a 28-foot-high structure on the lower Yuba River in California. The results of the study will assist other agencies in evaluating potential environmental impacts from mobilization of sediments if Daguerre Point Dam is modified or removed to improve the passage of anadromous fish. Methylmercury is of particular concern owing to its toxicity and propensity to bioaccumulate. A limited amount of recent work on hydraulic and dredge *tailings* in other watersheds has indicated that mercury and MeHg concentrations may be elevated in the fine-grained fractions of *placer mining debris*, particularly clay and silt. Mercury associated with tailings from *placer* gold mines is a source of continued contamination in Sierra Nevada watersheds and downstream water bodies, including the Sacramento–San Joaquin Delta and the San Francisco Bay of northern California.

Churn drilling was used to recover sediments and *heavy minerals* at 5-foot intervals from six locations upstream of Daguerre Point Dam. Maximum depth of penetration ranged from 17.5 to 35 feet below land surface, resulting in 31 discreet drilled intervals. Drilling in permeable, unconsolidated sediments below the streambed of the Yuba River released a significant volume of water along with the sediment, which complicated the sampling and characterization effort. Overflow of a silty fraction sampled at the drill site contained suspended sediment consisting predominantly of silt and clay, with Hg_T concentration ranging from 33 to 1,100 ng/g (nanogram per gram) dry weight. A sandy fraction, collected after sieving sediment through a 2-millimeter vibratory screen, contained from 14 to 82 percent sand and 1 to 29 percent silt plus clay, and had Hg_T concentrations ranging from 6.8 to 81 ng/g dry weight. A clay-silt fraction, sampled from material remaining in suspension after the sandy fraction settled for 15-20 minutes, contained mercury concentrations from 23 to 370 ng/g dry weight. Concentrations of MeHg were less than the detection limit (<0.001 ng/g dry weight) in 30 of 31 samples of the sandy fraction. In the suspended clay-silt fraction, MeHg was detected in 16 of 31 samples, in which it ranged in concentration from 0.04 (estimated) to 0.61 ng/g wet weight.

Potential rates of mercury methylation and demethylation were evaluated in seven samples using radiotracer methods. Mercury methylation (MeHg production) potentials were generally low, ranging from less than 0.15 to about 1.6 ng/g/d (nanogram per gram of dry sediment per day). Mercury demethylation (MeHg degradation) potentials were moderately high, ranging from 1.0 to 2.2 ng/g/d. The ratio of methylation potential (MP) to demethylation potential (DP) ranged from less than 0.14 to about 1.4 (median = 0.24, mean = 0.44, number of samples = 7), suggesting that the potential for net production of MeHg in deep sediments is generally low. The MeHg production rates and MP/DP ratios were higher in the shallower interval in two of the three holes where two depth intervals were assessed, whereas the MeHg concentrations were higher in the shallower interval for all three holes. A similar spatial distribution was found for concentrations of solid-phase sulfide (measured as total reduced sulfur and likely representing iron-sulfide and iron-disulfide compounds), which were much higher in shallower samples (about 700 to about 2,100 nanomoles per gram, dry sediment) than in deeper samples (32 to 55 nanomoles per gram, dry sediment) in these three holes. If reduced sulfur compounds are oxidized to sulfate as a consequence of sediment disturbance, the activity of sulfate-reducing bacteria might be stimulated, causing a short-term increase in methylation of inorganic Hg(II) (divalent mercury). The extent of increased Hg(II)-methylation would depend on the reactivity of the inorganic Hg(II) fraction associated with these sediments, which is currently unknown.

The relation between Hg_T concentration and particle size was evaluated quantitatively using a suite of 15 samples, which were separated into 6 size fractions using screens with the following sieve sizes: 2,000, 500, 297, 149, 60, and 30 μm (micrometer). A trend toward higher concentrations of mercury in samples having finer particles was observed. This trend is consistent with data obtained for other bulk samples (sandy, silty, and clay-silt fractions), which indicate higher concentrations of mercury associated with larger proportions of clay-size material (less than 4 μm).

Heavy-mineral concentrates were prepared to evaluate gold concentrations and to make direct observations of elemental mercury and gold-mercury *amalgam*. Elemental mercury (Hg^0) was observed coating gold and gold-amalgam grains and was isolated with the aid of a stereo microscope. Using a scanning electron microscope, Hg^0 and mercury-rich gold amalgam were observed on the surfaces of individual gold grains. Spherules of liquid Hg^0 up to 6 μm in diameter were observed in association with platy, aluminosilicate minerals and iron oxides.

In addition to mercury, concentrations of several other trace elements in the fine-grained sediment trapped behind Daguerre Point Dam are of potential environmental concern. Median concentration values of arsenic, chromium, copper, and nickel from 19 sediment samples (screened to less than 0.060 millimeter) were higher than consensus threshold effects levels for ecological toxicity, and maximum concentrations of lead, mercury, and zinc were also above the threshold effects levels.

Introduction

Improved passage of anadromous fish is a significant issue for resource agencies throughout the Pacific Northwest, including northern California. A proposed fish-passage-improvement project in the lower Yuba River is located at Daguerre Point Dam (*fig. 1*), in the center of the Yuba Goldfields. The proposed fish-passage-improvement alternatives include dam removal or modification, which would likely release sediments trapped behind Daguerre Point Dam to downstream environments. The Yuba Goldfields area has been affected by several generations of mining of *alluvial gold* and gravel deposits by various methods, dating back to the California Gold Rush of 1849. Mercury is known to be a contaminant in gold-mining wastes because of its use in amalgamation. This study addresses concerns about mercury and other constituents in potentially released sediments trapped behind Daguerre Point Dam.

Daguerre Point Dam and the Yuba Goldfields

Daguerre Point Dam is a 28-foot-high structure located about ten miles east of Marysville, California, in the Yuba Goldfields (*fig. 1*). The dam sits on a *bedrock* bench in the piedmont plain of the ancestral Yuba River. A cut 600 feet wide and 25 feet deep was dug in the bedrock bench for the footing of the dam, which was completed in 1910. The Yuba Goldfields (*fig. 2*) consist of more than 8,000 acres of dredged landscape and represent one of the largest tracts of mining *debris* in northern California. Sediment stored behind Daguerre Point Dam is a mixture of material from a variety of sources, reflecting several periods of historical mining in the Yuba River watershed. In addition, some sediments unaffected by mining may exist very near Daguerre Point Dam.

Prior to *hydraulic mining* and dredging, the Yuba River traversed the northern Sierra Nevada and discharged into the Sacramento Valley (*fig. 1*), depositing vast quantities of gold-bearing gravels in a large *alluvial* plain. Gold dredging began in California in March 1898 (Aubrey, 1910), with the working of *auriferous*, alluvial deposits at the mouths of the Feather, Yuba, and American Rivers. One of the largest alluvial concentrations of gold in California is within the Yuba Goldfields, where over 5 million ounces of gold have been produced from more than 1 billion cubic yards of material. Parts of the Yuba Goldfields were mined multiple times by evolving dredging methods. Each new period of dredging dug deeper and recovered smaller gold particles as technology improved. Today, the only recent gold-dredging operation in the conterminous United States is in areas of previously mined gravels in the Yuba Goldfields, including tailings from hydraulic gold mines that were discharged to the Yuba River prior to construction of Englebright Dam (*fig. 1*) in 1940 and unworked gold-bearing gravel at and near the contact with metamorphic bedrock, reaching depths of nearly 140 feet below the water surface.

The Daguerre Point Dam was built in the early 1900s to retain mining debris from hydraulic mines in the upper Yuba River watershed. This was one of the early attempts to retain the large quantities of hydraulic mining debris that was being transported down the Yuba River *channel*. Prior to dam construction, the river carried most of the hydraulic mining debris in the watershed to the edge of the Central Valley, where the lower gradients caused the debris to be deposited, filling and choking the river channel.

The first attempt to constrain tailings and debris in the lower Yuba River was made using a structure known as Barrier Number 1, located about 1 mile downstream of the Parks Bar Bridge and 4.5 miles upstream of Daguerre Point (*fig. 1*). Barrier Number 1, constructed in 1905, was 14 feet high and constrained 1,690,000 cubic yards of gravel that were transported in the river channel during the winter and spring of 1906 (Gilbert, 1917). Of this total, 920,000 cubic yards were constrained upstream of the barrier during the January 1906 flood alone. However, Barrier Number 1 failed the following year, in March 1907. Many acres of farmlands were repeatedly destroyed by flooding and silting in the Yuba River, Bear River, and American River watersheds, and properties in the cities of Marysville and Sacramento were threatened frequently by the rise of river beds.

After Daguerre Point Dam was completed in 1910, it rapidly filled to capacity with sediment and debris that moved downstream during flooding in 1911. The level of the streambed at Daguerre Point Dam was established in 1911. The present-day alluvial sediments in the Yuba River are comprised predominantly of mining debris that contains mercury from

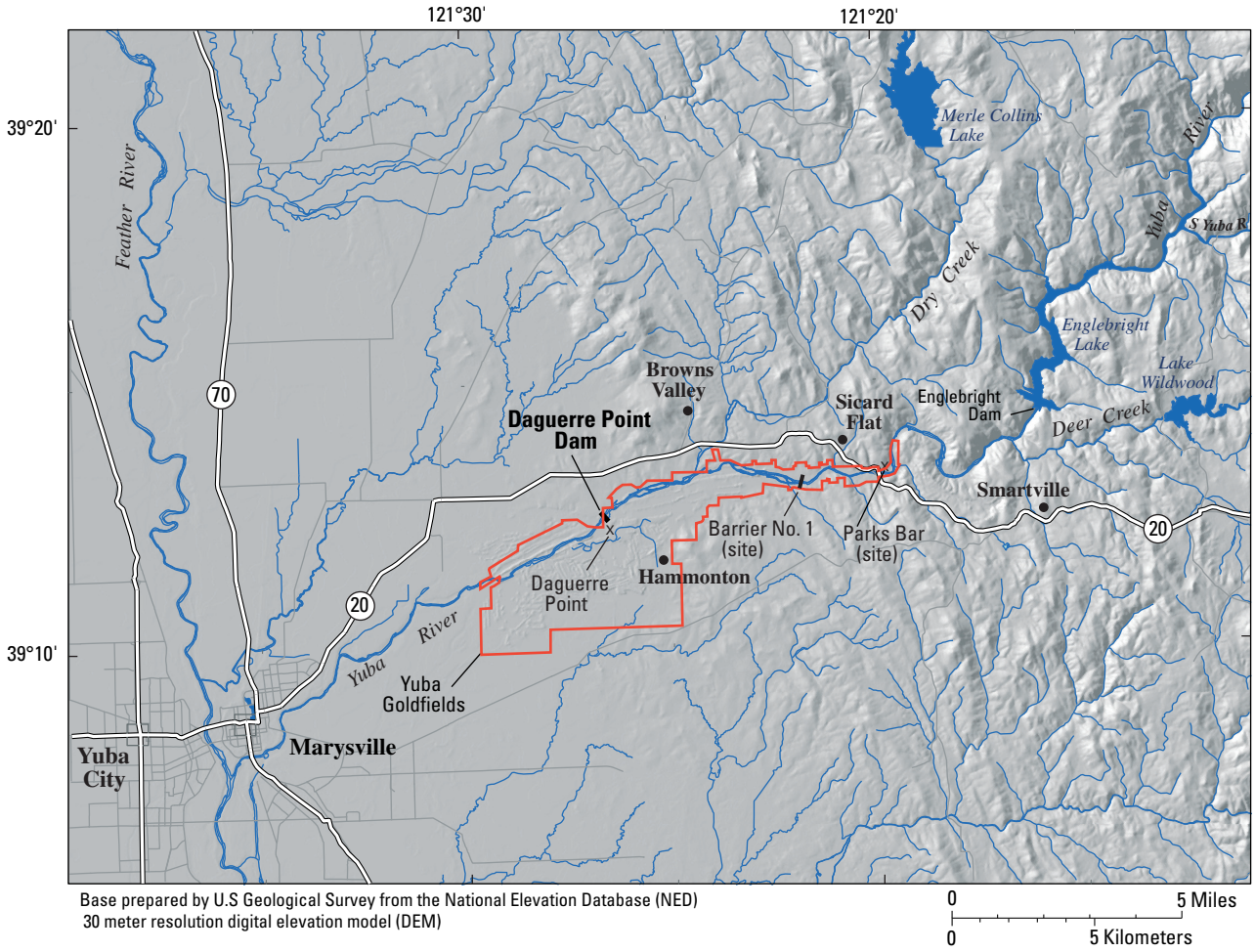

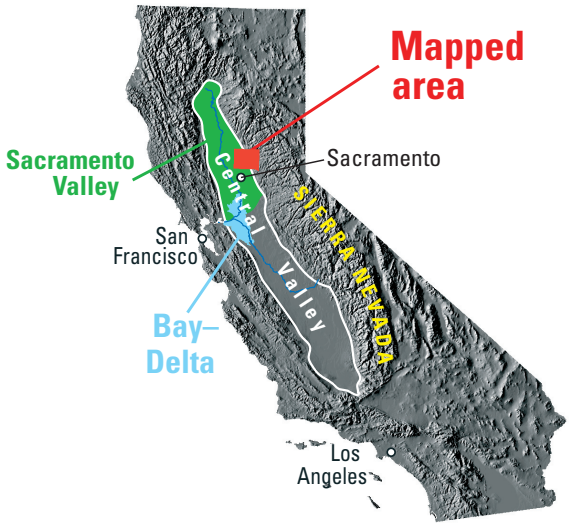

Figure 1. Map showing location of study area, Daguerre Point Dam, California.

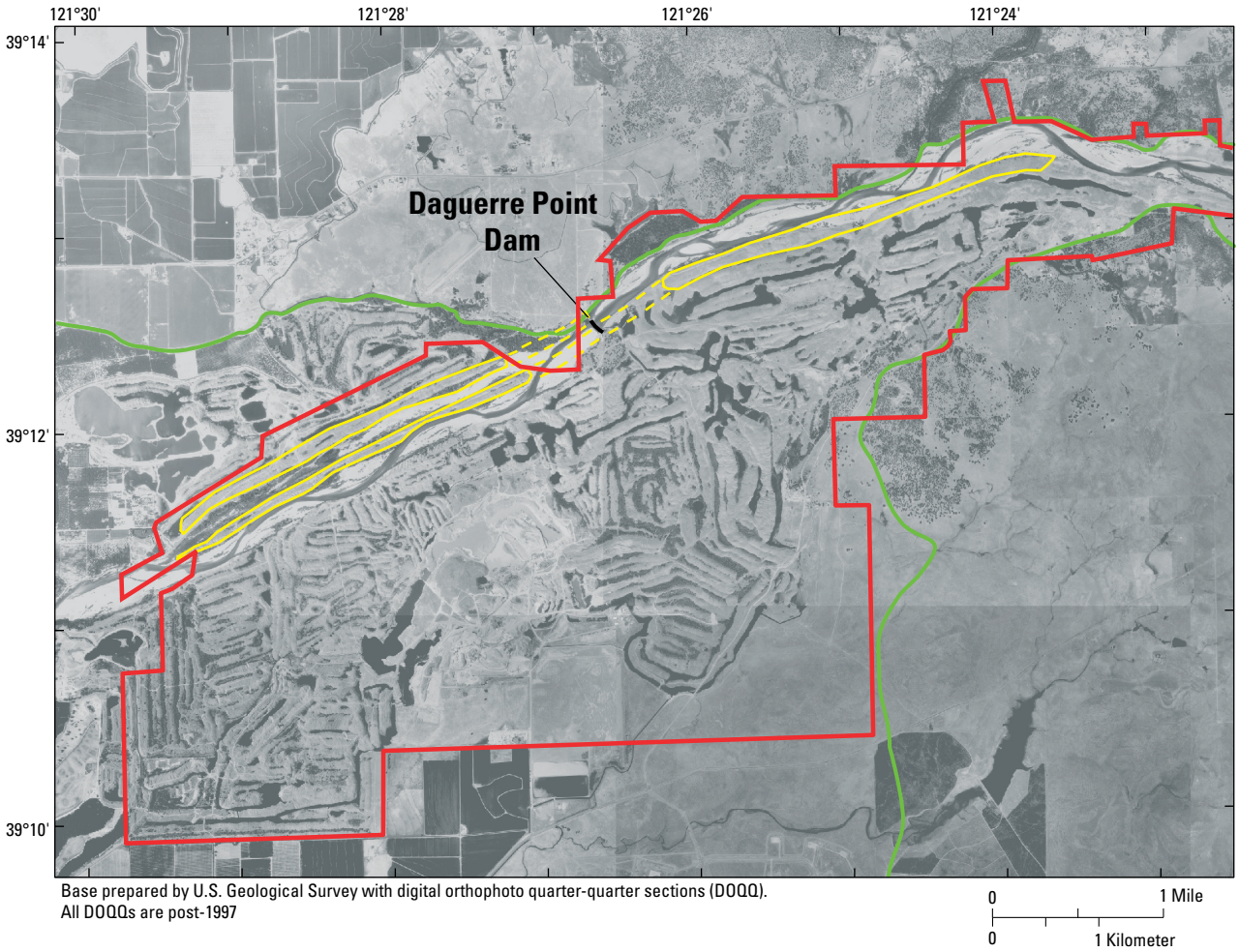

Figure 2. Aerial photograph showing Yuba Goldfields and location of training walls, Daguerre Point Dam, California.

the processing of gold-bearing gravels both in hydraulic mines and early dredging operations (Alpers and Hunerlach, 2000).

The Daguerre Point Dam was constructed in a cut above and to the north of the original Yuba River channel. The bedrock under Daguerre Point Dam is a portion of the Daguerre Point Terrace, a feature that facilitated the construction of a low dam at a relatively low cost. The current position of the Yuba River behind the Daguerre Point Dam is north of its pre-mining channel (*fig. 3*) and above its prior streambed elevation. Flood water was directed to and over the dam by large walls constructed of tailings stacked by specially constructed dredges. These constraining walls are known locally as training walls and currently hold the Yuba River in its position upstream of the dam (*fig. 2*). The training walls, which were constructed using dredge tailings, force the Yuba River to flow as far north as possible, allowing deeper gravels in the southern part of the Yuba Goldfields to be mined more economically and with less environmental impact than if the river's original course had been maintained. Downstream of Daguerre Point Dam, the Yuba River has abandoned the training walls and resumed a meandering course through the *fluvial* tailings. Down cutting of the streambed below the dam has exposed the bedrock of Daguerre Point.

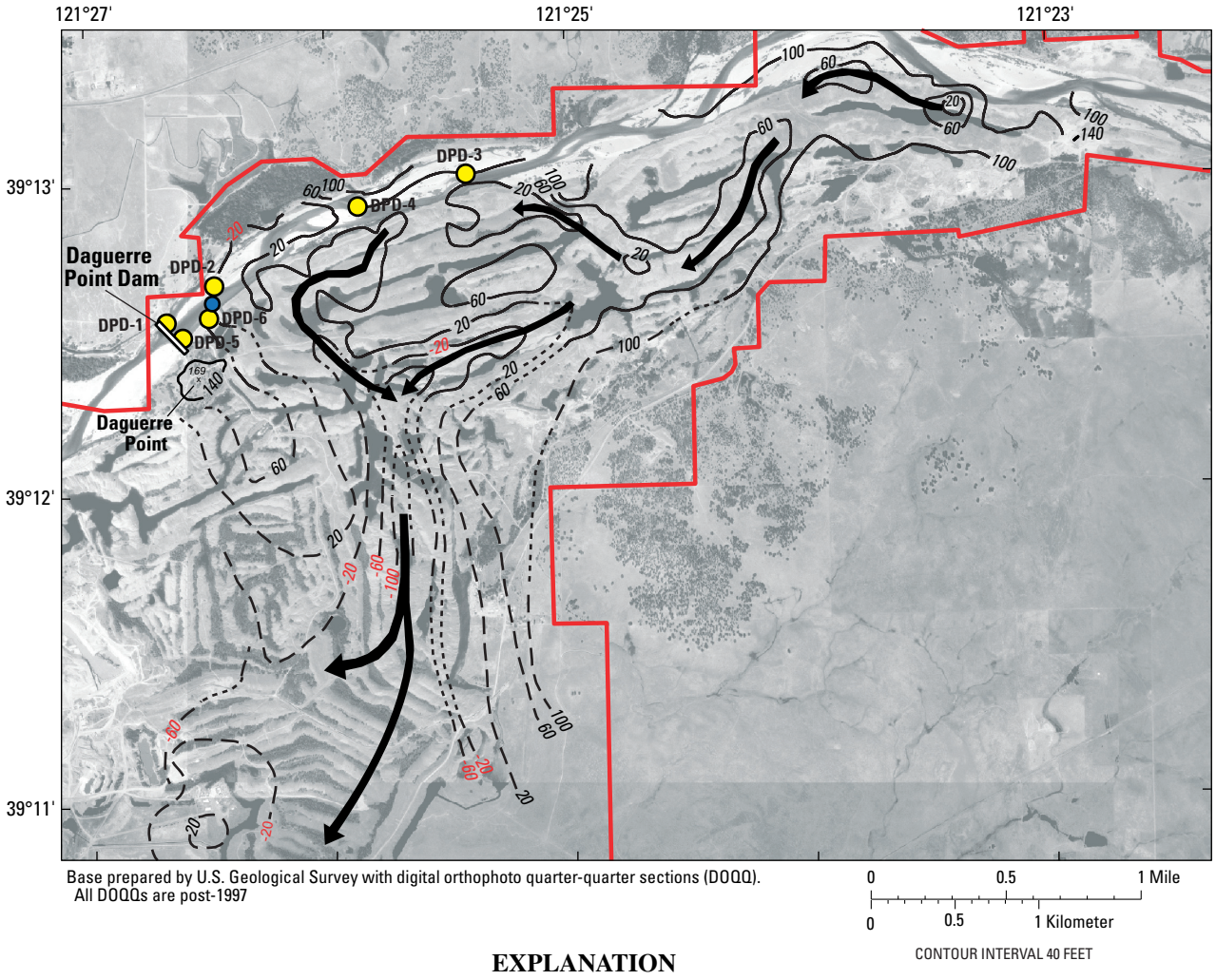

Figure 3. Map with contours representing elevation of top of bedrock, Daguerre Point Dam, California.

Fish Habitat and Environmental Concerns

A reconnaissance study in the northwestern Sierra Nevada (Slotton and others, 1997) indicated that mercury bioaccumulation in fish and biota is widespread and correlates in general with areas of historical gold mining. Alpers and Hunerlach (2000) combined the data from Slotton and others (1997) with historical mining records to demonstrate an overall correlation between mercury bioaccumulation and the intensity of hydraulic mining in the watersheds of the western slope of the northern Sierra Nevada. Mercury associated with tailings from placer gold mines is a source of continued contamination in Sierra Nevada watersheds and downstream water bodies, including the Sacramento–San Joaquin Delta and the San Francisco Bay of northern California (*fig. 1*). The Yuba River is one of the most intensely mined areas and also has some of the highest levels of mercury bioaccumulation. May and others (2000) documented significant bioaccumulation of MeHg in fish in Lake Englebright, located on the Yuba River several miles upstream of Daguerre Point Dam, and in four other reservoirs as well as several stream sites affected by hydraulic mining in the Yuba River and Bear River watersheds.

There are several species of anadromous fish, including steelhead trout and four distinct runs of Chinook salmon, for which available habitat in California has been greatly reduced by dams on rivers. There is considerable interest among federal and state agencies in restoring anadromous fish habitat and improving passage and survival of these fish in areas such as the lower Yuba River.

Fish ladders presently provide some passage of anadromous fish at Daguerre Point Dam; however, improved passage is needed (California Department of Water Resources, 2003). Of the six types of anadromous fish that are known to migrate into the Yuba River, four (white sturgeon, green sturgeon, striped bass, and American shad) are blocked by Daguerre Point Dam, and two (fall-run Chinook salmon, and steelhead trout) are hindered by inadequate fish ladders at the dam. Proposed modifications to Daguerre Point Dam intended to improve fish passage might result in release of sediments stored behind the dam to downstream environments. Increased sedimentation in downstream water bodies, including the Sacramento–San Joaquin Delta and the San Francisco Bay, could cause physical degradation of fish habitat by siltation, or chemical degradation by release of contaminants such as mercury (or methylmercury) or other trace metals that are presently stored in sediments behind Daguerre Point Dam.

Purpose and Scope

Removal or modification of the Daguerre Point Dam is being evaluated by various stakeholder agencies as a way to improve the ability of anadromous fish to access about 12 miles of the Yuba River below Englebright Dam (*fig. 1*). The purpose of this report is to provide data and information about the sediment trapped behind Daguerre Point Dam, specifically (1) the association of particle-size distribution and mercury and methylmercury concentration, and (2) the potential for mercury methylation and demethylation. Of particular concern to stakeholders is the distribution of silt- and clay-sized particles, which, if released to downstream environments, could cause degradation of fish habitat. This report presents the first characterization of mercury concentrations in sediments trapped behind Daguerre Point Dam, an area that has been affected by multiple periods of gold mining and associated mercury use.

Acknowledgments

The authors thank the numerous individuals at the U.S. Geological Survey (USGS) and other agencies who made this report possible. Personnel who assisted with field work for this study include Connie Clapton (California State University Sacramento Foundation) and Karl Davidek (USGS). USGS volunteer Michael J. Hunerlach and student intern Nick Kanowski helped with field logistics. Assistance by USGS personnel in the laboratory was provided by Ronald Antweiler, Dale Peart, Terry Plowman, and David Roth in Boulder, Colorado; by Mark Olson and Shane Olund in Middleton, Wisconsin; by Jennifer Agee and Le Kieu in Menlo Park, California; and by Daniel Gooding in Vancouver, Washington. Individuals from Cal Sierra Development Incorporated who facilitated understanding of the stratigraphy during drilling include Ben Coleman and Tony Massey, and especially Alberto Ramirez, who shared his vast knowledge of placer geology and mining history. Walter Cotter of the Browns Valley Irrigation District assisted in gaining access to the sampling sites. Ted Frink of the California Department of Water Resources and Paul Wisheropp of Entrix, Inc. participated in useful discussions regarding the hydrogeology of the lower Yuba River. John Nelson of the California Department of Fish and Game assisted with securing funding for this study in cooperation with the U.S. Bureau of Reclamation.

Hydrogeological Setting and Mining History

Geology of Gravel Deposits

The extensive gravel deposit in the Yuba Goldfields is located within Yuba County, north-central California, in the topographic transition zone between the western foothills of the Sierra Nevada and the eastern margin of the Great Valley (*fig. 1*). The Yuba Goldfields is one of three large floodplains that drain the principal gold-mining region of the northern Sierra Nevada in California; the others are the goldfields of the Feather River and the American River. Gravels in the Yuba Goldfields were deposited over the past 50 million years, beginning with the Eocene erosion of the Sierra Nevada; the gravels filled a large alluvial channel where the Yuba River currently emerges from the foothills. The ancestral Yuba River incised a deep channel into the metavolcanic bedrock in the reach between Parks Bar and Daguerre Point. About three miles upstream of Daguerre Point, the paleo-channel bifurcates and the bedrock gradient increases to the southwest around Daguerre Point (*fig. 3*). Daguerre Point is a metavolcanic greenstone barrier that formed the right bank of the deep channel where the ancestral Yuba River emptied onto a vast alluvial plain. About 0.7 miles south of Daguerre Point, the river channel begins to widen and the gravel deposit is more than 2 miles wide. The deposit rests on terraces that were uplifted and eroded at different times. The lowest bedrock of the channel reaches a depth of 100 feet below sea level southeast and south of Daguerre Point. The ancestral Yuba River followed the deep channel around Daguerre Point. The present Yuba River flows north of and parallel to the ancestral, deep channel, west to the confluence of the Feather River (*fig. 1*). Typically, the surface of the exposed gravel bars and the bed of the Yuba River upstream of Daguerre Point Dam are well armored with coarse gravel to a depth of several feet.

Gold particles were released during periods of erosion from rich, gold-bearing quartz veins in the upper Yuba River

watershed of the Sierra Nevada. Numerous gold-bearing quartz veins and veinlets of Middle Jurassic age exist in greenschist metamorphic grade host rocks in the Sierra Nevada. Abundant fine-grained gold particles were deposited in the *flood-plain* gravels of the modern Yuba River during several phases of glacial erosion in the Pleistocene. Quaternary gravels overlie older, Tertiary-aged volcanic rocks, post-volcanic gravels, and coarse gold-bearing gravels from the Tertiary Yuba River (Lindgren, 1911). Deltaic siltstones and sandstones of the Eocene Ione Formation overlie marine conglomerates of the Late Cretaceous Chico Formation, which form the basal contact with the Mesozoic metavolcanic greenstone bedrock. Rounded and subangular-to-subrounded clasts of coarse granite, rhyolite, and metavolcanic rocks dominate the lithology of the Quarternary gravels in a matrix of sand and silt. Thin horizons of sand, sandy silt, and silty clay formed lenses of variable thickness that extend throughout the deposit as a result of ancient flooding and natural levee breaching by the Yuba River as it meandered across a vast alluvial plain.

Mining Effects in the Lower Yuba River

Rich, shallow deposits of gold-bearing gravel near Parks Bar, about seven miles upstream of the present Daguerre Point Dam, were first worked around 1850. Soon after these shallow deposits were exhausted by *river mining*, miners exploited Quaternary terrace deposits at an elevation higher than that of the present river, which led miners to older, Tertiary-age deposits of the ancestral Yuba River. Around 1852, hydraulic mining of the Tertiary-age gravel deposits began farther upstream and continued for more than 32 years (Alpers and Hunerlach, 2000). Hydraulic mining moved nearly 500 million cubic yards of sand, gravel, and silt in the Yuba River system to the edge of the Central Valley, where much of it was deposited, filling and choking the Yuba River channel. Similar activity in other Sierra Nevada watersheds displaced approximately 1 billion additional cubic yards; the Yuba River was the site of more hydraulic mining debris than any other watershed in California (Lindgren, 1911; Gilbert, 1917).

The gold-rich placer deposits of the present Yuba River are mostly confined to the river banks, bars, benches, and flood plains. Small-scale placer mining in nearby streams and the active channel of the Yuba River ceased because the channel was buried by the large influx of hydraulic mining debris. Hydraulic mining occurred locally at Sicard Flat and Smartville (*fig. 1*), but was eventually terminated along with other hydraulic mining in the Sierra Nevada by the Sawyer Decision of 1884. Debris from hydraulic mining continued to be transported into the Yuba River, reaching a thickness of more than 80 feet within the Yuba Goldfields. The slurry of debris washed onto the Yuba River flood plain contained as much as 57 percent silt and sand (Gilbert, 1917) along with a high proportion of *black sand* and fine-grained gold, *floured mercury*, and amalgam. In an attempt to prevent flooding, Barrier Number 1 was constructed about 4.5 miles upstream of Daguerre Point in 1905 (Mining and Scientific Press, 1905). Prior to the completion of Daguerre Point Dam, Barrier Number 1 failed in March 1907, causing a large volume of debris to be transported by the Yuba River past the Daguerre Point location.

Overview of Mercury Use in Historical Mining

Liquid mercury (quicksilver) was used extensively from the 1850s through the mid-1900s for gold recovery in the Sierra Nevada. Mercury was first used during initial mining of placer gold deposits in riverbeds in the 1850s and its use was especially prevalent in hydraulic mining operations. Prior to the Sawyer Decision of 1884, hydraulic mining was largely unregulated. The Caminetti Act of 1893 allowed hydraulic mining to continue in the Sierra Nevada under the oversight of the California Debris Commission, and the activity continued until the 1930s (Yeend, 1974; Hagwood, 1981). More than 8 million pounds of mercury were lost to the environment during historical gold mining in the Sierra Nevada (Hunerlach and others, 1999; Alpers and Hunerlach, 2000; Churchill, 2000). Many of the historical mine sites remain as significant sources of mercury contamination as well as eroding sediment.

Mercury from the upstream mine sites has been partially transformed to MeHg and is currently bioaccumulating in fish in foothill reservoirs, including Englebright Lake on the Yuba River (May and others, 2000). For example, fourteen samples of smallmouth bass from Englebright Lake, ranging in total length from 285 to 358 mm, had Hg_T concentrations in skinless fillets of axial muscle tissue ranging from 0.53 to 0.96 parts per million (wet basis) (May and others, 2000). The data on mercury in fish tissue has led to fish consumption advisories for reservoirs and selected stream reaches in the Yuba River and Bear River watersheds, east and southeast, respectively, of the Daguerre Point Dam (Klasing and Brodberg, 2003).

Beginning in 1898, mercury also was used to recover gold collected using dredges. Up to 3,000 pounds of mercury was used per dredge per week (Janin, 1918). Mercury losses from *riffles* in gold-recovery sluices onboard the dredges in the Yuba Goldfields were from 2 to 5 percent per season, compared with the range of 10 to 30 percent per season for hydraulic mining (Alpers and Hunerlach, 2000; Churchill, 2000).

However, gold dredges commonly recovered more mercury than they lost because of their efficient recovery of heavy sand- and silt-sized particles and the fact that much of the material being dredged was either hydraulic tailings or previously dredged ground. Historical records from the Yuba Consolidated Goldfield indicate that dredging near Daguerre Point Dam took place on a nearly continuous basis from 1904 through 1968. Compilation of annual data for dredged areas indicates that dredging can be divided into three main periods: 1904-15, 1916-34, and 1942-68 (*fig. 4*). The mining company records indicate that extensive areas were re-dredged and that this was done primarily as technology improved allowing deeper digging. The area of the present Yuba River channel

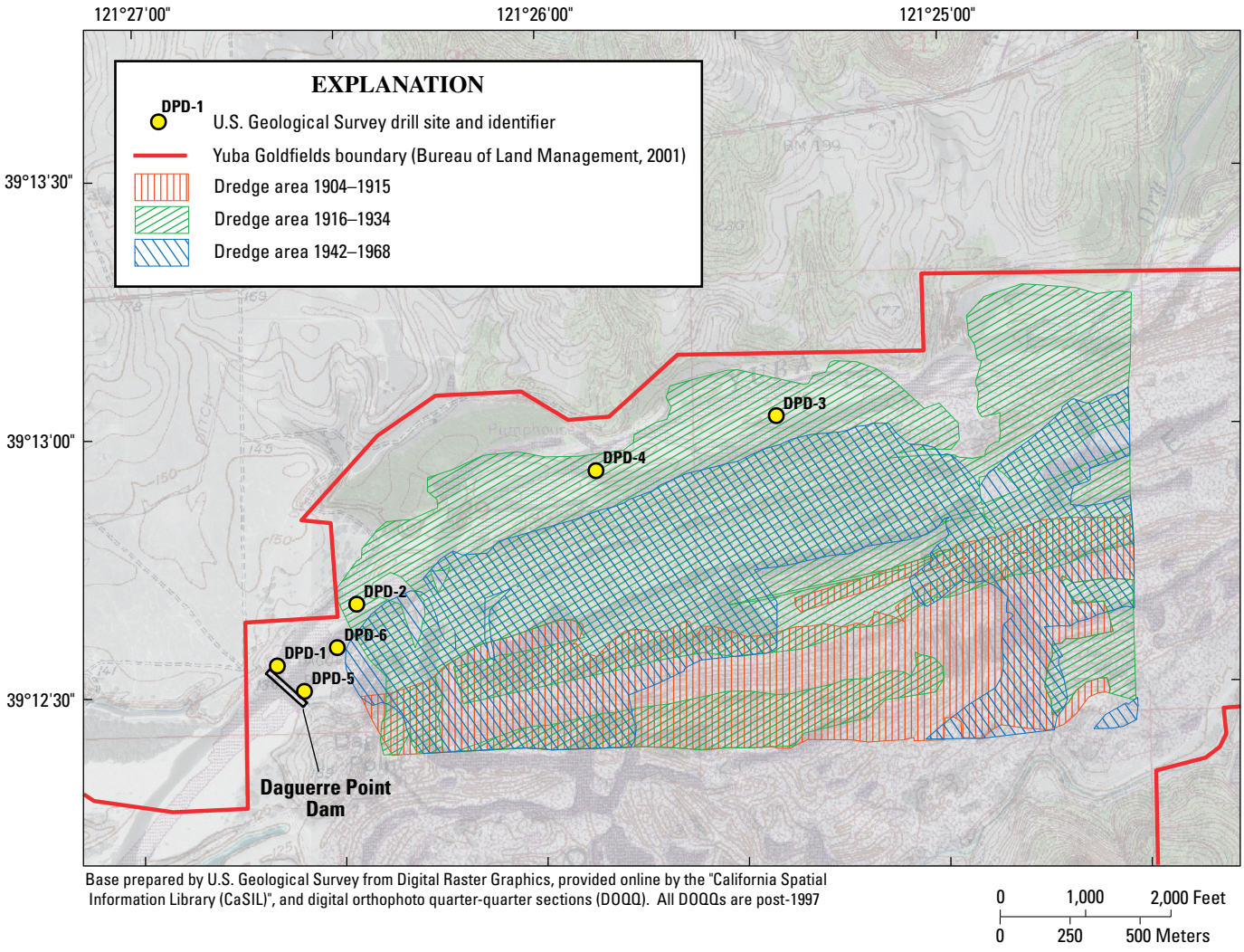

Figure 4. Map showing chronology of dredging upstream of Daguerre Point Dam, California.

upstream of Daguerre Point Dam was dredged primarily during 1916-34. The area north and west of this dredged area was apparently not dredged and most likely represents residual hydraulic mine tailings and (or) a mixture of hydraulic mine tailings and early dredged tailings (*fig. 5*).

Recovery of gold and gold-mercury amalgam was further enhanced starting around 1918 by installing *jigs* on the dredges. Early testing of heavy mineral concentrates from dredging showed a gain of 10 pounds of mercury for every 100 tons of black sand processed, corresponding to a mercury concentration of about 50 parts per million. Mercury use in the Yuba Goldfields stopped in 1990 (Alberto Ramirez, Mining Engineer, Cal Sierra Development Incorporated, oral commun., 2002); today, mercury is recovered as a by-product of gold and sand recovery.

Dredging

The *bucket-line dredge* was invented and first used in California around 1898, 14 years after the cessation of major hydraulic mining in the Sierra Nevada. In August 1904, mining operations began on the Yuba River near Hammonton (*fig. 1*) using the Yuba No. 1 and No. 2 bucket-line dredges; these were the first of their type to be able to dig 60 feet below the water line (Aubrey, 1910). Gold dredging was the first attempt to recover both the gold lost during hydraulic mining and the very fine gold distributed naturally in the gravel deposits of the Yuba River flood plain.

The gold dredge dug a deep trench across the alluvial plain using a series of buckets on a seamless conveyor. Within this trench, the dredge floated in a large pool and dumped

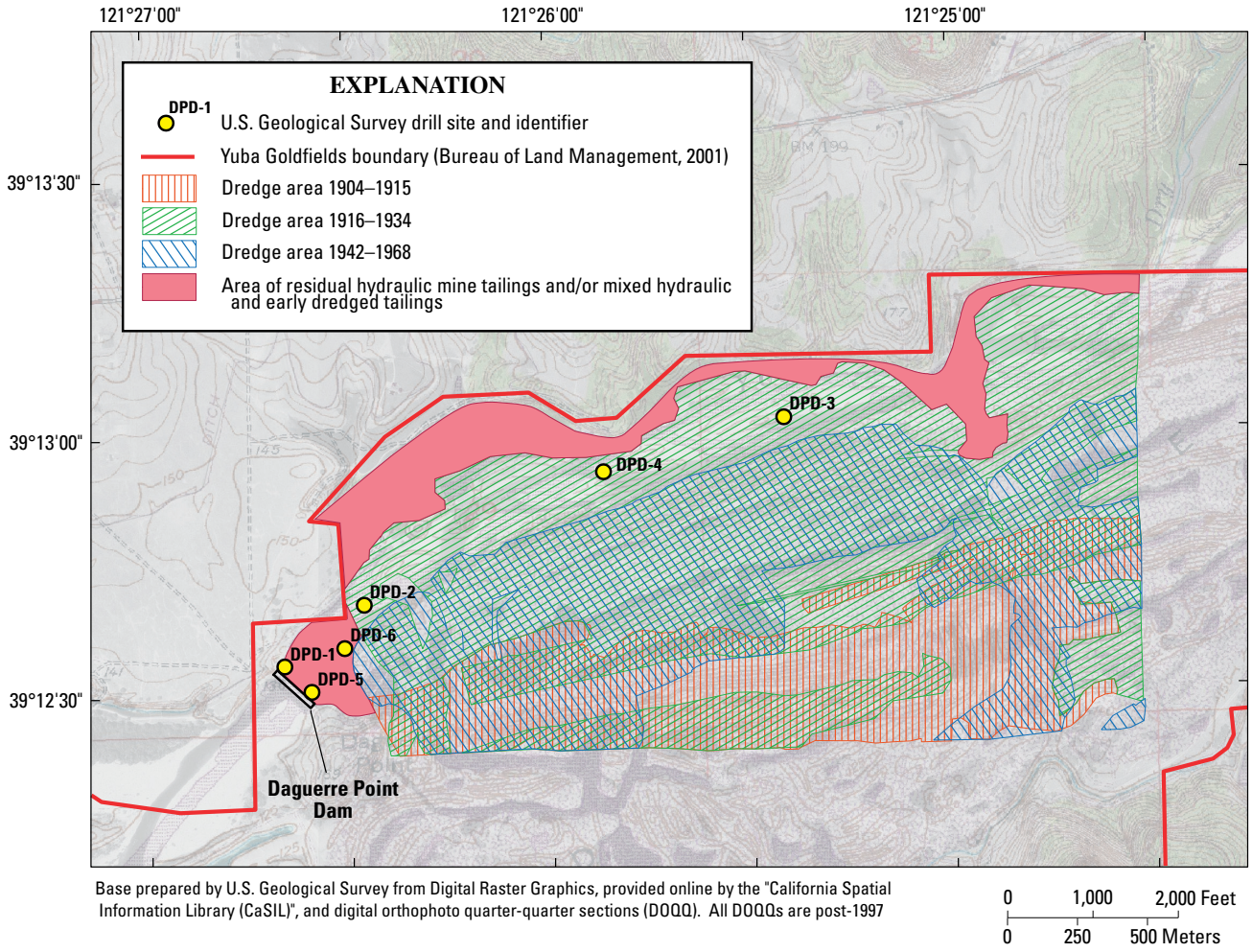

Figure 5. Map showing distribution of residual hydraulic mine tailings upstream of Daguerre Point Dam, California.

the processed gravel behind it as it progressed across the landscape. The gold-bearing gravel was separated inside the dredge into coarse and fine fractions. The fine fraction, consisting of sand, silt, and clay, was discharged into the pool and the coarser material was discharged to the rear and to the sides of the dredge. As a result, two distinct types of deposits accumulated in the pool inside the trench. A mixture of clay, silt, and sand, typically tens of feet thick, accumulated at the bottom of the pool, whereas gravel was stacked in piles up to 43 feet above the surface of the pool. The volume of gravel was not reduced by removing the clay and sand that previously occupied the interstices between the pebbles and coarse gravel. The total volume of the post-dredging deposits is greater than that of the undredged gravel and debris as a result of disruption and sorting of the material.

Since 1904, dredging has been the principal form of mining in the Yuba Goldfields. Dredging re-worked most of the hydraulic tailings that were deposited on top of the younger gold-bearing river gravels (Aubrey, 1910). By 1910, there were as many as 15 dredges operating near Hammonton (*fig. 1*). As dredging technology evolved and the top gravels were exploited, dredges were rebuilt to allow digging to greater depths below the water surface. Digging depths typically ranged from 60 to 80 feet below the water surface through 1939 and from 100 to 125 feet from 1939 to 2003. In 1959, four dredges mined more than 16 million cubic yards of gravel. Between 1898 and 2003, more than 1 billion (10^9) cubic yards of gold-bearing gravel were dredged in the Yuba Goldfields. In August 2001, only the Yuba No. 21 dredge was operating; operations on Yuba No. 21 have been halted since January 29, 2003 because of the sinking of this dredge.

At present (2004), no gold-mining dredges are operating in the Yuba Goldfields. Today, the extensive residual piles of coarse gravel are an important source of aggregate and sand. Water flowing through the gravels creates large tracts of wetland ponds throughout the mined landscape. In 1910,

fine-grained silt and sand were channeled to a "settling basin" about 2 miles south of Daguerre Point that was more than 1,200 acres. Because of the increased value of sand in recent years, miners have inverted the discharge of processed material from the dredge, sending the coarse gravels to the bottom of the pond while saving sand and fine-grained sediment for further processing.

Study Design and Methods

Drilling Methods

During August 2001, the USGS drilled a series of six holes (*fig. 6*) behind the Daguerre Point Dam, in the bed of the Yuba River. Site descriptions and locations are given in *table 1*. Based upon the lithology of the sediments behind the Daguerre Point Dam and evaluation of historical mining records, a *churn drill* (*fig. 7*) was selected for drilling and collecting composite samples. Churn drilling is used in deep or wet ground where sampling by pits, trenches, or other drills is not feasible and where quantitative recovery of heavy minerals is required. The churn drill uses a heavy steel casing with a drive shoe at the bottom, a chisel-shaped bit, and a sand pump for removing the sample from the hole. The sand pump is a vacuum pump made of a hollow steel cylinder, 8 feet long and 4 inches in diameter, equipped with a valve and a piston (or sucker rod) that travels the whole length of the cylinder. The piston goes to the bottom of the pump when lowered; when drawn up rapidly, it produces a vacuum, which draws in sand, silty water, gravel, and small cobbles. This method is very efficient for sampling alluvial material in which heavy minerals such as

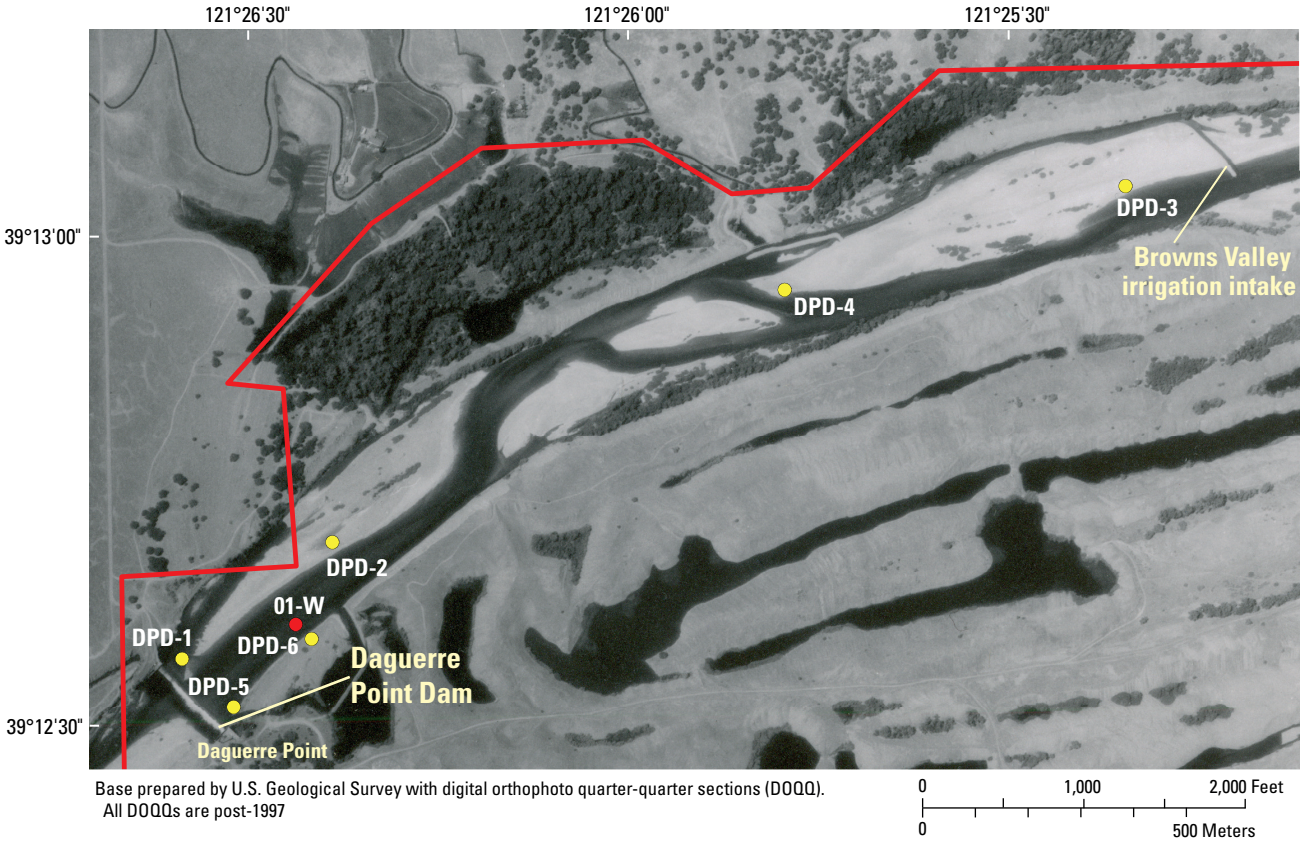

Figure 6. Aerial photograph showing locations of drilling upstream of Daguerre Point Dam, California.

Table 1. Description of drill sites upstream of Daguerre Point Dam, California.

[USGS, U.S. Geological Survey. ft, foot; mi, mile. DPD, Daguerre Point Dam]

USGS station number	Drill hole	Depth (ft)	Drilling start date	Site descriptions	Latitude (north)	Longitude (west)
391231121263201	DPD-1	0–17.5	8/14/2001	The sample location is at the far SW end of a gravel bar on the right bank side of the Yuba River about 200 ft upstream of Daguerre Point Dam.	39°12′34″	121°26′36″
391241121262401	DPD-2	0–35	8/15/2001	The sample location is at the far NE end of a gravel bar on the right bank side of the Yuba River about 400 ft upstream of Daguerre Point Dam.	39°12′41″	121°26′24″
391302121252101	DPD-3	0–20	8/20/2001	The sample location is at the far NE end of a gravel bar on the right bank side of the Yuba River about 1.2 mi upstream of Daguerre Point Dam.	39°13′02″	121°25′21″
391256121254801	DPD-4	0–30	8/21/2001	The sample location is near the SW end of a gravel bar on the right bank side of the Yuba River about 0.8 mi upstream of Daguerre Point Dam.	39°12′56″	121°25′48″
391231121263201	DPD-5	0–20	8/24/2001	The sample location is near the SE end of a gravel bar on the left bank side of the Yuba River about 200 ft upstream of Daguerre Point Dam.	39°12′31″	121°26′34″
391236121262701	DPD-6	0–30	8/27/2001	The sample location is near the SE end of a gravel bar on the left bank side of the Yuba River about 600 ft upstream of Daguerre Point Dam.	39°12′36″	121°26′27″

Figure 7. Photo of churn drill at site DPD-2, Daguerre Point Dam, California.

gold and gold-amalgam may be widely dispersed in unconsolidated sediments (Wells, 1973).

Drilling with the churn drill was accomplished by driving a 6-inch diameter steel casing to the desired depth interval and extracting the contents by means of the piston-plunger, which sucks up the contents of the discrete interval. If necessary, the material at the bottom of the hole was "churned" (broken up using the chisel-shaped bit) for several minutes to break up resistant rocks or hardpan clay layers. If necessary during churning, a hose was used to pump Yuba River water into the hole. It is estimated that 1 to 10 gallons of Yuba River water was introduced during the drilling of each 5-foot interval. Water quality in the Yuba River during drilling is discussed in a later section of the report. Sediment lithology was recorded for each 5-foot interval (*table A1*).

Hydrologic Conditions during Study

Diversion of Browns Valley Irrigation Ditch

The intake to the Browns Valley irrigation ditch (*fig. 6*) diverts water for agricultural use about 1.3 miles upstream of Daguerre Point Dam. Flow is diverted from the main Yuba River through a 40-foot-wide diversion channel. It was necessary to cross this channel to drill-holes DPD-3 and DPD-4. To maintain an uninterrupted flow of 200 ft^3/s (cubic foot per second), three 48-inch-diameter culverts were installed in the bed of the Browns Valley irrigation ditch and the mouth of the diversion was narrowed. A temporary gravel bridge was constructed over the corrugated steel culverts while the minimum flow required by the irrigation district was allowed to pass

through. This bridge allowed access to a 1-mile-long meander island in the river bed, located between 0.8 and 1.5 miles upstream of Daguerre Point Dam, while drill-holes DPD-3 and DPD-4 were drilled and sampled. Upon completion of drilling, the culverts were removed, the mouth of the diversion ditch was widened to its original configuration, and the diversion channel walls were stabilized with locally available gravels.

Discharge and Water Quality

The flow rate of the Yuba River changes with the seasons in response to the Mediterranean climate of northern California and to minimum flow requirements mandated for fish habitat (California State Water Resources Control Board, 2003). Discharge in the Yuba River and major tributaries is managed for the purposes of flood control, electric power generation, irrigation, and aquatic habitat. During drilling in August 2001, the Yuba River above Daguerre Point Dam had a moderate flow rate with an average discharge of 1,607 ft^3/s.

Because some Yuba River water was pumped into each open hole during drilling, a water-quality sample was collected to determine whether significant concentrations of mercury or methylmercury were added to the downhole sediments. A grab sample for water quality was collected from the main channel of the Yuba River between drill-hole numbers DPD-6 and DPD-2 (*fig. 6*). Analytical results for the water-quality sample are given in *table D1*.

Collecting and Processing Samples

A flow chart describing the sample collection and processing procedures is shown in *figure 8*. Sediment samples from the six drill holes were composited in 5-foot intervals, with minor exceptions described below. Samples of sediment and produced water from the churn drill were transferred into an acid-rinsed, stainless steel trough and then allowed to flow into an acid-rinsed, 5-gallon plastic bucket. For most intervals, three to four 5-gallon buckets were partially filled with sediment for each 5-foot interval, for a total retained volume of 12 to 15 gallons. A volume of 10 to 65 gallons of water containing fine sediment was discarded (silty fraction; yellow areas in *figure 8*). The silty fraction was sampled by collecting 1 L per 5-gallon bucket of discharged drill water; the 1-L subsamples were composited in a 20-L teflon-lined, stainless-steel churn, from which 1-L subsamples were drawn for analysis of Hg_T concentration and particle-size distribution. For selected intervals at this stage, a 0.5-L subsample of the retained material was taken for analysis of mercury methylation and demethylation potential and related ancillary parameters.

The retained sediment for each 5-foot interval was transferred to an acid rinsed, stainless-steel, 76-cm-diameter vibratory screen (manufactured by SWECO) with openings of 2 mm. For each interval, fine-grained sediments were separated from the greater-than 2-mm sediments with recirculated process water. Unscreened sediment was continuously washed on top of the vibratory screen until no fine material was seen on the gravel. The gravel fraction that did not pass through the screen was set aside in clean, plastic, 5-gallon buckets. The sandy fraction that passed through the 2-mm screen (sand, silt, and clay) was homogenized in an acid-rinsed, plastic tub.

After stirring it in the plastic tub to a slurry-like consistency using acid-rinsed plastic spoons, the sandy fraction was subsampled for Hg_T, particle-size distribution, and trace metals in a 1-L, acid-rinsed plastic bottle that was subsequently chilled on wet ice. An additional 1-L subsample of the sandy fraction was taken for archive purposes and frozen on dry ice. Samples for analysis of Hg_T and MeHg in the sandy fraction were collected in acid-rinsed 60-mL Teflon vials and frozen immediately on dry ice. After the sandy fraction was allowed to settle for 15–20 minutes, a sample of the very fine-grained suspended sediment, the clay-silt fraction, was collected in an acid-rinsed, 30-mL Teflon centrifuge tube and frozen immediately on dry ice for Hg_T and MeHg analyses. A composite sample of the clay-silt fraction was collected for analysis of particle-size distribution and Hg_T in a 1-L, plastic bottle, which was chilled. After subsampling was complete, all buckets and subsamples were weighed and the excess volume of the clay-silt fraction was discarded by decanting.

The residual sandy fraction that remained after decanting was recombined with the gravel fraction (more than 2 mm) and sent to Cal Sierra Development Incorporated for standard sieve analysis of particle-size distribution of particles at least 0.075 mm. The heavy mineral fraction was separated from the sample using a conventional screen with openings less than 2 mm, then concentrated using a gravity shaker table. The concentrated heavy-mineral fraction was air-dried and weighed. For each interval, visible gold and gold-amalgam grains were separated from the heavy metal fraction by panning and were hand picked with the aid of a microscope.

Heavy-mineral concentrates and gold analysis were processed and calculated by Cal Sierra Development Incorporated. The heavy-mineral concentrates were dried and sieved by USGS personnel using the following screen sizes: 1 mm, 0.5 mm, 0.25 mm, and 0.063 mm. Individual grains of gold and gold-amalgam were hand selected using a stereo binocular microscope and subsequently mounted for examination using the USGS scanning electron microscope (SEM) and energy dispersive X-ray (EDX) analyzer in Menlo Park, Calif. Relatively large visible grains of gold were observed during drilling in holes DPD-1 and DPD-5, which correlates with the higher gold *tenor* and visual gold particles observed in concentrates from these locations.

The residual sandy fraction from 15 intervals in holes DPD-4, -5, and -6 was sieved for additional analysis of Hg_T as a function of grain size. These samples were separated by sieving into six size-bins (also referred to as particle-size subclasses) using screens with the following sieve sizes: 2,000, 500, 297, 149, 60, and 30 μm (micrometer). Material from 500 to 2,000 μm (2 mm) is referred to as coarse sand; material between 297 and 500 μm is considered to be medium sand; 149 to 297 μm is fine sand; and 60 to 149 μm is very

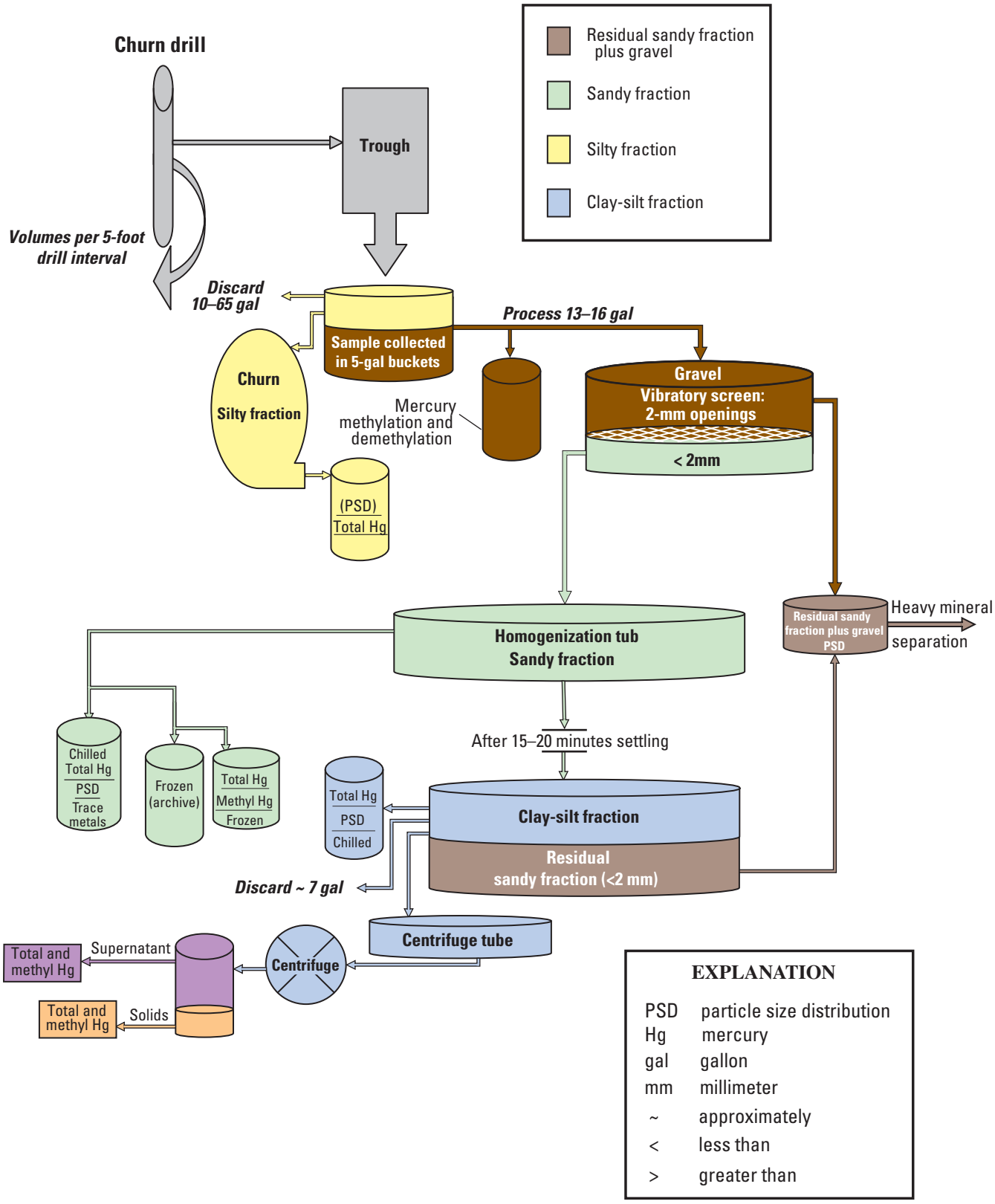

Figure 8. Flow-sheet showing drilling and processing of sample flow-stream.

fine sand. The material between 30 and 60 μm is referred to as coarse silt, and the material passing through the 30 μm-screen consists of medium and fine silt with clay.

Laboratory Methods

Particle-Size Distribution

The residual sandy fraction plus gravel was analyzed by Cal Sierra Development Incorporated. Particle size was evaluated for a suite of 31 samples representing individual drilled intervals. The samples were separated into 10 size fractions using screens with the following sieve sizes: 75, 50, 25, 4.75, 2.36, 1.18, 0.60, 0.30, 0.15 and 0.075 mm (*table B1*).

Particle-size distributions in the sandy, silty, and clay-silt fractions were determined by the USGS Cascades Volcanic Observatory (CVO) sediment laboratory in Vancouver, Washington. Conventional sieving was used to determine the size distribution of coarse material from 2 to 0.063 mm. The particle-size distribution of material smaller than 0.063 mm was determined using a SediGraph 5100 particle-size analyzer. The particle-size distributions determined by the SediGraph for these subsamples are described as 14 size fractions ranging from 0.063 mm to 0.00025 mm (equal to 0.25 μm). The results of sieving and using the Sedigraph were combined to make a single distribution of particle sizes for each subsampled fraction (*tables B2*, *B3*, and *B4*).

Heavy Mineral Concentration and Grain-Size Separation

Cal Sierra Development Incorporated used a gravity shaker-table to separate heavy mineral concentrates from the bulk-sediment samples. Individual gold and gold-amalgam grains were counted and a gold tenor was calculated based on the initial volume of the sample. Concentrates of the heavy minerals were returned to the USGS for further analysis. The heavy mineral concentrates were air-dried, weighed, and sieved using the following screen sizes: 1 mm, 0.5 mm, 0.25 mm, and 0.063 mm. Particle-size separates were weighed and compared to original weights to determine a percentage distribution (*table C1*). Individual grains of gold and gold-amalgam were hand-selected using a stereo binocular microscope and subsequently were mounted for examination by SEM and EDX. Mineral grains were identified by morphology, and their overall abundance was visually estimated (*table C2*).

Analysis of Mercury and Methylmercury

Analysis of Hg_T in the silty fraction, the clay-silt fraction, and the six sieved, fine particle-size bins was by the USGS National Research Program laboratory in Boulder, Colorado, using cold-vapor atomic fluorescence spectroscopy (CVAFS) without amalgamation. Complete digestion of sediment samples was done in a microwave oven using HCl-HNO_3-HF in Teflon containers. Approximately 100 mg of dry material was used for each digestion. Additional details regarding the analytical method and related quality-assurance procedures are described by Alpers and others (2000).

Analysis of Hg_T and MeHg in the sandy fraction and the clay-silt fraction (centrifuge tubes) was done at the USGS Wisconsin District Mercury Laboratory (WDML) in Middleton, Wisconsin, using CVAFS methods with double amalgamation. Methylmercury was isolated using ethylation-extraction methods described by Olson and DeWild (1999) and by DeWild and others (2002).

Prior to analysis, sediments were digested using HCl and HNO_3 at room temperature in Teflon containers. For MeHg analysis, solids (0.5 to 1.0 g) were placed into a centrifuge tube. Potassium bromide (KBr), copper sulfate ($CuSO_4$), and methylene chloride (CH_2Cl_2) were sequentially added. The mixture was allowed to react for an hour and then was shaken for an hour to ensure complete extraction of the MeHg. Following shaking, the samples were centrifuged to break any emulsion that had formed. An aliquot of the CH_2Cl_2 was cleanly transferred to a vial containing reagent water. These vials were placed in a heating block until all CH_2Cl_2 evaporated and the MeHg was back-extracted into the reagent water. The pH of the extractant was adjusted to 4.9 (to maximize ethylation potential) using acetate buffer. The extractant then was ethylated using sodium tetraethyl borate ($NaBEt_4$) and allowed to react for 15 minutes. After reaction with $NaBEt_4$, the extractant was purged with nitrogen gas (N_2) for 20 minutes and the ethylated Hg species were collected on a sample trap containing Carbotrap. These ethylated Hg species were desorbed thermally from the sample trap, separated using a gas chromatographic (GC) column, reduced using a pyrolytic column, and detected using a cold vapor atomic fluorescence spectrometry (CVAFS) detector.

Analysis of Trace Elements and Major Elements

Analysis of trace elements and major elements in sediment samples was done by the USGS research laboratory in Boulder, Colorado, using inductively coupled plasma (ICP) methods. Samples were digested with strong acids in Teflon containers in a similar manner to the Hg_T analyses. Trace elements other than mercury were analyzed by ICP-Mass Spectrometry (ICP-MS); major elements (Ca, Mg, Na, K, Si, Fe, and Mn) were analyzed by ICP-Atomic Emission Spectroscopy (ICP-AES). Additional details regarding analytical procedures are described by Alpers and others (2000) and Taylor (2001).

Mercury Methylation and Demethylation Potentials

Mercury methylation and demethylation rate potentials were analyzed for seven samples collected from drill-holes DPD-1, -3, -5 and -6. Two depth intervals (shallow and deep) were sampled from three of the four drill holes; only a deep interval was sampled from hole DPD-6. Sediment from each

analyzed section was transferred to a acid-cleaned, plastic 5-gallon bucket. A screen with 2-mm openings was used to collect a subsample, which was transferred to an acid-cleaned, glass mason jar; the jar was filled completely with sediment to minimize atmospheric oxygen. Upon collection, samples were stored temporarily on wet ice until refrigerated (5 °C). Storage time was 3–16 days before subsampling at the USGS laboratory in Menlo Park, California. Physical descriptions of each sediment sample along with the collection date, location, and estimated in-place sediment temperature at the time of collection were tabulated (*table A2*).

All subsample processing for microbial assays and ancillary sediment characterization was done in a glove bag flushed with nitrogen gas (N_2) to maintain anaerobic conditions. Sediment from each subsampled interval was transferred to a clean zip-lock bag and manually homogenized. Subsamples for each process or analyte were taken from the homogenized sample using acid-cleaned, stainless-steel tools. The sediment was weighed (± 0.1 g precision) and placed into the appropriate containers.

Standard radiotracers were used to measure potential rates of both MeHg production (Hg(II) methylation) and MeHg degradation (demethylation) (Marvin-DiPasquale and others, 2003). An amendment containing 1.5 μCi/100 μL of radio-labeled divalent mercury (^{203}Hg(II)), with a half-life of 46.5 days, was used per 3.0-g sediment sample for the MeHg-production rate assay. The ^{203}Hg(II) specific activity of the injection solution was 1.15 mCi/mg, which resulted in a total Hg(II) amendment of 436 ng/g wet sediment. Mercury demethylation rates were determined by amending separate subsamples with MeHg tagged with radio-labeled carbon (^{14}C-MeHg or $^{14}CH_3HgCl$) at a concentration of 9.4 nCi/100 μL, resulting in total MeHg additions (as Hg) of 10.5 ng/g wet sediment. Sample sets for each interval tested for both microbial Hg(II)-methylation (MeHg production) and demethylation (MeHg degradation) assays consisted of duplicate, live (incubated) samples and one control sample killed by flash freezing at the beginning of the experiment (time zero). Both MeHg production and degradation sample sets were incubated simultaneously for 4 hours at 19 °C. It is assumed that both Hg-transformation processes are first-order for the purposes of calculating potential rates (Marvin-DiPasquale and others, 2003). Potential rates are subsequently calculated as the product of the radiotracer-derived rate constant and the final concentration of radiotracer amendment in the whole sediment, and are thus independent of the amount of original Hg(II) or MeHg that might have been present in each sample.

Each of the seven sediment depth intervals was subsampled for several ancillary chemical parameters, including, pH, oxidation-reduction (redox) potential, loss-on-ignition, acid volatile sulfide, and total reduced sulfur. The pH and oxidation-reduction (redox) potential were determined by inserting an electrode directly into sediment. Organic content was measured by weight loss on ignition (American Public Health Association, 1981). Two forms of sulfur—acid volatile sulfur and total reduced sulfur—were determined using methods described by Ulrich and others (1997). Organic content and both forms of solid-phase sulfur were measured in duplicate samples from each sediment depth interval.

Dissolved organic carbon (DOC) concentrations were assessed by adding deionized water (Milli-Q, 10 mL) to the sediment (10 g) to obtain enough pore water for analysis. The exact weight of the sediment and the water added per tube was recorded, and subsequent pore-water analyte concentrations were calculated taking this pore-water dilution into account. Samples were shaken until they became a homogenous slurry, which was then centrifuged (3,000 rpm for 15 minutes) in 45-cm^3 polystyrene, screw-cap tubes. The resulting supernatant was filtered (0.45-μm nylon syringe, in-line filter) inside an O_2-free glove bag. The DOC samples were frozen until analysis, which was done using high-temperature oxidation with infrared detection (Qian and Mopper, 1996).

Quality Assurance and Quality Control

Particle-Size Distribution

The SediGraph 5100 Particle Size Analyzer determines particle size by the highly accurate and reproducible X-ray sedimentation method which measures the gravity-induced settling rates of different size particles in a liquid having known properties. The SediGraph instrument at CVO is calibrated daily using garnet reference material and analysis conditions recommended by the manufacturer. Each sample processed through the SediGraph system was analyzed in duplicate. Comparison of the two analyses should indicate agreement within 10 percent for each size class. If this criterion was not met, then the system was checked for malfunctions and the sample was re-analyzed a third time. If the disagreement persisted, the sample was removed and the equipment was thoroughly cleaned and inspected, and a calibration check was done before further analysis. All final results satisfied the quality-assurance criterion.

Mercury, Methylmercury, and Trace Elements

The reliability of field and laboratory methods used for characterization of mercury, methylmercury, and trace element concentrations in this study was assessed by analyzing blank, spiked, and replicate samples collected or prepared during environmental sampling. In addition, standard reference materials (SRM) were analyzed routinely with each batch of environmental samples at each laboratory. Detailed results are provided for replicates, blanks, spikes, and SRMs for the USGS laboratories in Boulder, Colorado, and Middleton, Wisconsin (*tables D2-8*). In general, the blanks and spike recoveries for Hg_T, MeHg, and trace elements were within acceptable ranges for these analytes. Also, analyses of SRMs for Hg_T, MeHg, and trace elements were within acceptable ranges at both USGS laboratories.

The sample of Yuba River water collected during drilling of hole DPD-5 had very low concentrations of Hg_T in both

filtered and unfiltered splits; concentrations of Hg_T were less than 1.2 ng/L (*table D1*). Concentrations of MeHg in the Yuba River water were below the method detection limit (<0.04 ng/L) in both filtered and unfiltered splits. This indicates that the injection of water during drilling likely had a negligible chemical effect on concentrations of Hg_T and MeHg in the sediment samples that were recovered.

Possible contamination of environmental samples at all steps in the procedures, including collection and processing through laboratory analysis, was evaluated by analyzing field blanks consisting of deonized (Milli-Q) water. After cleaning the sampling equipment in the field, deionized water was put in contact with the sampling and sample-processing equipment and then poured into sample bottles and preserved in a manner identical to that for the environmental samples. Four unfiltered equipment blanks and one filtered process blank were taken after the drilling of hole DPD-6 (*table D2*). In general, the field blank mercury concentrations were less than 2.5 ng/L, indicating no significant mercury contamination.

Total mercury concentration in laboratory blanks analyzed by the USGS laboratory in Boulder, Colorado, ranged from 0.2 to 1.2 ng/L (*table D3*). A spike experiment consisting of an addition of 5 ng/L to a laboratory blank gave a Hg_T concentration of 5.14 ng/L, a recovery of 103 percent, which is well within the acceptable range.

Three different standard reference water samples (SRWS) for Hg_T were analyzed by the Boulder, Colorado laboratory, as summarized in *table D3*. Based on a total of 25 to 32 observations of each SRWS, the analyzed concentrations were consistently within the standard deviation of most probable values. The standard reference material Buffalo River Sediment 2704 (National Institute of Standards and Technology) was digested six times (*table D4*). Averaged results for all trace elements of primary interest (As, Cd, Cr, Cu, Ni, Pb, Sb, and Zn) agreed with concentrations certified within the published standard deviations. Digestion blanks for trace elements and major elements (*table D5*) generally contained an insignificant amount of trace elements of primary interest, with minor exceptions. Three separate spike recovery experiments for selected elements (As, Ca, Cd, Cu, Fe, Mg, Pb, and Zn) were consistently in the acceptable range of 92 to 112 percent (*table D6*).

The standard reference material for MeHg used by the USGS laboratory in Middleton, Wisconsin, was IAEA-405, a polluted marine sediment provided by the International Atomic Energy Agency. The certified concentration of MeHg in IAEA-405 is 5.49 ng/g (dry weight), with a 95 percent confidence interval from 4.96 to 6.02 ng/g. The certified value was determined using a distillation procedure that has been shown to form significant amounts of artifact MeHg when the MeHg fraction is less than 1 percent of the inorganic pool (Hintelmann and others, 1997; Hintelmann, 1999), which is true for IAEA-405. Using the same extraction method for MeHg determination that was used in this study, multiple analyses (19) by the USGS Wisconsin laboratory resulted in a 76 percent recovery of the SRM literature value. Because the certified value may be biased high and multiple analyses from the USGS laboratory produced a consistently lower value, the accepted range of recovery for this standard has been established at 55 to 95 percent. During the analysis of MeHg in samples for the present study, four analyses of IAEA-405 gave concentrations of 4.21, 4.50, 4.85, and 5.20 ng/g (dry weight), which correspond to recoveries ranging from 76.7 to 94.7 percent, within the accepted range of recovery for the laboratory.

Two types of replicate sediment subsamples were analyzed: (1) replicate subsamples digested separately (field replicates) and (2) replicate subsamples from a single digestion (laboratory replicates). Varied results of analyses of field replicates indicate sample inhomogeneity or inconsistent sampling technique, whereas the comparison of laboratory replicates indicates variability in analytical results. A measure of variability between replicate samples is the Relative Percent Difference (RPD), defined as the absolute value of the quotient of the difference between two values and their average:

$$RPD = |(r1-r2)/[(r1+r2)/2]|,$$

where r1 and r2 are the replicate analyses. Acceptability of values of RPD depends on several factors, including proximity to the method detection limit (MDL) and natural heterogeneity factors. For most constituents in concentrations well above the MDL, RPD values less than 15–25 percent are expected, whereas larger RPD values are expected for concentrations near the MDL. Field replicates of unprocessed samples may have larger RPD values than laboratory replicates of processed (filtered or digested) samples because of a greater degree of inhomogeneity in unprocessed samples.

Results for three pairs of field replicate samples analyzed for trace and major elements by the USGS research laboratory in Boulder, Colorado, are compared (*table D7*). Values of RPD for the principal trace elements of interest (As, Cd, Cr, Cu, Ni, Pb, Sb, and Zn) were consistently less than 11 percent for at least two of the three replicate pairs.

Results of replicate subsamples analyzed by the USGS Wisconsin District Laboratory are compared (*table D8*). Values of RPD for four laboratory replicates of Hg_T in the clay-silt fraction range from 1.7 percent to 38.1 percent, with a geometric mean of 8.4 percent; RPD values for four laboratory replicates of Hg_T in the sandy fraction range from 1.1 percent to about 30 percent, with a geometric mean of 4.5 percent. Two field replicate samples of the clay-silt fraction and one field replicate of the sandy fraction were collected. Values of RPD for Hg_T in the field replicates of the clay-silt fraction range from 1.3 to 5.9 percent; the RPD value for the sandy fraction is 43.6 percent, indicating a high degree of inhomogeneity. Such

inhomogeneity of mercury distribution in coarser material is an expected manifestation of the "*nugget effect*," because of the nonuniform distribution of gold-mercury amalgam grains and mercury-stained gold grains. At least one analysis of each of the sediment samples chosen for replicate analysis of MeHg was below the MDL, so it was not possible to calculate RPD values. A high degree of variability is typical for constituents near the MDL.

Results

Particle-Size Distribution

Several sediment fractions from each drilled interval were analyzed for particle-size distribution. Detailed particle-size analysis of the following sediment fractions was done: (1) residual sandy fraction plus gravel, (2) sandy fraction, (3) silty fraction, and (4) clay-silt fraction.

Residual Sandy Fraction Plus Gravel

The particle-size distributions of the residual sandy fraction plus gravel from the 31 drilled intervals varied moderately between drill-hole locations (*fig. 9*). The most abundant size classes were sand (defined in *table 2* as 0.075 to 4.75 mm) and gravel (>4.75 mm), as summarized in *table 2*. Gravel concentration varied from 2 to 85 weight percent and generally decreased with depth in all drill holes except for DPD-2, where gravel concentration increased with depth to about 25 feet, followed by a sharp decrease at 35 feet. There was a moderate increase of gravel from 15 to 30 feet in hole DPD-6. The increase in the 5- to 10-foot and 15- to 20-foot intervals in hole DPD-5 was probably due to fragments of weathered bedrock that were broken during drilling. Sand concentration varied from 14 to 82 weight percent and generally increased with depth in holes DPD-1, -2, -3, and -4. Sand decreased with depth in drill-hole DPD-6. Drill-hole DPD-5 had two distinct sand lenses between 0 and 10 feet and 10 and 20 feet. Silt and clay (<0.075 mm) concentrations varied from 1 to 29 weight percent and generally increased with depth in holes DPD-1, -3, and -4 and generally decreased with depth in hole DPD-6. In hole DPD-5, the silt and clay correlate with the sand lenses. Hole DPD-2 showed a decrease in silt and clay proportions down to 25 feet and an increase in the 25- to 35-foot interval.

Sandy Fraction

The sandy fraction (consisting of a slurry of sand, silt, and clay) was homogenized in a plastic tub after being sieved through the 2-mm vibratory screen. Sand was the most dominant size class in this fraction, as shown in *table 3* and *figure 10*. The concentration of sand (defined as 0.063 to 2 mm) in this fraction ranged from about 65 to 98 percent, concentration of silt (0.004 to 0.063 mm) ranged from about 2 to 32 percent, and the concentration of clay (<0.004 mm) ranged from about 0.1 to 3.4 percent.

Silty Fraction

The silty fraction (material in suspension in the slurry collected as overflow from the collection buckets and composited in a churn at the drill site, *fig. 8*) consisted mostly of silt and clay with minor amounts of fine sand (*table 4*, *fig. 10*). Particle-size distributions ranged from about 0.2 to 11 percent sand, 7 to 61 percent silt, and 35 to 91 percent clay.

To quantify losses of sediment (and mercury) from the suspended silty overflow fraction, a set of 22 samples were analyzed for total sediment concentration and 16 selected sample intervals were analyzed for distribution of particle sizes 2 mm through 0.00025 mm. The 16 selected samples ranged from about 20 to 73 percent silt and from about 27 to 80 percent clay. Total suspended sediment concentrations in the silty fraction samples ranged from about 2,400 mg/L to 254,000 mg/L (*table B5*).

Clay-Silt Fraction

The clay-silt fraction consisted of silt- and clay-sized particles that passed through the 2-mm vibratory screen separation and remained in suspension after settling for 15 to 20 minutes (*fig. 8*). There was a high concentration of clay-sized particles relative to silt in this fraction (*table 5*). The silt (0.004 to 0.063 mm) concentration in this fraction ranged from about 9 to 70 percent. Clay (<0.004 mm) concentration in this fraction ranged from about 26 to 91 percent. Sand (>0.063 mm) in this fraction constituted less than 1 percent except in the 25- to 30-foot depth intervals in drill-holes DPD-2 and 6, which had about 29 and 18 percent sand, respectively, and in the 30- to 35-foot interval of DPD-2, which had 5 percent. Higher concentrations of silt and clay in some intervals are probably due to the breaking up of large masses of clay during separation with the vibratory screen.

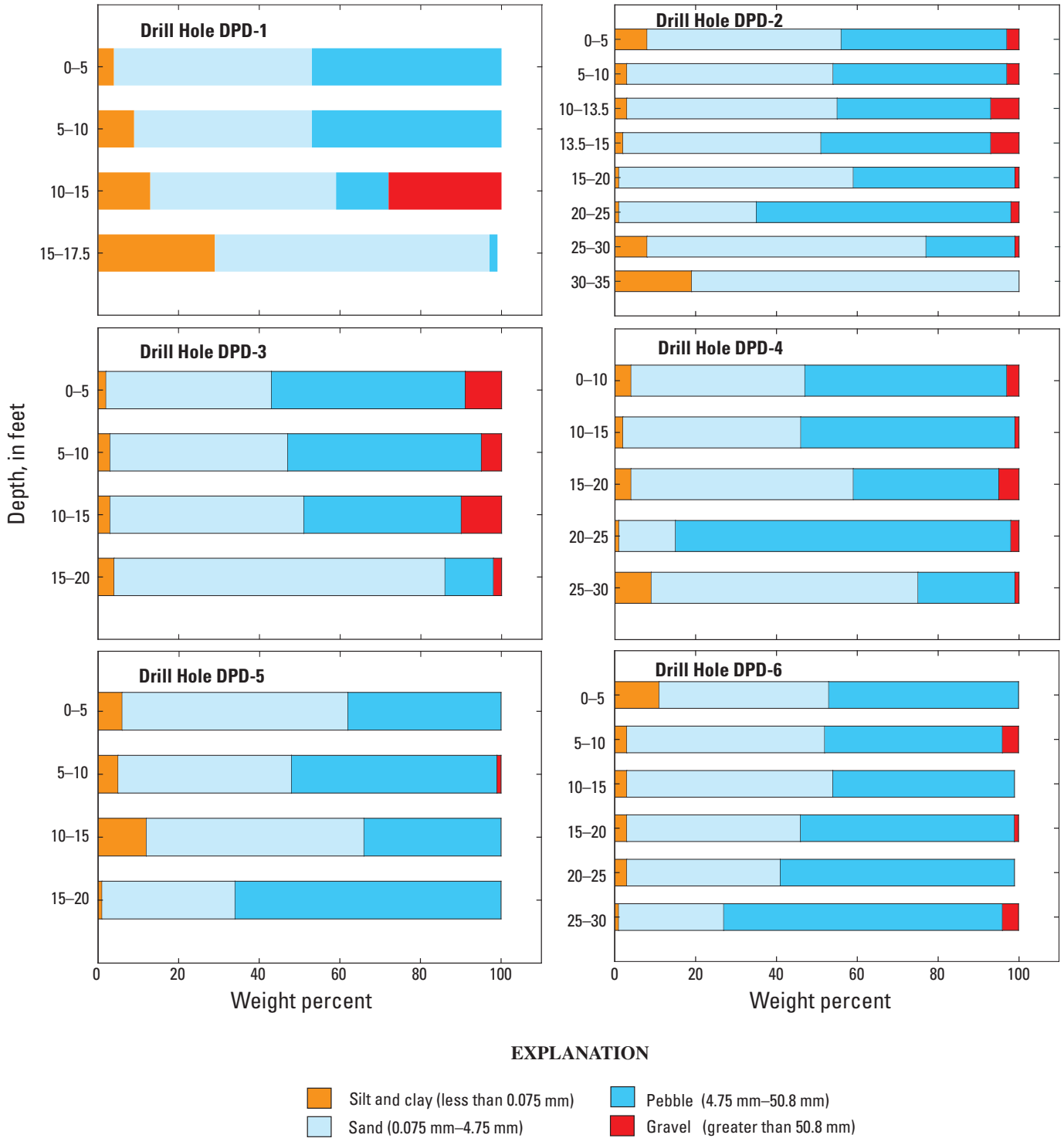

Figure 9. Bar chart diagram showing particle-size distribution of residual sandy fraction plus gravel at each drill hole, Daguerre Point Dam, California.
mm, millimeter.

Table 2. Particle-size distribution and depth profiles of the residual sandy fraction plus gravel, Daguerre Point Dam, California.

[DPD, Daguerre Point Dam. ft, foot; mm, millimeter. >, greater than; <, less than]

Drill hole/Depth (ft)	Silt and clay	Sand	Gravel
Size (mm)	< 0.075	0.075 – 4.75	> 4.75
	Weight percent		
	DPD–1		
0–5	4	49	47
5–10	9	44	47
10–15	13	46	41
15–17.5	29	68	2
	DPD–2		
0–5	8	48	44
5–10	3	51	46
10–13.5	3	53	45
13.5–15	2	49	49
15–20	1	58	41
20–25	1	34	65
25–30	8	69	23
30–35	19	81	0
	DPD–3		
0–5	2	41	57
5–10	3	44	53
10–15	2	48	49
15–20	4	82	14
	DPD–4		
0–10	4	43	53
10–15	2	44	54
15–20	4	55	41
20–25	1	14	85
25–30	9	66	25
	DPD–5		
0–5	6	56	38
5–10	5	43	52
10–15	12	54	34
15–20	1	33	66
	DPD–6		
0–5	11	42	47
5–10	3	49	48
10–15	3	51	45
15–20	3	43	54
20–25	3	38	58
25–30	1	26	73

Table 3. Particle-size distribution and depth profiles of the sandy fraction, Daguerre Point Dam, California.

[DPD, Daguerre Point Dam. ft, foot; mm, millimeter. <, less than]

Drill hole/Depth (ft)	Clay	Silt	Sand
Size (mm)	<0.004	0.004 – 0.063	0.063 – 2
	Weight percent		
	DPD–1		
0–5	0	14	86
5–10	0	18	82
10–15	1	27	72
15–17.5	4	32	64
	DPD–2		
0–5	0	8	92
5–10	0	6	94
10–13.5	0	4	96
13.5–15	0	5	95
15–20	0	3	97
25–30	0	6	94
30–35	1	26	73
	DPD–3		
0–5	0	4	96
5–10	0	6	94
10–15	0	7	93
15–20	.2	8.5	91.3
	DPD–4		
0–10	0	3	97
10–15	0	2	98
15–20	0	4	96
20–25	0	4	96
25–30	0	8	92
	DPD–5		
0–5	0	6	94
5–10	0	6	94
10–15	0	8	92
15–20	0	5	95
	DPD–6		
0–5	0	9	91
5–10	0	6	94
10–15	0	3	97
15–20	0	8	92
20–25	0	11	89
25–30	1	13	86

Synthesis and Spatial Distribution

Some of the sandiest sediments were found in the deepest sections of the drill holes (*table 2*). Sand exceeded 80 percent in the deepest intervals of DPD-2 and DPD-3 and almost 70 percent in the deepest intervals of DPD-1 and DPD-4. A total silt and clay content of about 19 percent was measured in the lowest interval of sediment from DPD-2. The high sand and silt value for the lowest depth interval of hole DPD-2 may actually be due to sediment stratification from previous dredging operations. The highest silt and clay content, 29 percent, was measured in the deepest interval of hole DPD-1 (15- to 17.5-foot depth) and is probably due to decomposed bedrock. This site was located closest to the Daguerre Point Dam.

Overall ranges in particle-size distribution for the residual sandy fraction plus gravel and the sandy, silty, and clay-silt fractions from 0.00025 to 50.8 mm are compared on a semi-log plot (*fig. 11*). There is a clear separation in the size distributions between the two coarse fractions (residual sandy fraction

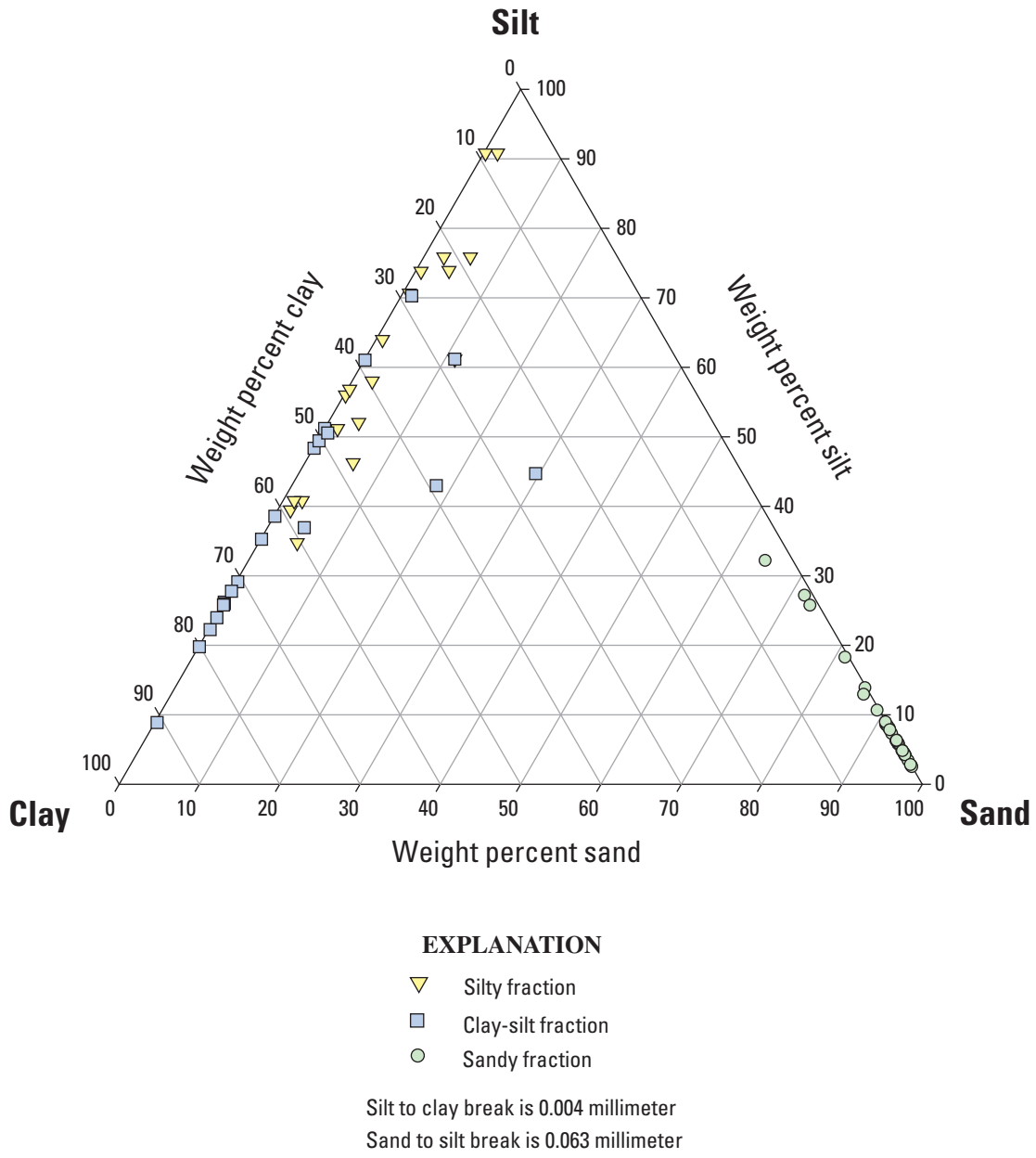

Figure 10. Ternary diagram showing particle-size classes of sandy fraction, silty fraction, and clay-silt fraction, Daguerre Point Dam, California.

Table 4. Particle-size distribution and depth profiles of the silty fraction, Daguerre Point Dam, California.

[DPD, Daguerre Point Dam. ft, foot; mm, millimeter. >, greater than; <, less than]

Drill hole/Depth (ft)	Clay	Silt	Sand
Size (mm)	<0.004	0.004 – 0.063	>0.063
	Weight percent		
DPD-2			
0–5	56	44	0
5–10	57	43	0
15–20	64	35	1
20–25	58	40	2
25–30	35	60	5
30–35	40	59	1
DPD-3			
15–20	91	7	2
DPD-4			
10–15	52	44	4
15–20	46	48	6
DPD-5			
0–5	90	10	0
5–10	74	25	1
10–15	41	57	2
15–20	76	22	2
DPD-6			
0–5	41	58	1
5–10	76	18	6
10–15	74	22	4
15–20	71	28	1
20–25	51	47	2
25–30	61	28	11

Table 5. Particle-size distribution and depth profiles of the clay-silt fraction, Daguerre Point Dam, California.

[DPD, Daguerre Point Dam. ft, foot; mm, millimeter. >, greater than; <, less than]

Drill hole/Depth (ft)	Clay	Silt	Sand
Size (mm)	<0.004	0.004 – 0.063	>0.063
	Weight percent		
DPD-2			
20–25	90	9	1
25–30	26	45	29
30–35	58	37	5
DPD-3			
0–5	91	9	0
5–10	78	22	0
10–15	74	26	0
15–20	28	70	1
DPD-4			
10–15	76	24	0
15–20	74	26	0
20–25	74	26	0
25–30	71	29	0
DPD-5			
0–5	49	51	0
5–10	80	20	0
10–15	72	28	0
15–20	61	39	0
DPD-6			
0–5	39	61	0
5–10	52	48	0
10–15	65	35	0
15–20	50	49	1
20–25	49	51	0
25–30	39	43	18

plus gravel and sandy fraction) and the two fine fractions (silty and clay-silt fractions), which represent the suspended material at two places in the sample-processing stream (*fig. 8*). The residual sandy fraction plus gravel (brown in *fig. 11*) shows the widest range of distributions. The sandy fraction (green in *figure 11*) fits mostly within the range of distributions of the residual sandy fraction plus gravel. The clay-silt fraction (blue in *figure 11*) contains some particles of fine and very fine sand that did not settle during the 15 to 20 minute period. The silty fraction (yellow in *figure 11*) contains the highest proportion of clay-sized particles and fits well within the range of distributions of the clay-silt fraction, which also includes a high proportion of suspended clay-sized particles.

Mercury Geochemistry

There is a high degree of spatial variability in mercury concentrations for each of the different particle-size fractions. Total mercury concentrations generally increase with depth in holes DPD-2, -3, and -6 in all particle-size fractions; the variations with depth are less systematic in the other three holes (*fig. 12*). Total mercury concentrations generally increase as sediment decreases in grain-size (*fig. 13*). Mercury concentrations in the sandy fraction are consistently lower than the concentrations in the other, finer-grained fractions by a factor of between about 3 and 30 (*fig. 12*). Total mercury concentrations in the sandy fraction ranged from 6.8 ng/g to 80.7 ng/g dry weight (*table 6*). Total mercury concentrations in the silty fraction ranged from 33 to 1,100 ng/g (*table 7*). Total mercury concentrations

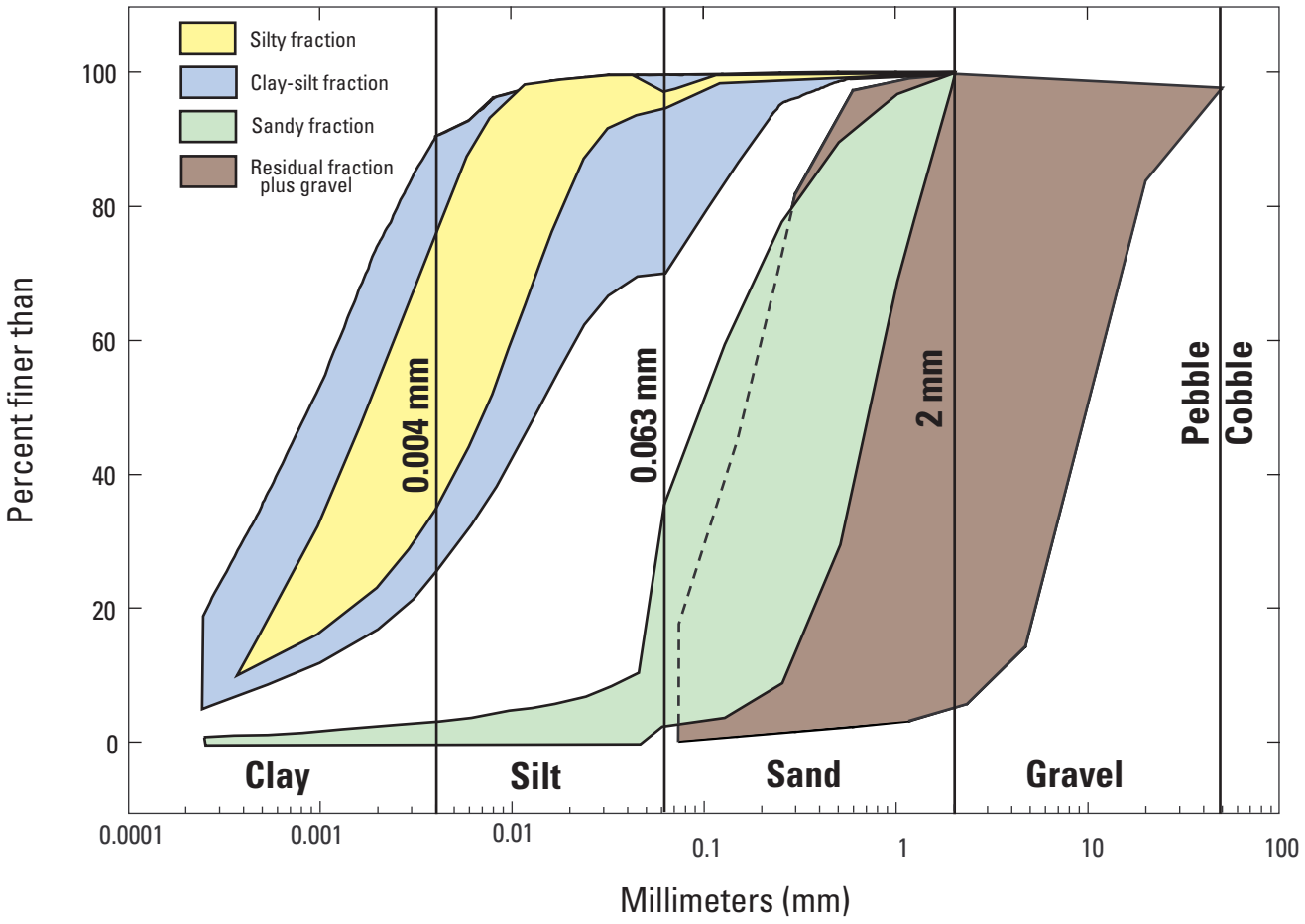

Figure 11. Graph showing summary of particle-size distributions, Daguerre Point Dam, California.

in the clay-silt fraction ranged from 23 to 370 ng/g (*table 7*). Concentrations of Hg_T in the centrifuge tube solids (wet weight) ranged from 0.3 to about 320 ng/g (*table 8*). (Note that centrifuge solids are reported only on a wet weight basis because limited material precluded accurate determination of water content.)

Fifteen subsamples of the sandy fraction were separated by sieving into six sediment bins (particle-size subclasses) to evaluate the effect of particle size on Hg_T concentration. Median values for mercury concentration increased sharply as the size decreased (*table 9*). The median values in the sand subclasses ranged from 1.9 ng/g in coarse sand (dry weight for all values), to 4.4 ng/g in medium sand, to 8.6 and 7.5 ng/g in fine and very fine sand, respectively. In sharp contrast, the median value for coarse silt was 21.6 ng/g, and for the finest size subclass (less than 30 µm [0.030 mm], containing medium silt, fine silt, and clay), the median concentration was 43.3 ng/g. As indicated in *figures 12* and *13* and in *tables 6-8*, the Hg_T concentration in the sandy fraction is consistently lower than that in the silty and clay-silt fractions from the same depth interval. If it is assumed that separation into various size fractions did not change the fundamental chemical properties of the sediment with regard to the concentration of mercury, it can be inferred that the fine silt (~0.004 to ~0.015 mm) and clay (less than about 0.004 mm) size fractions must contain, on the average, higher mercury concentrations than the two finest subclasses represented in *table 9*. Physical separation of the fine silt and clay particle size classes followed by mercury analysis would be the preferred manner to test this assertion; ultra-clean methods for doing such separations are currently being researched by the USGS.

Methylmercury (MeHg) concentrations were determined in two fractions: the sandy fraction and the clay-silt fraction solids isolated by centrifugation (*fig. 8*). In the sandy fraction, concentrations of MeHg were less than the MDL of 0.001 ng/g in all but one of 31 sampled intervals; the 0- to 5-foot interval of hole DPD-5 had a MeHg concentration of 0.083 ng/g (*table 6*). MeHg concentrations were above the MDL in about half of clay-silt fraction solids; where detected, the concentration of MeHg ranged from 0.04 (estimated) to 0.61 ng/g, wet weight

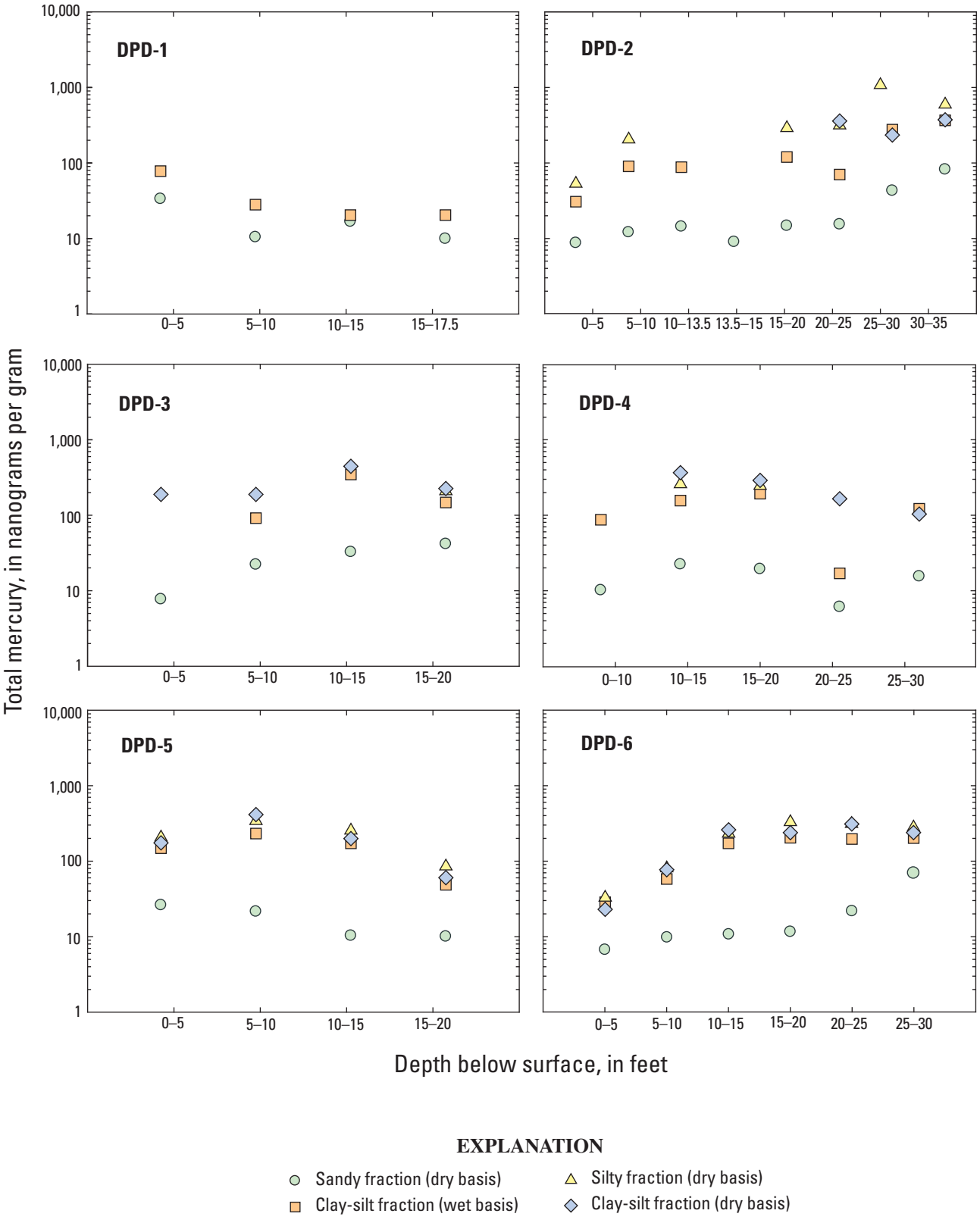

Figure 12. Graph showing down-hole concentration of total mercury in different sediment fractions, Daguerre Point Dam, California.

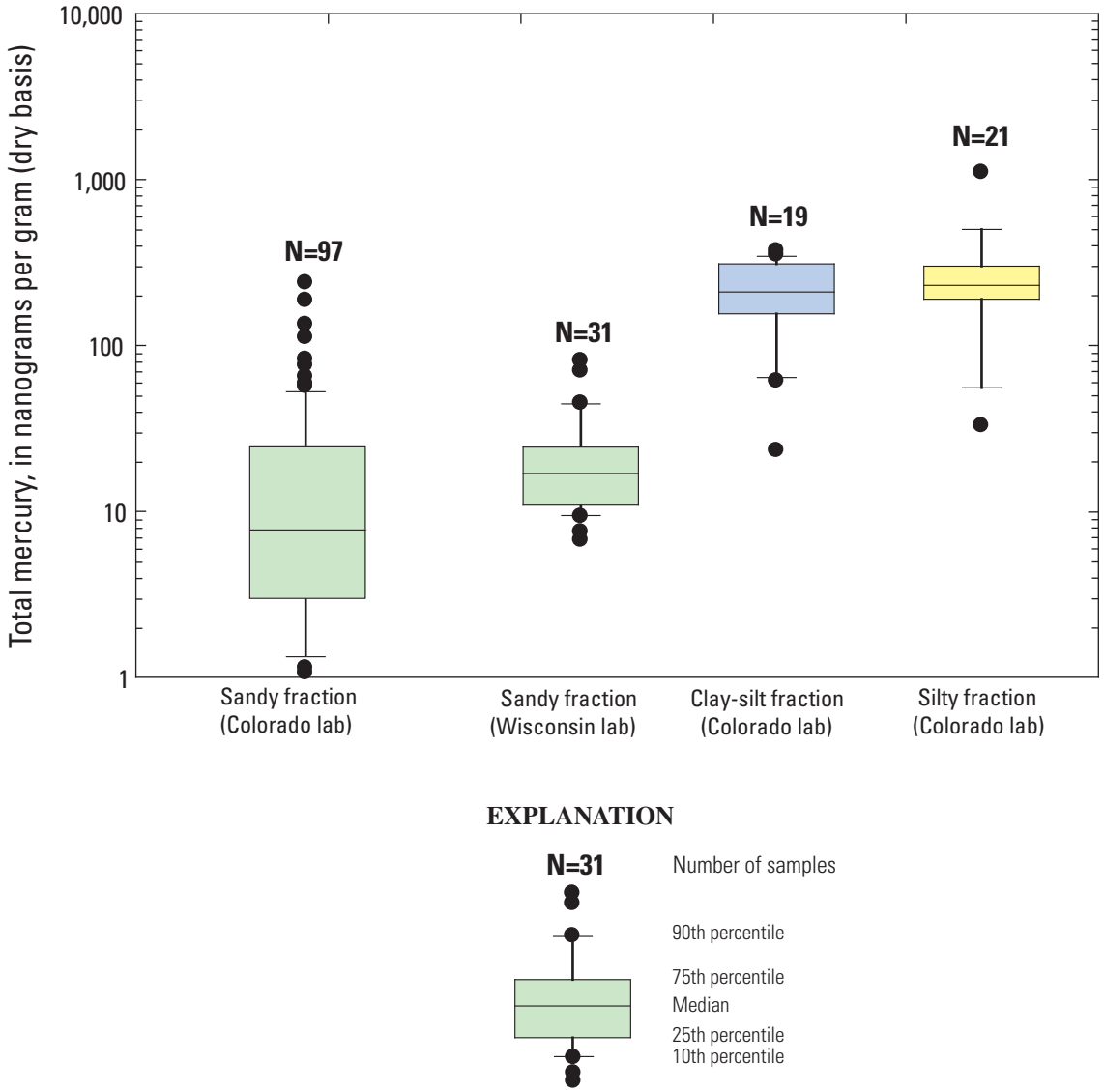

Figure 13. Graph showing boxplots of total mercury concentration in different sediment fractions, Daguerre Point Dam, California.

(*table 8*). Detection limits were higher for the clay-silt fraction solids because the samples collected in 30-mL Teflon™ centrifuge tubes were small, and less solid material was available for digestion. Seven of the 16 sample intervals with detectable MeHg had MeHg concentrations greater than 0.1 ng/g; these intervals were from five separate drill holes: DPD-1, -2, -3, -4, and -5. Drill-hole DPD-3 was the only hole in which MeHg was detected in samples from all depth intervals. A large degree of heterogeneity with regard to MeHg concentrations was observed in the study area.

The relation between concentrations of MeHg and Hg_T in the silt-clay fraction solids was plotted to identify drilled intervals having relatively high concentrations of MeHg (*fig. 14*). In *figure 14*, the diagonal lines represent constant values of the ratio of MeHg to Hg_T. Samples for which MeHg concentrations were below detection are plotted at half of the MDL for MeHg with an error bar representing the possible range of MeHg concentrations from zero to the MDL (zero values do not exist on logarithmic axes). The maximum possible values of MeHg/Hg_T for these samples can be seen in *figure 14*. Four

Table 6. Total mercury and methylmercury concentrations in the sandy fraction, Daguerre Point Dam, California.

[DPD, Daguerre Point Dam; ft, foot; ng/g wet, nanogram per gram wet weight; ng/g dry, nanogram per gram dry weight; LTD, less than detection limit]

Drill hole/Depth (ft)	Date	Time	Methylmercury		Total mercury	
			Concentration (ng/g wet)	Detection limit (ng/g wet)	Concentration (ng/g wet)	Concentration (ng/g dry)
DPD–1						
0–5	8/14/01	1100	LTD	0.001	26.7	32.9
5–10	8/14/01	1800	LTD	.001	9.2	11.4
10–15	8/14/01	1430	LTD	.001	14.5	17.5
15–17.5	8/14/01	1500	LTD	.001	7.3	10.9
DPD–2						
0–5	8/15/01	1200	LTD	0.001	8.3	10.1
5–10	8/15/01	1400	LTD	.001	11.5	14.1
10–13.5	8/15/01	1600	LTD	.001	13.2	16.5
13.5–15	8/15/01	1030	LTD	.001	8.8	10.8
15–20	8/16/01	1200	LTD	.001	18.2	20.6
20–25	8/16/01	1330	LTD	.001	16.9	20.3
25–30	8/16/01	1500	LTD	.001	34.4	44.9
30–35	8/16/01	1700	LTD	.001	60.5	80.7
DPD–3						
0–5	8/20/01	1030	LTD	0.001	7.5	9.2
5–10	8/20/01	1100	LTD	.001	19.3	24.3
10–15	8/20/01	1330	LTD	.001	26.6	34.4
15–20	8/20/01	1500	LTD	.001	33.8	43.0
DPD–4						
0–10	8/21/01	1300	LTD	0.001	9.9	11.9
10–15	8/21/01	1530	LTD	.001	19.9	24.4
15–20	8/22/01	0900	LTD	.001	16.5	21.3
20–25	8/22/01	1100	LTD	.001	6.1	7.5
25–30	8/22/01	1230	LTD	.001	14.2	17.5
DPD–5						
0–5	8/24/01	1030	0.083	0.001	22.9	28.5
5–10	8/24/01	1130	LTD	.001	19.8	23.8
10–15	8/24/01	1430	LTD	.001	10.1	12.3
15–20	8/24/01	1530	LTD	.001	9.4	12.0
DPD–6						
0–5	8/27/01	1530	LTD	0.001	5.5	6.8
5–10	8/28/01	0930	LTD	.001	8.1	9.9
10–15	8/28/01	1130	LTD	.001	8.6	10.8
15–20	8/28/01	1330	LTD	.001	9.3	11.6
20–25	8/28/01	1430	LTD	.001	17.3	21.8
25–30	8/28/01	1530	LTD	.001	57.2	70.1

of the samples that have the highest concentrations of MeHg (from holes DPD-1, -2, -4, and -5) also have the highest values of $MeHg/Hg_T$, in the range of 0.2 to 0.5 percent. Another interval from hole DPD-4, which has relatively low concentrations of MeHg and Hg_T, has a value of $MeHg/Hg_T$ of about 0.2. All other intervals for which MeHg was detected have values of $MeHg/Hg_T$ between 0.01 and 0.1 percent.

The relation between Hg_T concentration (in clay-silt fraction solids from centrifugation) and gold concentration (in heavy mineral concentrates) is shown in *figure 15A*. The highest gold tenor values, greater than 100 mg/yd^3, were seen in three intervals from hole DPD-1; these intervals had low concentrations of mercury also (about 18 to 33 ng/g, wet weight; also see *table 8*). Six intervals had gold tenor values between 50 and 100 mg/yd^3; three of these samples were from hole DPD-5, the others were from DPD-2 and 4 (*table C1*). Mercury concentrations in these six intervals ranged from 33 to 207 ng/g (wet weight) (*table 8*). Gold tenor in other

Table 7. Mercury concentrations in the silty and clay-silt fractions from sample processing streams, Daguerre Point Dam, California.

[Samples analyzed by the U.S. Geological Survey laboratory in Boulder, Colo. DPD, Daguerre Point Dam. ft, foot; ng/g wet, nanogram per gram wet weight; ng/g dry, nanogram per gram dry weight; —, no data]

Drill hole/ Depth (ft)	Date	Time	Silty fraction (ng/g dry)	Clay-silt fraction (ng/g dry)
DPD–2				
0–5	8/15/01	1200	56	—
5–10	8/15/01	1400	190	—
10–13.5	8/15/01	1600	—	—
13.5–15	8/16/01	1030	—	—
15–20	8/16/01	1200	260	—
20–25	8/16/01	1330	280	310
25–30	8/16/01	1500	1,100	210
30–35	8/16/01	1700	500	320
DPD–3				
0–5	8/20/01	1030	—	170
5–10	8/20/01	1100	—	170
10–15	8/20/01	1330	—	370
15–20	8/20/01	1500	190	200
DPD–4				
0–10	8/21/01	1300	—	—
10–15	8/21/01	1530	230	310
15–20	8/22/01	0900	220	250
20–25	8/22/01	1100	—	150
25–30	8/22/01	1230	—	98
DPD–5				
0–5	8/24/01	1030	190	160
5–10	8/24/01	1130	300	350
10–15	8/24/01	1430	230	180
15–20	8/24/01	1530	85	61
DPD–6				
0–5	8/27/01	1530	33	23
5–10	8/28/01	0930	80	77
10–15	8/28/01	1130	230	260
15–20	8/28/01	1330	330	240
20–25	8/28/01	1430	310	310
25–30	8/28/01	1530	280	240

intervals ranged from trace amounts (estimated at 1 mg/yd^3) to about 170 mg/yd^3 (*table C1*); these intervals had the full range of mercury values (0.3 to 315 ng/g, wet weight) (*table 8*). Geometric means of gold tenor and mercury concentration were computed for each drill hole and are plotted in *figure 15B* along with standard deviations. This plot indicates that hole DPD-1 is distinct from the other five holes in terms of both gold and mercury content, and hole DPD-5 is somewhat elevated in gold tenor relative to the drill-holes DPD-2, -3, -4, and -6.

Trace Elements

Concentrations of trace elements and major elements were determined for material screened to less than 0.060 mm in 19 drilled intervals from holes DPD-1, -4, -5, and -6 (*table 10A*). Samples from 2 of the 19 intervals were analyzed in duplicate. In addition to mercury, some trace elements that may harm the environment if fish passage is improved are arsenic, antimony, cadmium, chromium, copper, lead, nickel, and zinc. Minimum, median, and maximum values for the 19 intervals for the trace elements of potential environmental concern are shown in *table 10B*, together with sediment-quality criteria. The sediment-quality criteria are Threshold Effects Concentrations (TEC) and Probable Effects Concentrations (PEC) that were compiled by MacDonald and others (2000) based on values with regard to limits for ecological toxicity accepted by various agencies and researchers.

Four of the trace elements from the 19 intervals analyzed have median concentrations that exceed the TEC values of MacDonald and others (2000): arsenic, chromium, copper, and nickel (*table 10B*). For three of these metals (Cr, Cu, and Ni), all 19 concentrations measured in this study exceeded the TEC value limit. In addition, the maximum concentrations of lead, mercury, and zinc were above the TEC values. Median concentrations exceeded the PEC value for only chromium and nickel.

It is possible that the arsenic, chromium, copper, and nickel in the Daguerre Point sediments exist in forms that are less bioavailable than those in the other areas on which the TEC and PEC values are based. Site-specific toxicity testing is required to determine if these trace elements pose a significant risk to aquatic life.

Analyses of gold concentrations from the sieved fraction, less than 0.060 mm, ranged from less than detection (<0.005 mg/kg [or µg/g]) to a maximum value of 0.017 mg/kg (*table 10A*). In comparison, the gold tenor values from the heavy mineral concentrates ranged from trace (~1 mg/yd^3) to 170 mg/yd^3 (*table C1*). These data can be compared by converting the geochemical data to a volumetric basis using a density of 1,500 kg/yd^3. The converted range of measured values is <8 mg/yd^3 to 26 mg/yd^3. These values are within the overall range of the gold tenor values derived from the heavy-mineral concentrates, but are generally lower. Apparently, some of the gold, especially in intervals with higher tenor, exists as material coarser than 0.060 mm, likely in sand-sized particles. Another important factor in interpreting gold concentrations is the nugget effect. The analyses in *table 10A* are based on very small samples (about 100 mg), whereas the heavy-mineral concentrates (*table C1*) are based on much larger samples (several kg). Therefore, the gold tenor results from the heavy-mineral concentrates are considered to be more representative of actual in-place gold concentrations.

Table 8. Mercury and methylmercury concentrations in the clay-silt fraction after centrifuge separation, Daguerre Point Dam, California.

[DPD, Daguerre Point Dam; No., number; LTD, less than detection; E, estimated; ft, foot; ng/g wet, nanogram per gram wet weight; n/a, not applicable]

Drill hole/Depth (ft)	Centrifuge tube No.	Date	Time	Methylmercury		Total mercury
				Concentration (ng/g wet)	Detection limit (ng/g)	Concentration (ng/g wet)
DPD–1						
0–5	EXT013	8/14/01	1100	0.182	0.02	70.6
5–10	EXT058	8/14/01	1200	LTD	.01	33.3
10–15	EXT024	8/14/01	1430	LTD	.06	21.3
15–17.5	EXT075	8/14/01	1500	LTD	.05	17.9
DPD–2						
0–5	EXT080	8/15/01	1200	LTD	0.02	33.4
5–10	EXT077	8/15/01	1400	LTD	.02	88.1
10–13.5	EXT057	8/15/01	1600	0.230	.02	86.4
13.5–15	EXT020	8/16/01	1030	.137	.03	n/a
15–20	EXT066	8/16/01	1200	LTD	.02	114
20–25	EXT055	8/16/01	1330	LTD	.009	69.7
25–30	EXT054	8/16/01	1500	LTD	.006	247
[1]25–30	EXT074	8/16/01	1500	LTD	.07	244
30–35	EXT069	8/16/01	1700	.04E	.04	315
DPD–3						
0–5	EXT011	8/20/01	1030	0.261	0.01	0.3
5–10	EXT022	8/20/01	1100	.063	.009	88.0
10–15	EXT010	8/20/01	1330	.049	.01	295
15–20	EXT018	8/20/01	1500	.072	.07	136
DPD–4						
0–10	EXT029	8/21/01	1300	LTD	0.009	83.6
10–15	EXT039	8/21/01	1530	0.611	.07	143
15–20	EXT030	8/22/01	0900	.107	.02	173
20–25	EXT065	8/22/01	1100	.04E	.14	19.5
25–30	EXT079	8/22/01	1230	.056	.010	114
DPD–5						
0–5	EXT049	8/24/01	1030	0.318	0.02	138
5–10	EXT042	8/24/01	1130	.056	.01	207
10–15	EXT061	8/24/01	1430	LTD	.14	158
15–20	EXT072	8/24/01	1530	LTD	.09	50.2
DPD–6						
0–5	EXT062	8/27/01	1530	LTD	0.12	28.3
5–10	EXT032	8/28/01	0930	LTD	.14	58.4
10–15	EXT014	8/28/01	1130	0.081	.08	173
15–20	EXT028	8/28/01	1330	LTD	.13	205
20–25	EXT046	8/28/01	1430	.069	.04	198
25–30	EXT012	8/28/01	1530	LTD	.06	204
[1]25–30	EXT019	8/28/01	1530	LTD	.07	196
Blank[2]	EXT052	8/28/01	1630	LTD	n/a	n/a

[1]Field replicate.

[2]Field blank.

Heavy Mineral Concentrates

Gold Tenor and Speciation

The highest tenor of gold concentration found was 170 mg/yd^3 in drill-hole DPD-1 near the bedrock contact (*table C1*). Drill-hole DPD-5 had relatively high gold concentrations in all three tested intervals. Drill-hole DPD-2 had moderate gold concentrations at certain intervals. Drill-holes DPD-3, -4 and -6 had the lowest gold concentrations, except for the 15- to 20-foot interval of DPD-4. Visible grains of gold (sand-sized) were observed in drill cuttings during drilling of holes DPD-1 and -5.

Table 9. Total mercury concentration (ng/g dry weight) for sieved fine particle sizes, Daguerre Point Dam, California.

[ft, foot; mm, millimeter; ng/g, nanogram per gram; >, greater than; <, less than; DPD, Daguerre Point Dam]

Drill hole/Depth (ft)	Medium and fine silt, with clay	Coarse silt	Very fine sand	Fine sand	Medium sand	Coarse sand
Size (mm)	**<0.030**	**0.030 – 0.060**	**0.060 – 0.149**	**0.149 – 0.297**	**0.297 – 0.500**	**>0.500**
			Concentrations of mercury (ng/g)			
			DPD–4			
0–10	57.4	17.5	5.3	3.0	2.0	0.9
10–15	63.1	25.1	18.7	8.6	6.0	1.0
15–20	182	24.1	19.5	13.7	8.0	4.8
20–25	9.5	2.2	2.3	9.8	6.9	22.5
25–30	43.3	4.6	7.3	24.9	24.0	38.9
			DPD–5			
0–5	74.0	24.8	16.4	6.8	4.3	2.3
5–10	130	25.3	232	9.1	4.4	2.9
10–15	109	46.5	12.8	7.3	3.3	2.0
15–20	27.1	7.7	3.5	3.6	3.5	2.9
			DPD–6			
0–5	9.9	2.3	0.2	0.4	2.2	1.3
5–10	24.1	21.6	5.8	2.0	1.8	.5
10–15	24.1	21.6	5.8	2.0	1.8	.5
15–20	26.9	15.0	24.2	11.9	27.3	.5
20–25	24.4	50.4	17.9	10.1	10.3	.5
25–30	80.3	55.1	7.5	34.7	7.1	1.9
Minimum	9.5	2.2	0.2	0.4	1.8	0.5
Median	43.3	21.6	7.5	8.6	4.4	1.9
Maximum	182	55.1	232	34.7	27.3	38.9

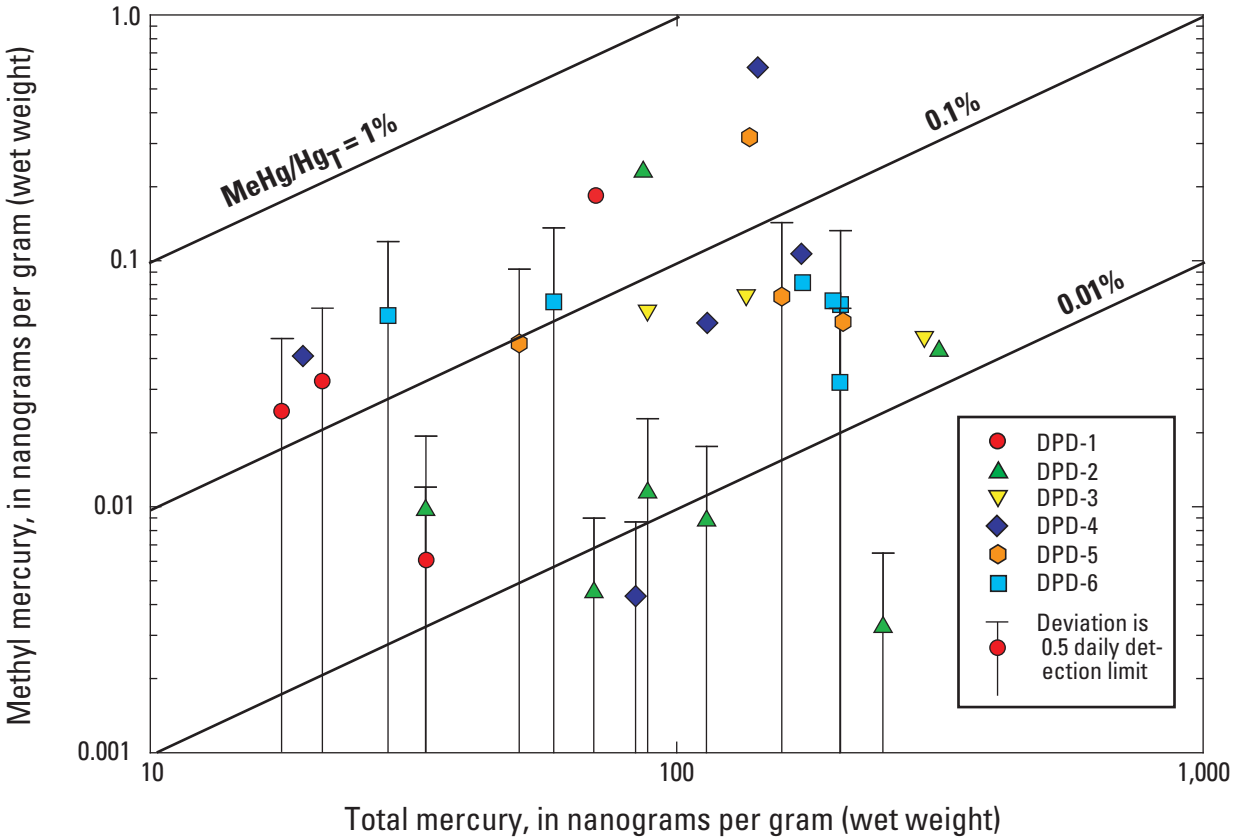

Figure 14. Graph showing relation of methylmercury and total mercury in the clay-silt fraction (centrifuge tube solids), Daguerre Point Dam, California.
MeHg, methylmercury; Hg_T, total mercury; %, percent.

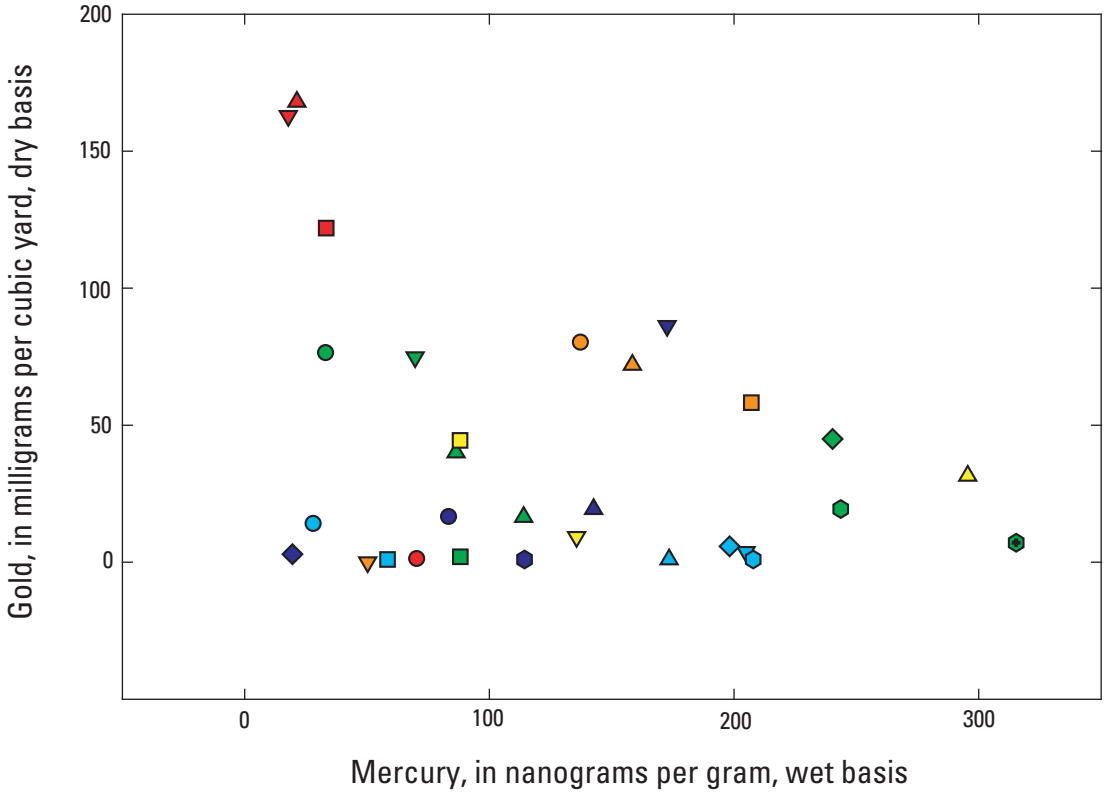

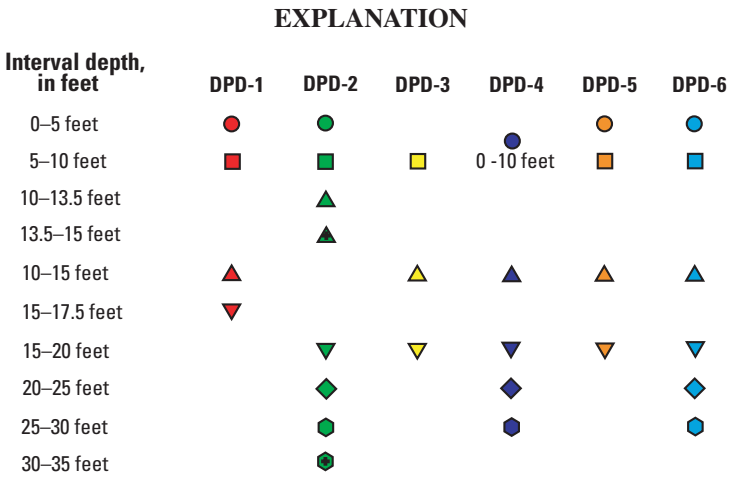

Figure 15A. Graphs showing the relation of gold and mercury in the clay-silt fraction, Daguerre Point Dam, California.

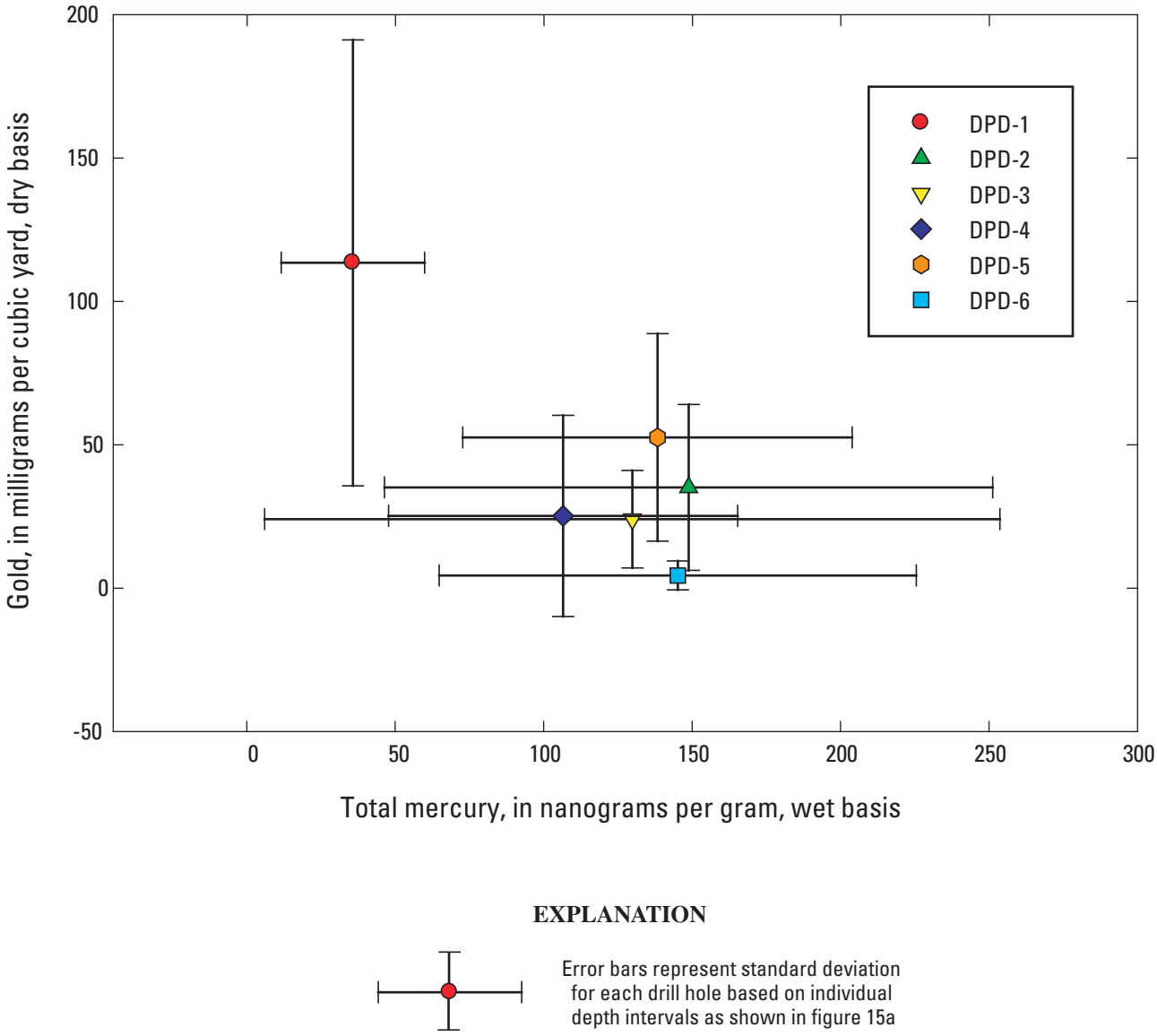

Figure 15B. Graph showing the relation of gold and mercury in the clay-silt fraction for each drill hole, Daguerre Point Dam, California.

Gold grains were generally well rounded (*fig. 16*) and range in size from 0.25 mm to almost 2 mm. Although elemental mercury was not observed with the naked eye on individual gold-grains, evidence of mercury was found with the aid of a binocular microscope and was confirmed with SEM observations, described in the next section.

Mercury Speciation

An SEM with EDX analyzer was used to observe individual microscopic gold grains, which showed evidence of mercury amalgamation. These gold grains had a pitted surface texture with shrinkage cracks (*fig. 17*) that yielded moderate to strong mercury spectra. The shrinkage cracks may indicate a surface amalgam layer from which some mercury has been lost. A grain of gold amalgam from the 0- to 5-foot interval of hole DPD-1 showed 10- to 30-µm stacked platelets of coarse-grained amalgam. Gold amalgam is very soft and brittle and readily breaks away from parts of gold grains that do not contain mercury (*fig. 16*).

Table 10A. Concentration of selected elements in sediment screened to less than 0.060 millimeter, Daguerre Point Dam, California.

[ft, foot; Wt%, weight percent; Avg, average; SD, standard deviation; DPD, Daguerre Point Dam. µg/g, microgram per gram; <, less than]

Drill hole/Depth (ft)	Al Aluminum Wt%		As Arsenic µg/g		Au Gold µg/g		B Boron µg/g		Ba Barium µg/g		Be Beryllium µg/g		Bi Bismuth µg/g	
	Avg	SD	Avg	SD	Avg	SD	Avg	SD	Avg	SD	Avg	SD	Avg	SD
DPD-1														
0–5	4.3	0.2	6.5	0.5	0.006	0.002	46	7	278	13	0.65	0.04	0.21	0.06
5–10	3.9	.3	7.2	.7	.006	.005	78	10	385	32	.82	.04	.12	.03
10–15	8.5	.1	8.0	.3	.008	.003	207	12	507	2	1.1	.1	.43	.08
15–17.5	9.0	.3	8.8	.5	.006	.000	75	9	441	18	1.2	.0	.14	.02
DPD-4														
0–10	3.9	0.2	11	1	0.006	0.003	99	0	441	24	0.81	0.15	<0.04	0.02
10–15	5.1	.1	32	2	.008	.004	128	1	591	0	1.0	.1	<.04	.03
15–20	5.6	.2	20	1	.012	.002	96	3	755	5	1.0	.1	<.04	.01
20–25	3.8	.2	10	1	.005	.000	157	5	330	17	.74	.06	.11	.01
25–30	5.9	.0	14	0	.008	.003	83	13	442	1	.97	.10	.06	.07
DPD-5														
0–5	7.2	0.1	22	0	0.009	0.007	126	6	904	0	1.5	0.1	0.26	0.06
5–10	5.6	.1	22	0	.017	.003	167	2	488	9	1.1	.0	<.04	.07
10–15	5.5	.1	23	0	<.007	.001	129	5	486	2	1.1	.1	.19	.01
15–20	3.6	.2	11	0	.007	.004	49	4	269	3	.90	.07	.23	.12
DPD-6														
0–5	3.3	0.1	4.7	0.4	<0.005	0.001	73	7	260	9	0.71	0.09	0.06	0.02
5–10	3.6	.1	7.4	.1	<.005	.001	82	1	377	1	.76	.06	.11	.04
10–15	6.7	.2	17	0	.007	.002	77	7	477	9	1.2	.0	.29	.02
15–20	7.1	.2	11	0	<.005	.002	103	1	413	18	1.0	.0	1.1	.1
20–25	8.0	.1	14	0	.006	.002	43	2	600	17	1.1	.1	.20	.01
25–30	6.4	.2	20	1	.009	.003	134	14	414	19	1.6	.1	.26	.05
Minimum	3.3		4.7		<0.005		43		260		0.65		<0.04	
Median	5.6		11		.006		96		441		1.02		.14	
Maximum	9.0		32		.017		207		904		1.6		1.1	

Drill hole/Depth (ft)	Ca Calcium Wt%		Cd Cadmium µg/g		Ce Cerium µg/g		Co Cobalt µg/g		Cr Chromium µg/g		Cs Cesium µg/g		Cu Copper µg/g	
	Avg	SD	Avg	SD	Avg	SD	Avg	SD	Avg	SD	Avg	SD	Avg	SD
DPD-1														
0–5	1.6	0.1	0.20	0.01	16	0	16	1	88	3	0.54	0.11	42	2
5–10	.89	.05	.19	.02	14	1	19	1	131	7	.71	.07	42	2
10–15	1.9	.0	.22	.03	32	0	30	1	161	6	2.7	.1	52	1
15–17.5	1.5	.1	.25	.01	28	1	24	1	155	7	1.4	.1	61	2
DPD-4														
0–10	1.7	0.0	0.14	0.03	17	1	26	1	159	2	1.0	0.1	63	3
10–15	1.8	.1	.28	.10	19	1	38	1	195	2	1.5	.3	98	4
15–20	1.7	.1	.31	.01	16	1	31	0	172	1	1.2	.1	103	2
20–25	2.5	.1	.21	.03	8.2	.0	34	1	167	0	.5	.0	97	4
25–30	1.7	.1	.23	.05	19	0	47	2	136	5	1.2	.1	115	2
DPD-5														
0–5	3.5	0.0	0.48	0.05	37	1	43	1	244	2	1.7	0.1	94	3
5–10	1.9	.1	.40	.06	21	1	33	1	190	8	1.0	.0	106	3
10–15	1.8	.0	.29	.05	19	0	27	1	189	7	1.5	.1	75	2
15–20	.95	.02	.24	.03	9.5	0.0	35	1	155	5	1.0	.1	54	1
DPD-6														
0–5	1.2	0.0	0.19	0.02	13	1	16	0	90	4	2.2	0.0	43	2
5–10	1.3	.0	.16	.03	14	1	15	0	117	1	.55	.06	40	1
10–15	1.8	.0	.40	.02	15	0	37	0	188	6	2.4	.1	108	2
15–20	1.8	.1	.30	.04	14	0	36	2	146	2	1.5	.0	104	2
20–25	2.1	.0	.31	.02	16	0	30	1	143	6	1.4	.1	85	4
25–30	.80	.03	.55	.02	7.7	.4	48	0	147	3	1.0	.1	127	3
Minimum	0.80		0.14		7.7		15		88		0.5		40	
Median	1.7		.25		16		31		155		1.2		85	
Maximum	3.5		.55		37		48		244		2.7		127	

Table 10A. Concentration of selected elements in sediment screened to less than 0.060 millimeter, Daguerre Point Dam, California.—Continued

[ft, foot; Wt%, weight percent; Avg, average; SD, standard deviation; DPD, Daguerre Point Dam. µg/g, microgram per gram; <, less than]

Drill hole/Depth (ft)	Dy Dysprosium µg/g		Er Erbium µg/g		Eu Europium µg/g		Fe Iron Wt%		Ga Gallium µg/g		Gd Gadolinium µg/g		Ho Holmium µg/g	
	Avg	SD	Avg	SD	Avg	SD	Avg	SD	Avg	SD	Avg	SD	Avg	SD
DPD-1														
0–5	1.3	0.1	0.72	0.03	0.34	0.01	3.8	0.1	10	0	1.3	0.1	0.26	0.00
5–10	1.3	.0	.79	.03	.37	.02	4.6	.2	13	1	1.4	.1	.27	.02
10–15	3.5	.0	1.9	.0	1.0	.0	5.7	.1	17	0	3.6	.0	.66	.01
15–17.5	3.1	.2	1.6	.0	.89	.00	6.1	.1	18	0	3.2	.1	.58	.01
DPD-4														
0–10	1.3	0.0	0.77	0.03	0.38	0.04	4.9	0.1	12	1	1.3	0.0	0.22	0.01
10–15	1.5	.1	.85	.06	.42	.04	7.7	.0	15	0	1.5	.0	.30	.01
15–20	1.5	.1	.90	.00	.45	.02	7.1	.2	16	0	1.6	.0	.32	.00
20–25	1.2	.1	.72	.05	.31	.01	6.7	.3	12	0	1.1	.1	.25	.01
25–30	1.6	.1	.93	.03	.48	.03	7.5	.7	16	0	1.6	.0	.31	.00
DPD-5														
0–5	2.4	0.0	1.31	0.04	0.72	0.03	9.6	0.0	20	1	2.5	0.1	0.46	0.02
5–10	1.6	.0	.93	.03	.53	.02	6.8	.3	16	0	1.8	.0	.33	.01
10–15	1.5	.1	.80	.05	.41	.01	6.7	.4	16	0	1.5	.1	.28	.01
15–20	.85	.02	.52	.01	.26	.01	5.6	.2	13	0	.87	.06	.17	.01
DPD-6														
0–5	.88	.02	.49	.02	.23	.01	4.6	.1	11	0	.80	.03	.17	.01
5–10	.93	.04	.51	.01	.25	.01	4.8	.1	11	0	.85	.05	.18	.01
10–15	1.6	.1	.91	.02	.38	.03	7.7	.2	17	1	1.5	.1	.28	.01
15–20	1.3	.1	.71	.01	.38	.01	7.1	.3	16	1	1.3	.1	.26	.01
20–25	2.2	.0	1.3	.0	.59	.02	6.9	.1	17	0	2.2	.1	.43	.00
25–30	.91	.06	.51	.03	.24	.01	7.7	.2	20	1	.90	.05	.18	.01
Minimum	0.85		0.49		0.23		3.8		10		0.80		0.17	
Median	1.5		.80		.38		6.7		16		1.5		.28	
Maximum	3.5		1.9		1.0		9.6		20		3.6		.66	

Drill hole/Depth (ft)	K Potassium Wt%		La Lanthanum µg/g		Li Lithium µg/g		Lu Lutetium µg/g		Mg Magnesium Wt%		Mn Manganese µg/g		Mo Molybdenum µg/g	
	Avg	SD	Avg	SD	Avg	SD	Avg	SD	Avg	SD	Avg	SD	Avg	SD
DPD-1														
0–5	0.59	0.03	7.3	0.1	5.7	0.4	0.11	0.01	0.56	0.02	711	30	4.4	0.7
5–10	.77	.02	5.9	.5	7.8	.8	.11	.01	.39	.02	750	37	2.9	.5
10–15	.79	.01	14	0	13	0	.28	.01	.65	.01	1,260	19	3.8	.4
15–17.5	.79	.03	12	1	18	0	.25	.01	.91	.01	740	34	1.5	.9
DPD-4														
0–10	0.74	0.05	7.1	0.5	8.6	0.3	0.098	0.007	0.97	0.01	1,050	29	13	0
10–15	.78	.02	7.9	.5	14	1	.12	.00	1.6	.0	960	25	51	2
15–20	.81	.02	6.4	.0	16	1	.14	.00	1.5	.0	972	46	9.9	.5
20–25	.56	.03	2.9	.1	9.7	.5	.09	.01	.93	.05	1,720	28	33	2
25–30	.95	.02	7.0	.2	16	0	.13	.01	1.6	.1	2,340	188	10	0
DPD-5														
0–5	1.3	0.0	15	0	11	1	0.18	0.01	1.5	0.0	1,980	21	14	0
5–10	.90	.03	8.7	.2	15	1	.14	.00	1.5	.1	1,750	101	9.1	.5
10–15	1.0	.0	8.0	.1	12	0	.124	.010	1.1	.1	1,230	63	91	3
15–20	.62	.01	3.7	.1	8.7	.5	.068	.006	.44	0.01	1,590	18	39	0
DPD-6														
0–5	0.60	0.02	4.7	0.1	4.0	0.3	0.073	0.00	0.62	0.01	759	22	5.5	0.9
5–10	.64	.01	5.3	.2	4.7	.2	.076	.004	.70	.00	743	29	4.6	.5
10–15	.96	.04	6.2	.3	17	0	.13	.01	1.4	.0	1,480	43	26	0
15–20	.88	.02	5.8	.2	16	0	.11	.00	1.4	.1	1,440	79	5.1	.6
20–25	.83	.02	7.7	.2	19	1	.18	.01	1.0	.0	1,280	17	7.7	.3
25–30	.96	.02	2.8	.1	24	1	.080	.001	.76	.00	2,200	31	2.2	.2
Minimum	0.56		2.8		4.0		0.068		0.39		711		1.5	
Median	.79		7.0		13		.12		1.0		1,260		9.1	
Maximum	1.3		15		24		.28		1.6		2,340		91	

Table 10A. Concentration of selected elements in sediment screened to less than 0.060 millimeter, Daguerre Point Dam, California.—Continued

[ft, foot; Wt%, weight percent; Avg, average; SD, standard deviation; DPD, Daguerre Point Dam. µg/g, microgram per gram; <, less than]

Drill hole/Depth (ft)	Na Sodium Wt%		Nd Neodymium µg/g		Ni Nickel µg/g		P Phosphorous µg/g		Pb Lead µg/g		Pr Praseodymium µg/g		Rb Rubidium µg/g	
	Avg	SD	Avg	SD	Avg	SD	Avg	SD	Avg	SD	Avg	SD	Avg	SD
DPD-1														
0–5	1.1	0.0	7.0	0.3	42	2	540	13	6.1	0.4	1.8	0.0	17	1
5–10	.98	.05	6.8	.6	48	3	451	37	8.2	.6	1.6	.0	23	2
10–15	1.1	.0	17	0	73	2	377	10	11	0	4.1	.0	24	1
15–17.5	.91	.03	15	1	88	1	407	5	11	0	3.7	.2	24	1
DPD-4														
0–10	0.97	0.01	7.3	0.0	75	1	699	9	9.3	0.7	1.8	0.1	16	1
10–15	1.1	.0	8.0	.1	121	0	1,010	16	17	1	2.1	.0	23	1
15–20	1.1	.1	7.5	.0	100	1	732	52	20	1	1.8	.0	23	1
20–25	1.5	.1	4.3	.0	103	5	659	6	8.7	.6	1.0	.1	7.0	.3
25–30	.99	.01	8.3	.1	100	3	635	33	13	0	2.0	.1	24	1
DPD-5														
0–5	1.6	0.0	14	0	94	3	1,230	51	20	0	3.5	0.0	35	1
5–10	1.2	.1	9.0	.0	112	3	787	21	16	1	2.3	.1	22	1
10–15	1.2	.0	7.9	.2	86	3	765	45	41	0	2.0	.1	28	1
15–20	.89	.03	4.3	.1	90	2	376	20	105	0	1.0	.0	12	0
DPD-6														
0–5	1.2	0.1	4.3	0.1	36	1	1,190	14	6.4	0.2	1.1	0.1	13	1
5–10	1.0	.0	5.0	.2	47	1	634	16	7.8	.1	1.3	.1	16	1
10–15	1.2	.0	6.9	.3	107	3	859	19	163	1	1.6	.0	29	0
15–20	1.3	.0	6.4	.3	96	3	726	8	15	1	1.6	.1	23	1
20–25	1.0	.1	8.9	.2	87	4	765	27	23	1	2.2	.1	17	0
25–30	.56	.03	3.7	.2	147	5	797	46	25	1	.88	.05	13	1
Minimum	0.56		3.7		36		377		6.1		0.88		7.0	
Median	1.1		7.3		90		726		15		1.8		23	
Maximum	1.6		17		147		1,230		163		4.1		35	

Drill hole/Depth (ft)	Re Rhenium µg/g		S Sulfur Wt%		Sb Antimony µg/g		Sc Scandium µg/g		Se Selenium µg/g		Sm Samarium µg/g		Sr Strontium µg/g	
	Avg	SD	Avg	SD	Avg	SD	Avg	SD	Avg	SD	Avg	SD	Avg	SD
DPD-1														
0–5	<0.003	0.001	0.03	0.01	0.85	0.15	7.3	0.7	<0.8	1.3	1.5	0.1	160	8
5–10	<.003	.000	.04	.00	.83	.06	6.9	.8	<.8	.1	1.6	.2	126	9
10–15	<.003	.001	.04	.01	.92	.03	16	1	.8	.6	3.8	.1	191	6
15–17.5	<.003	.001	.02	.01	.85	.06	17	0	<.8	.2	3.3	.0	147	6
DPD-4														
0–10	<0.004	0.002	0.30	0.01	1.1	0.2	8.1	0.9	<0.9	0.5	1.5	0.1	246	3
10–15	<.004	.006	1.2	.0	2.7	.4	12	1	1.4	.4	1.7	.1	206	2
15–20	.004	.002	.37	.02	1.8	.1	16	0	<.9	1.3	1.7	.1	196	14
20–25	.003	.001	.18	.00	.88	.00	15	1	1.6	.2	1.1	.1	168	8
25–30	<.004	.002	.17	.00	1.1	.1	14	1	<.9	.5	1.8	.0	158	3
DPD-5														
0–5	0.003	0.003	0.06	0.01	1.6	0.1	14	1	<1	0	2.8	0.1	301	2
5–10	<.004	.003	.04	.01	1.3	.2	14	1	<.9	.3	1.8	.0	203	14
10–15	.003	.002	.05	.01	5.1	.1	10	1	<1	0	1.7	.0	212	7
15–20	<.003	.000	<.02	.01	16	0	6.2	.4	<.8	.4	.97	.03	127	5
DPD-6														
0–5	<0.003	0.001	0.02	0.01	0.65	0.03	5.6	0.5	0.9	0.6	0.86	0.10	183	8
5–10	<.003	.001	.06	.00	.72	.03	6.5	.9	<.8	.1	1.0	.0	181	6
10–15	<.003	.001	.05	.01	19	0	11	1	<.8	.2	1.6	.0	189	2
15–20	<.003	.001	.02	.02	1.3	.1	11	1	<.8	.7	1.4	.1	190	4
20–25	.004	.001	.10	.00	3.8	.0	14	1	<.8	.8	2.2	.0	202	8
25–30	<.003	.001	.03	.00	1.7	.0	12	0	<.8	.2	.93	.00	90	4
Minimum	<0.003		<0.02		0.65		5.6		<0.8		0.93		90	
Median	<.003		.05		1.3		12		<.8		1.6		189	
Maximum	.004		1.2		19		17		1.6		3.8		301	

Table 10A. Concentration of selected elements in sediment screened to less than 0.060 millimeter, Daguerre Point Dam, California.—Continued

[ft, foot; Wt%, weight percent; Avg, average; SD, standard deviation; DPD, Daguerre Point Dam. µg/g, microgram per gram; <, less than]

Drill hole/Depth (ft)	Tb Terbium µg/g		Te Tellurium µg/g		Th Thorium µg/g		Ti Titanium Wt%		Tl Thallium µg/g		Tm Thulium µg/g		U Uranium µg/g	
	Avg	SD	Avg	SD	Avg	SD	Avg	SD	Avg	SD	Avg	SD	Avg	SD
DPD-1														
0–5	0.21	0.01	<0.07	0.03	2.5	0.0	0.31	0.01	0.05	0.02	0.11	0.01	1.0	0.0
5–10	.22	.01	<.07	.04	2.5	.1	.60	.02	.18	.09	.12	.01	1.6	.1
10–15	.56	.01	<.07	.04	5.6	.1	.76	.02	.19	.05	.28	.00	1.9	.1
15–17.5	.48	.01	.09	.03	6.4	.2	.65	.01	.19	.01	.26	.02	1.9	.1
DPD-4														
0–10	0.20	0.00	0.09	0.08	2.0	0.0	0.31	0.01	0.26	0.06	0.087	0.003	1.2	0.1
10–15	.24	.02	.07	.04	2.8	.1	.44	.02	.19	.03	.13	.01	1.9	.1
15–20	.26	.01	.10	.03	2.5	.1	.55	.02	.21	.03	.13	.01	1.6	.1
20–25	.18	.00	.10	.03	.9	.0	.41	.02	.13	.02	.11	.00	.94	.06
25–30	.26	.00	<.05	.02	2.6	.1	.46	.02	.19	.01	.13	.01	1.3	.1
DPD-5														
0–5	0.36	0.00	<0.09	0.02	4.4	0.1	0.88	0.02	0.46	0.06	0.19	0.01	2.2	0.1
5–10	.27	.00	.13	.04	3.0	.1	.54	.03	.30	.05	.13	.00	1.8	.0
10–15	.23	.02	.17	.11	3.1	.1	.56	.03	.24	.11	.126	.012	1.8	.0
15–20	.15	.01	.11	.00	1.5	.0	.57	.02	.12	.02	.071	.003	1.3	.0
DPD-6														
0–5	0.14	0.01	0.09	0.03	1.6	0.1	0.37	0.01	0.14	0.01	0.078	0.005	1.2	0.0
5–10	.15	.01	<.07	.03	1.8	.0	.40	.01	.16	.06	.075	.004	.99	.03
10–15	.23	.01	.10	.07	2.7	.1	.54	.01	.20	.02	.12	.01	1.6	.1
15–20	.22	.00	<.07	.02	2.5	.1	.54	.02	.18	.03	.11	.01	1.4	.1
20–25	.34	.00	.10	.03	3.3	.0	.55	.03	.17	.04	.18	.01	1.6	.1
25–30	.14	.01	.27	.04	2.3	.1	.55	.01	.23	.09	.075	.002	2.0	.1
Minimum	0.14		<0.05		0.9		0.31		0.05		0.071		0.94	
Median	.23		.09		2.5		.54		.19		.12		1.6	
Maximum	.56		.27		6.4		.88		.46		.28		2.2	

Drill hole/Depth (ft)	V Vanadium µg/g		W Tungsten µg/g		Y Yttrium µg/g		Yb Ytterbium µg/g		Zn Zinc µg/g		Zr Zirconium µg/g		Mass Digested (g)
	Avg	SD	Avg	SD	Avg	SD	Avg	SD	Avg	SD	Avg	SD	
DPD-1													
0–5	135	6	0.48	0.03	6.4	0.3	0.68	0.06	62	3	43	3	0.101
5–10	175	10	.83	.04	6.2	.4	.73	.06	64	3	60	2	.102
10–15	217	5	1.3	.0	16	0	1.8	.1	92	3	77	2	.101
15–17.5	218	8	1.1	.1	14	0	1.7	.0	94	5	75	3	.100
DPD-4													
0–10	136	8	0.66	0.01	5.8	0.5	0.65	0.05	81	4	43	2	0.106
10–15	221	4	1.1	.0	7.1	.3	.88	.02	138	14	50	1	.106
15–20	257	1	1.1	.0	7.0	.0	.85	.05	114	5	53	0	.102
20–25	200	10	.61	.03	6.0	.2	.65	.04	90	1	252	97	.100
25–30	221	1	.91	.02	7.3	.0	.86	.02	115	13	47	0	.101
DPD-5													
0–5	333	9	1.3	0.0	12	0	1.3	0.1	163	7	77	1	0.133
5–10	225	7	1.2	.0	7.9	.2	.90	.01	109	9	54	1	.108
10–15	231	10	1.1	.0	7.0	.2	.76	.02	111	2	58	2	.132
15–20	195	6	.82	.03	4.0	.1	.46	.01	82	1	54	2	.101
DPD-6													
0–5	149	6	0.44	0.01	4.9	0.2	0.44	0.02	61	2	36	1	0.103
5–10	168	3	.48	.02	4.9	.3	.49	.02	66	1	40	2	.101
10–15	229	6	1.0	.1	7.2	.2	.85	.00	132	3	60	1	.105
15–20	222	8	.85	.00	6.3	.1	.71	.03	118	3	53	1	.103
20–25	207	8	.92	.02	10	0	1.2	.0	109	3	59	2	.101
25–30	219	7	1.4	.1	3.8	.1	.47	.00	144	3	69	2	.101
Minimum	136		0.44		3.8		0.44		61		36		0.100
Median	218		.92		7.0		.76		109		54		.102
Maximum	333		1.4		16		1.8		163		252		.133

Table 10B. Trace-element concentrations in fine-grained Daguerre Point sediment and sediment quality criteria (ecological toxicity), Daguerre Point Dam, California.

[Mercury concentrations based on analysis of clay-silt fraction separated by centrifugation (*table 8*). Other metal concentrations based on analysis of material screened to less than 0.060 mm (*table 10A*). Bold values exceed TEC concentrations; TEC, threshold effects concentration. PEC, probable effects concentration; NG, not given; mg/kg, milligram per kilogram (parts per million)]

Metals	Concentrations (mg/kg)			Consensus-based TEC[1]	Consensus-based PEC[1]
	Minimum	Median	Maximum		
Arsenic	4.7	**11**	**32**	9.79	33
Antimony	.65	1.3	19	NG	NG
Cadmium	.14	.25	.55	.99	4.98
Chromium	**88**	**155**	**244**	43.4	111
Copper	**40**	**85**	**127**	31.6	149
Lead	6.1	15	**163**	35.8	128
Mercury	.018	.13	**.32**	.18	1.06
Nickel	**36**	**90**	**147**	22.7	48.6
Zinc	61	109	**163**	121	459

[1]Values from MacDonald and others (2000).

Elemental mercury spherules from 4 to 6 μm in diameter were observed on a grain of gold amalgam from the 30- to 35-foot interval of drill-hole DPD-2 (*fig. 18*). These mercury spherules are associated with platy aluminosilicate minerals and iron oxides less than 0.4 μm in diameter. In addition, a gold-amalgam grain with mercury was observed in a sample from the 25- to 30-foot interval of drill-hole DPD-2.

Other Heavy Minerals

Quantities of heavy minerals in concentrates prepared from drilled sediment intervals upstream of Daguerre Point Dam vary with the type of mining. Higher concentrations of heavy minerals tend to be associated with undredged hydraulic tailings, whereas lesser amounts are associated with undisturbed, pre-mining gravels (*fig. 19*). Individual euhedral to subhedral grains of pyrite, magnetite, spessartine garnet, chromite, ilmenite, zircon, and sphene were observed in the heavy-mineral concentrates (*table C2*).

Magnetite, chromite, and ilmenite were the most common minerals in the mineral concentrates. The highest concentration of pyrite grains was found in the 0- to 5-foot interval of hole DPD-1. Pyrite concentrations were also relatively high in the 20- to 25-foot interval of DPD-2 and the 5- to 10-foot interval of DPD-3. Concentrations of pyrite grains tended to increase as the grain-size decreased in the heavy-mineral fraction, which may be a consequence of breakage during churn drilling. Fine-grained pyrite (<1 mm) with coarsely crystalline textures may represent detrital sulfides from gold-quartz lode mines nearby in Browns Valley that were active before 1942 and were transported via Dry Creek, just upstream of DPD-3 (*figs. 1* and *3*). Zircon grains were less abundant than other heavy minerals and were randomly distributed throughout the particle sizes. Garnets were found in the 0.500- to 1-mm size fractions of most intervals; the proportions of garnet were highest in the deeper sections of holes DPD-1, DPD-2, and DPD-3 (*table C2*).

Mercury Methylation and Demethylation Potentials

In other studies, it has been shown that surface sediments typically have a much higher potential for MeHg production than deeper sediments (Marvin-DePasquale and others, 2003). The amount of radiotracer $^{203}Hg(II)$ converted to $CH_3{}^{203}Hg+$ (MeHg with radiotracer Hg) ranged from <0.03 to 0.31 percent per day for deep core samples from DPD, which corresponds to Hg-methylation potential rates of less than about 0.15 to 1.57 ng/g dry sed/d (*table 11*). This range is at the low end of Hg-methylation rates. This trend reflects the general decrease in overall microbial activity with sediment depth, as organic matter needed to drive heterotrophic microbial metabolism decreases with depth. In addition, the activity of sulfate-reducing bacteria is limited at greater depths where pore-water sulfate tends to be depleted (Marvin-DiPasquale and Capone, 1998). Because this bacterial group is primarily responsible for Hg-methylation (Compeau and Bartha, 1985; Gilmour and others, 1992), we can expect Hg-methylation to decrease with increasing depth. Such depth profiles have been observed in other systems and in shallower sediment profiles (Marvin-DiPasquale and others, 2003). For two holes (DPD-1 and DPD-3) of the three from which samples were taken at two depths, the upper layer sample had the higher $^{203}Hg(II)$-methylation rate. The opposite trend occurred at hole DPD-5, which likely represents original Yuba River bed sediment, below the zone impacted by hydraulic mining debris.

The amount of $^{14}CH_3HgCl$ that degraded to $^{14}CO_2 + {}^{14}CH_4$ (combined) in the deeper sediments ranged from 6.5 to 17.7 percent per day, which corresponds to 1.0 to 2.2 ng/g dry sed/d (*table 11*). In general, the overall decrease in microbial activity likely is due to labile organic matter decreasing with depth and likely accounts for this vertical trend. However, unlike the situation for Hg-methylation, which is promoted primarily by sulfate-reducing bacteria, a wider variety of heterotrophic bacterial groups can carry out MeHg degradation; aerobes, denitrifiers, sulfate reducers, and methanogens have been implicated in this process (Oremland and others, 1991; Marvin-DiPasquale and Oremland, 1998). Similar to the trend for Hg-methylation, the upper portions of drill-holes DPD-1 and DPD-3 had higher MeHg-degradation rates than the lower portion, and the reverse vertical trend was observed for drill-hole DPD-5. In fact, the deeper zone of DPD-5 exhibited the

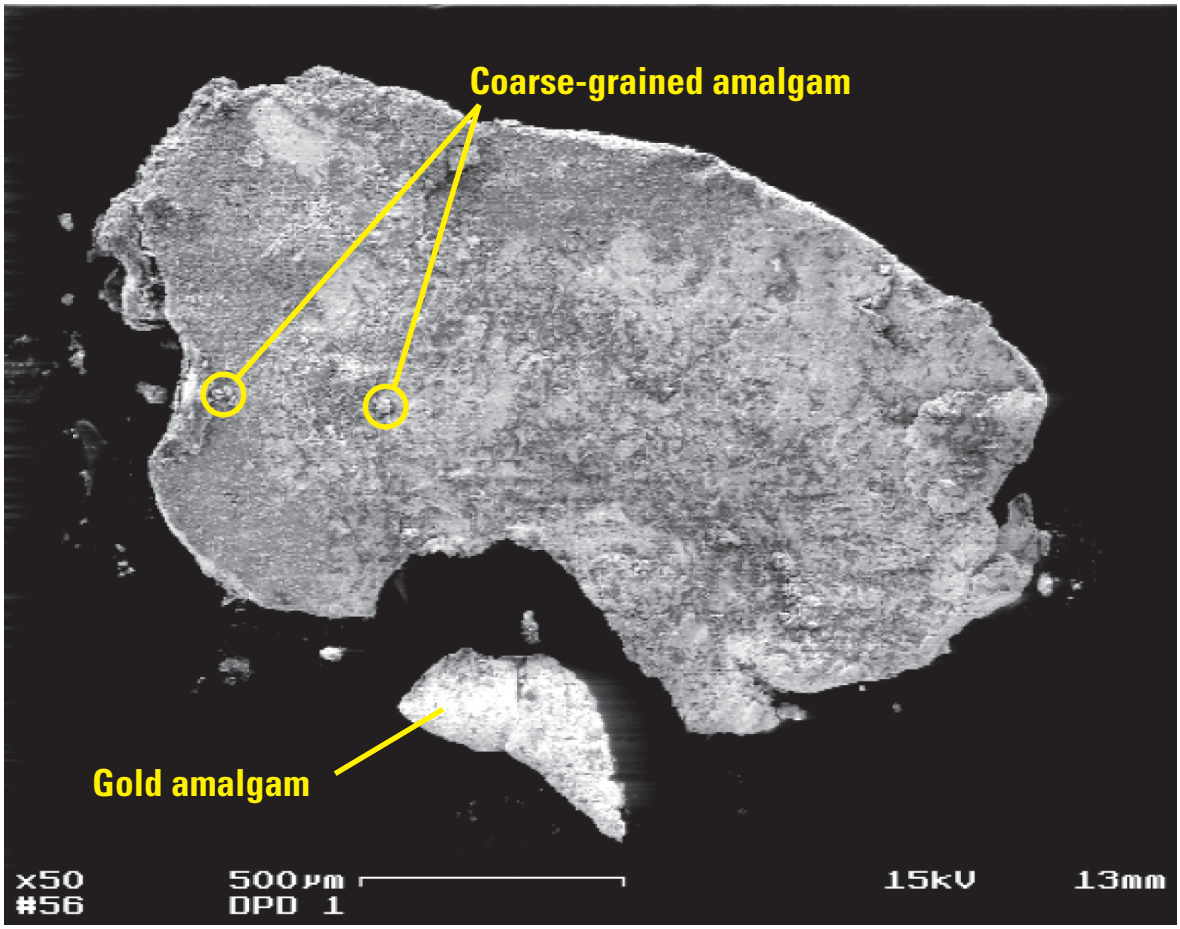

Figure 16. Scanning electron micrograph of broken gold-amalgam fragment from a gold grain, Daguerre Point Dam, California.

highest MeHg degradation rate in the entire sample set (N = 7). These results suggest that this deeper layer of original bed sediment had generally higher microbial activity than the overlying sediment, composed largely of hydraulic mining debris. The sediment layers with the greatest microbial activity gave rise to both increased levels of MeHg and higher levels of ^{14}C-MeHg degradation. Further, there was a generally positive relation, albeit statistically insignificant (P = 0.12), between ^{203}Hg(II)-methylation and ^{14}C-MeHg demethylation potentials (*fig. 20*).

Characterization of ancillary environmental variables revealed that samples from the upper intervals of core holes DPD-1, -3, and -5 generally had higher levels of solid-phase reduced sulfur than samples from the deeper intervals (*table 12*); the sulfur as acid volatile sulfide (AVS) ranged from 11 to 854 nmol/g dry sediment, and total reduced sulfur (TRS) ranged from 32 to 2,060 nmol/g dry sediment. Conversely, loss on ignition (LOI), a proxy for organic matter, ranged from 0.35 to 1.14 percent by weight and was higher in the deeper intervals for all of these profiles. In contrast, the trend in pore water DOC (8 to 63 mg/L) was not consistent with the trend in LOI. Sediment percent dry weight ranged from 68 to 87 percent, sediment pH ranged from 6.8 to 7.8, and sediment redox ranged from –409 mV to +477 mV. That the highest redox values were for the deeper samples from holes DPD-3 and -6 (*table 12*) was unexpected. The deeper sediments were buried many years ago (as discussed in a later section of the report), and the upper part of the core from DPD-3 was –379 mV. While oxygenated ground-water inflow can not be excluded as an explanation (inflow of Yuba River water through porous gravel), it is also possible that the high redox values reflect oxidation of these sediments during the sample collection and processing. If the latter is true, then the MeHg production and degradation potential assays also could have been similarly affected.

No significant relations were found between MeHg production or degradation potential and any of the above-mentioned environmental variables. However, the ratio of Hg(II)-methylation potential to MeHg degradation (or demethylation)

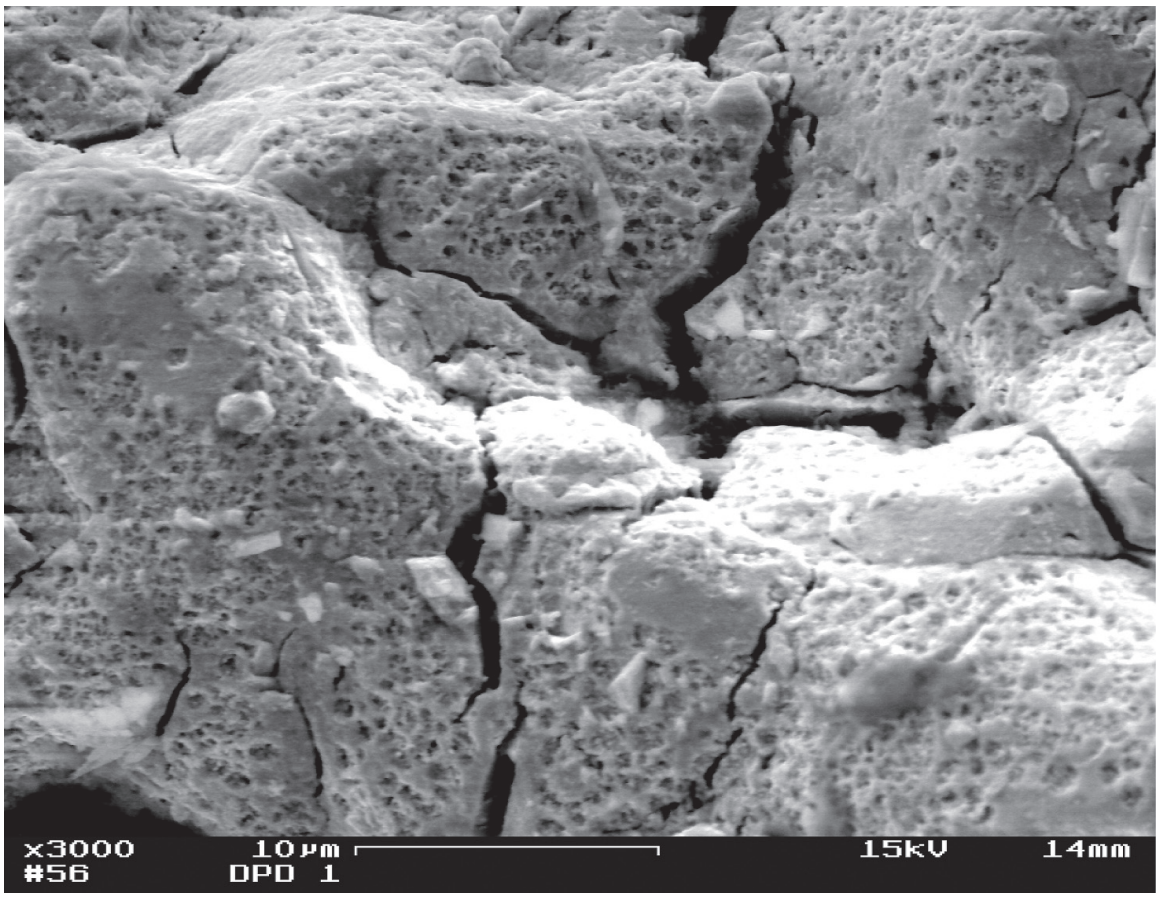

Figure 17. High-magnification scanning electron micrograph of gold-amalgam particle showing pitted surface, Daguerre Point Dam, California.

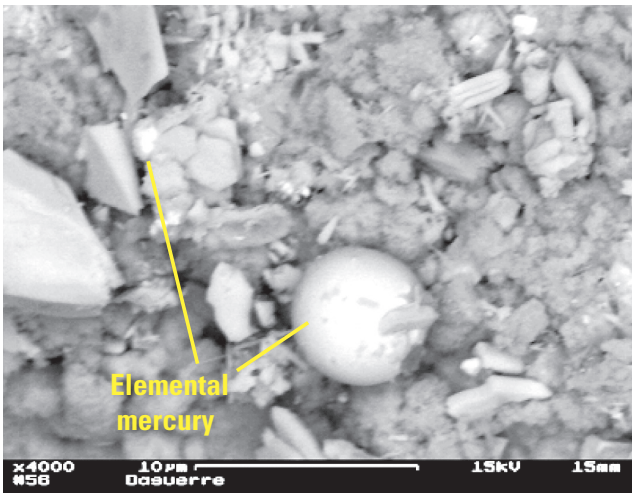

Figure 18. Scanning electron micrograph of elemental mercury in clay-silt fraction from 25 to 30 feet in drill hole DPD-2, Daguerre Point Dam, California.

potential (MP/DP, *table 11*) is highest for the two samples with highest sediment pH; the data were fit with non-linear, second-order polynomial function (*fig. 21*). Furthermore, using a multiple linear regression, we found that 96 percent of the variability in the ^{203}Hg-methylation rates could be explained by three variables (pH, E_h, and DOC) with the following equation:

$$^{203}\text{Hg-methylation} = 1.30[\text{pH}] - 1.12 \times 10^{-3}[E_h] - 1.98 \times 10^{-2}[\text{DOC}] - 8.45,$$

for $R^2 = 0.96$ and $P < 0.01$, where R is the regression correlation coefficient and P is the probability value.

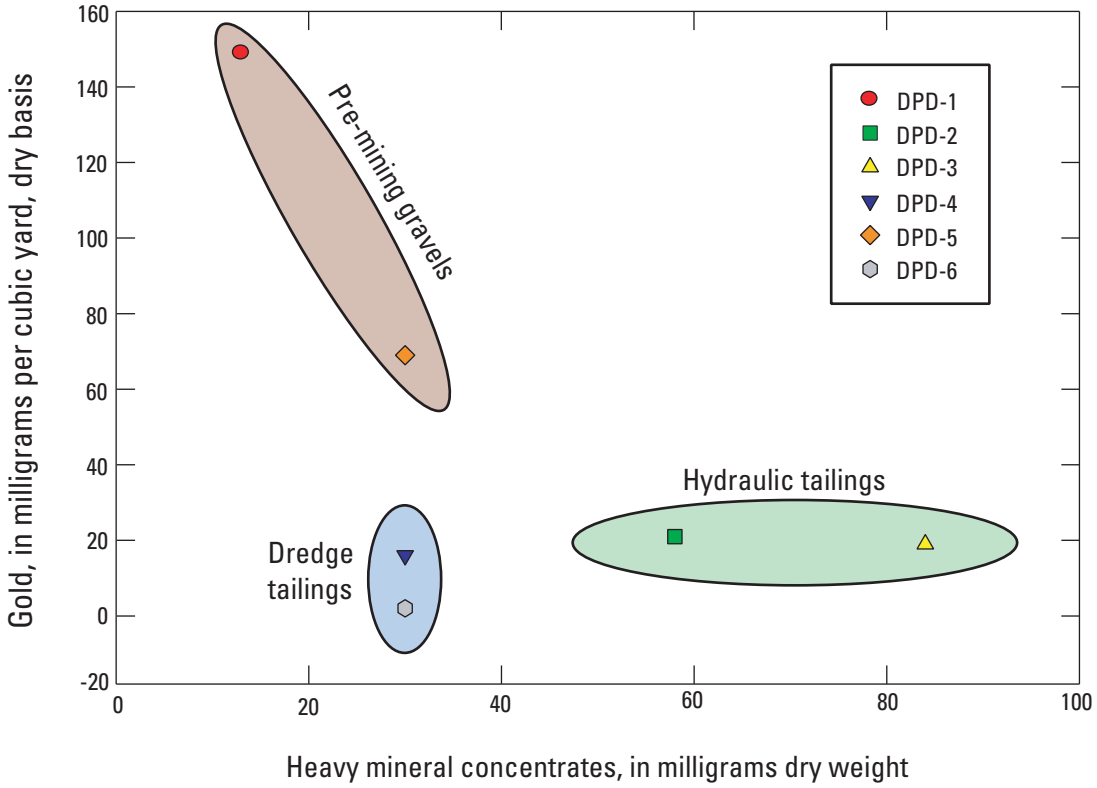

Figure 19. Graph showing geometric mean of gold tenor and heavy mineral concentrates, Daguerre Point Dam, California.

Table 11. Potential rates of mercury methylation and methylmercury degradation, Daguerre Point Dam, California.

[Standard deviations from the mean are given in parentheses when there are two replacates. $CH_3{}^{203}Hg^+$, methylmercury ion with radio-labeled mercury. $^{203}Hg(II)$, radio-laveled divalent mercury; ^{14}C-MeHg, methylmercury with radio-labeled carbon; $^{14}CH_3HgCl$, carbon-14 labeled methylmercury choloride; MP/DP, Hg-methylation/MeHg-degradation ratio, based on potential rate data; $^{14}CO_2$, carbon dioxide with radio-labeled carbom; $^{14}CH_4$, methane with radio-labeled carbon; ^{14}C-Total, the sum of $^{14}CO_2 + {}^{14}CH_4$. %/day, percent per day; DPD, Daguerre Point Dam. ft, foot; ng/g dry sed/d, nanogram per gram dry sediment per day; <, less than; n/a, not applicable]

Drill hole/ Depth (ft)	$^{203}Hg(II)$-methylation (%/day)[1]	$^{203}Hg(II)$-methylation (ng/g dry sed/d)[2]	^{14}C-MeHg degradation (%/day)[3]	^{14}C-MeHg degradation (ng/g dry sed/d)[4]	MP/DP	pH	$^{14}CO_2/{}^{14}C$-total[5]
			DPD-1				
0–5	0.08 (0.03)	0.42 (0.15)	12.6 (0.1)	1.5 (0.0)	0.28	6.8	0.91
10–15	<.03	<.15	6.5 (0.7)	1.0 (0.1)	<.15	6.8	1.00
			DPD-3				
3–5	0.31 (0.19)	1.57 (0.94)	9.9 (3.3)	1.1 (0.4)	1.37	7.8	0.50
15–20	<.03	<.15	8.1 (0.1)	1.0 (0.1)	<.15	7.2	.90
			DPD-5				
3–5	0.05	0.27	9.0 (2.2)	1.1 (0.1)	0.24	7.4	0.56
15–20	.29 (0.01)	1.55 (0.03)	17.7 (0.6)	2.2 (0.3)	.72	7.5	.25
			DPD-6				
25–30	<0.03	<0.15	8.2 (2.1)	1.1 (0.3)	<0.14	7.0	0.80
Median	0.05	0.27	9.0	1.1	0.24	7.2	0.8
Mean	n/a	n/a	n/a	n/a	0.44	n/a	n/a

[1] Percentage of radiolabeled $^{203}Hg(II)$ recovered as ^{203}Hg-methylmercury after 4-hour incubation, expressed on a per day basis.

[2] Hg-methylation potential normalized to sediment dry weight and calculated based on an amendment of 436 nanogram $^{203}Hg(II)$ per gram weight sediment.

[3] Percentage of radiolabeled $^{14}CH_3HgCl$ recovered as $^{14}CO_2$ plus $^{14}CH_4$ after 4-hour incubation, expressed on a per day basis.

[4] MeHg-degradation potential normalized to sediment dry weight and calculated based on an amendment of 10.5 nanogram $^{14}CH_3HgCl$(as Hg) per gram wet sediment.

[5] $^{14}CO_2/{}^{14}C$-total; this ratio gives some indication of whether the MeHg degradation pathway was largely oxidative (resulting in $^{14}CO_2$) or reductive (resulting in $^{14}CH_4$).

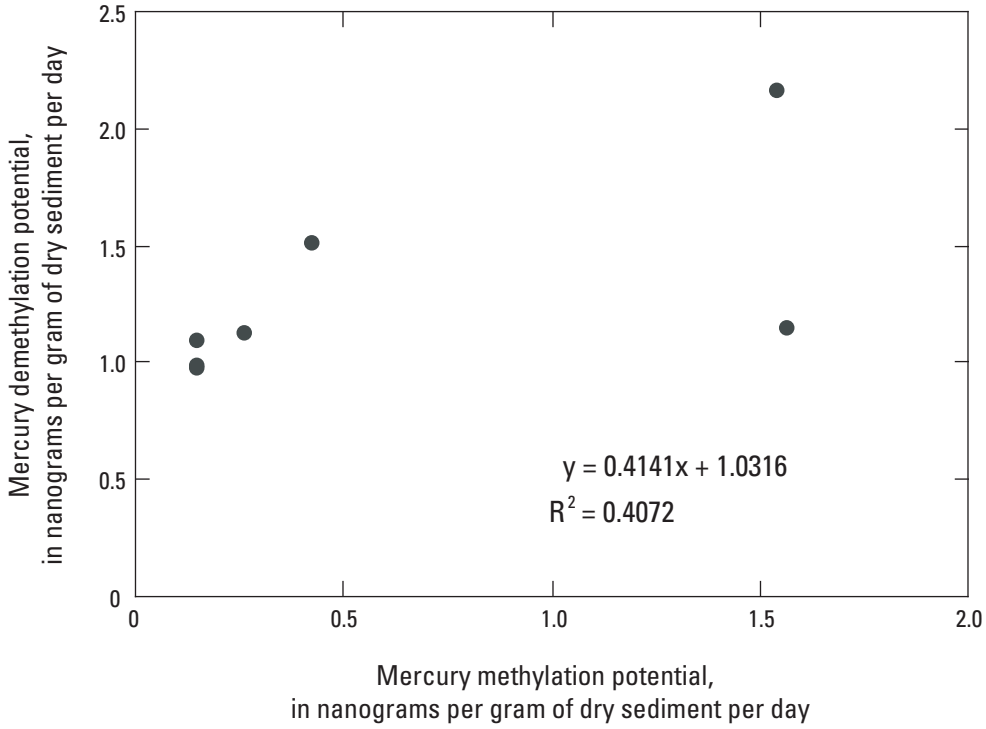

Figure 20. Graph showing relation between rates of mercury methylation potential and mercury demethylation potential, Daguerre Point Dam, California.

Table 12. Concentrations of acid volatile sulfur and total reduced sulfur in selected samples, Daguerre Point Dam, California.

[Acid volatile sulfur (AVS) assay = FeS; total reduced-sulfur (TRS) assay = FeS and FeS_2; TRS-AVS = FeS_2. DOC, dissolved organic carbon; DPD, Daguerre Point Dam. ft, foot; nmol/g dry sed, nanomole per gram dry sediment; mV, millivolt; mg/L, milligram per liter]

Drill hole/ Depth (ft)	Sediment						Pore water DOC (mg/L)[2]
	Acid volatile sulfur (nmol/g dry sed)	Total reduced sulfur (nmol/g dry sed)	Percentage weight loss on ignition	pH (standard units)	Redox E_h (mV)[1]	Percentage dry weight	
			DPD–1				
0–5	854	2,056	0.40	6.8	-335	84	10
10–15	19	34	1.14	6.8	-290	68	39
			DPD–3				
3–5	766	1,193	0.25	7.8	-379	87	27
15–20	19	32	.60	7.2	477	83	12
			DPD–5				
3–5	183	698	0.35	7.4	-409	81	63
15–20	16	55	.53	7.5	-379	80	8
			DPD–6				
25–30	11	649	0.72	7.0	249	77	11

[1] $E_h = E_m + E_r$, where E_m = the measured value (in mV) taken with the platinum electrode and E_r is the temperature-dependent correction for a standard hydrogen reference electrode (+207 to +211 mV).

[2] Sediment was first diluted with Milli-Q water to obtain enough sample for dissolved organic carbon analysis.

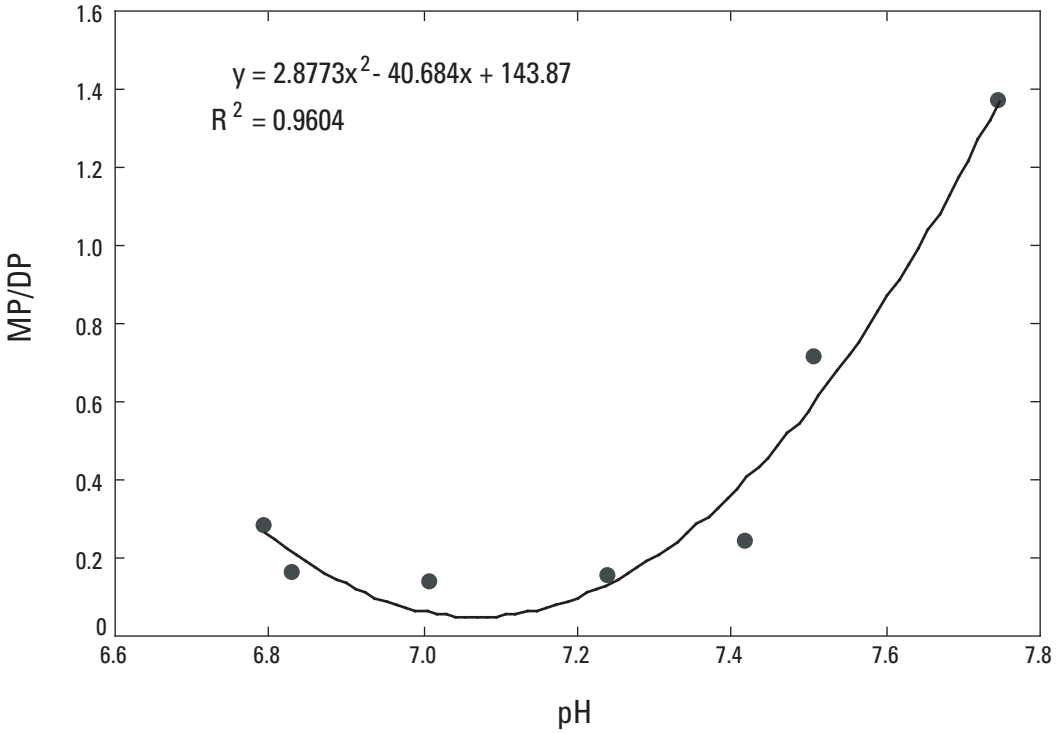

Figure 21. Graph showing ratio of mercury methylation potential (MP) to mercury demethylation potential (DP) as function of sediment pH, Daguerre Point Dam, California.

Discussion

Relation of Sediment Characteristics to Mining History

On the basis of results of this study and historical accounts, we hypothesize that the highest concentrations of mercury in sediments within the Yuba Goldfields are associated with undredged hydraulic mining tailings and the earliest dredged sediments. The dredging history of the area upstream of Daguerre Point Dam (*fig. 4*) is well documented. Field observations indicate that the area immediately north and west of the area dredged during 1916–34 consists primarily of remobilized hydraulic mine tailings (*fig. 5*). Because of the action of the Yuba River and the proximity to dredge tailings, it is likely that some of the sediment in this area consists of a mixture of hydraulic tailings and dredge tailings. Drill-holes DPD-5 and DPD-6 intersected sediments interpreted to consist of a mixture of hydraulic tailings and dredge tailings from the period 1916–68. The lowest concentration of mercury was found in drill-hole DPD-1, located in an area containing gravel relatively undisturbed by mining, according to analyses of mercury, gold, and heavy mineral concentrates (*figs. 15* and *19*). We suggest that the relatively low concentration of mercury (10.9 to 32.9 ng/g dry weight) in sediments from hole DPD-1 was transported to this location as bed load during flood events. Similarly, elevated gold values in the upper 5-foot intervals of DPD-2 and -5 (*fig. 15A*) may be because of flood gold deposition. Generally, moderate concentrations of mercury (7.50 to 80.7 ng/g dry weight) in sediments from holes DPD-2, -3, and -4 were consistent with that in dredged and re-dredged sediments. Exceptions were the two deepest intervals of hole DPD-2, which may have higher mercury concentrations as a result of mixing with hydraulic mine tailings.

The distribution of mercury corresponds well with that of gold and gold-mercury amalgam grains. The highest mercury concentration observed in this study was 1,100 ng/g, in the silty fraction of the 25- to 30-foot interval of hole DPD-2 (*table 7*); this anomalously high concentration was probably caused by a particle of amalgam, thus producing a nugget effect. This high concentration correlates with observations of abundant amalgam and traces of mercury in the heavy-mineral concentrate from the same interval (*table C2*).

There is a positive correlation between Hg_T concentration and the abundance of fine particles. In general, the finer the average particle size, the higher the concentration of Hg_T, indicating that most mercury is associated with the finer particle-size fractions of the sediments. This relation is demonstrated by the consistently lower concentrations of Hg_T in the sandy fraction compared with the finer grained silty and clay-silt fractions (*figs. 12* and *13*), and by the consistent increase in median mercury concentrations of sieved sediment fractions with decreasing grain size in the sand and silt size subclasses (*table 9*). Similarly, a positive relation between higher mercury concentration and finer particle size in dredge tailings and hydraulic mine tailings has been documented previously for sediment fractions <2 mm and <0.063 mm in the Clear Creek

drainage basin in Shasta County in northern California (Ashley and others, 2002).

The relation between the gold tenor in each drill hole and the mass of heavy mineral concentrates (*fig. 19*) helps to distinguish hydraulic mine tailings from dredge tailings. Hydraulic mine tailings contain a significantly higher proportion of heavy minerals (*table C2*), which are partially removed during dredging, thus decreasing the amount in dredge tailings. Upstream of Daguerre Point Dam, dredge tailings are distinguished by many discordant lenses of fine-grained sediment because of the different settling velocities of particles in old dredge ponds and infilling with coarser sediment from past dredging and flooding.

Loss of Mercury during Drilling

Drilling in permeable sediments below the elevation of the Yuba River produced a significant volume of water along with sediment, which complicated the sampling and characterization effort. Overflow generated from each drill hole contained suspended sediment consisting predominantly of silt and clay (silty fraction, *figs. 8*, *10*, and *11*). Because the highest concentrations of mercury observed in this study are in the relatively fine-grained fractions, it is clear that some mercury was lost. To calculate the in-place concentration of mercury in sediments prior to drilling, it is necessary to combine mercury concentration data for the various size fractions produced from the process stream (*fig. 8*). The total amount of mercury in the sediment deposit behind Daguerre Point Dam remains uncertain because we do not know quantitatively the proportion of fine material lost from every drilled interval in the overflow streams (silty fraction and clay-silt fraction). The volumes and (or) masses of material recovered and discarded were determined for each drilled interval. For the selected intervals for which the concentration of suspended sediment was determined in the waste streams, a mass balance approach can be used to estimate the relative proportions of fine and coarse sediment in the in-place deposit. Mass balance calculations were not completed as part of this report, but could be done with existing data (*tables 3-9*, *tables B1-B5*).

Environmental Factors Influencing Mercury Methylation and Demethylation

Although only seven samples were used to calculate the potential rates of mercury methylation and demethylation (*table 11*) in this study, it was encouraging to find that a combination of factors controlling the availability of Hg(II) to sulfate-reducing bacteria could be used to explain essentially all of the variability in the Hg-methylation potential rate measurement. No comparable combination of environmental factors adequately explained the variability in ^{14}C-MeHg-degradation (mercury demethylation). However, there was a decrease in the $^{14}CO_2/(^{14}CO_2 + {}^{14}CH_4)$ end-product ratio (simplified as the ratio CO_2/C) with increasing pH (*fig. 22*). It has been reported that this ratio increases with increasing sulfate concentration (and presumably increasing rates of microbial sulfate reduction) in Florida Everglades sediments (Marvin-DiPasquale and others, 2000). Methylmercury degradation can proceed by a number of pathways, including reductive *mer* detoxification (Robinson and Tuovinen, 1984) and oxidative demethylation (Oremland and others, 1991, 1995). In the former process, MeHg degrades to CH_4 as a detoxification response by bacteria to high levels of MeHg. In the case of oxidative demethylation, CO_2 alone or CO_2 plus CH_4 are the primary end-products, and it has been hypothesized that the outcome depends on whether the dominant bacterial groups responsible for the degradation are sulfate reducers or methanogens, respectively (Marvin-DiPasquale and others, 2000). Thus, the shift to lower values of CO_2/C in the end-product of MeHg degradation with increasing pH may imply differences in the primary microbial communities in different pH environments at different depths.

The correspondence of elevated concentrations of reduced sulfur (AVS and TRS) with Hg-methylation potential in the shallow samples from holes DPD-1 and -3 may have been at least partially affected by the process of sampling. As the reduced sulfur-rich cores were being taken, some oxygenated, overlying water likely entered the coring hole and was mixed with the deep sediment substrate. The sediment was then homogenized in a bucket in the open atmosphere, which likely reoxidized some reduced sulfur to sulfate. Prior to drilling, the in-place sulfate concentrations may have been very low, or fully depleted, below the top few feet of the sediment profile. Thus, the sampling process may have stimulated sulfate-reducing bacteria, previously limited by low sulfate concentrations. Theoretically, this could have initiated a pulse

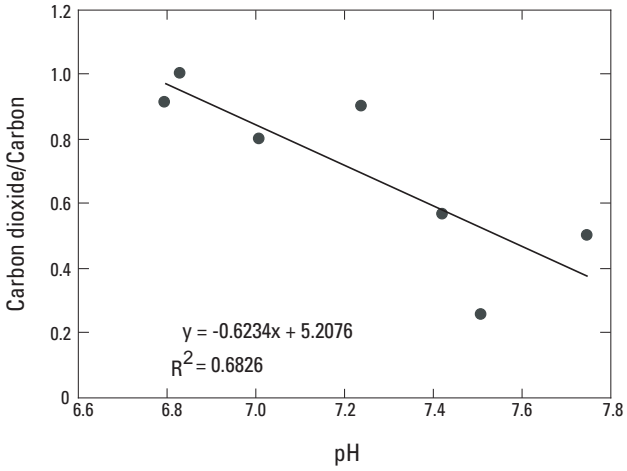

Figure 22. Graph showing carbon-14 end-product ratio (CO_2/C) from mercury demethylation experiments as a function of sediment pH, Daguerre Point Dam, California.

of Hg-methylation activity and an increase in MeHg concentration. Although this is speculative (higher Hg-methylation potentials were also seen at the deeper depth for drill-hole DPD-5), the discussion is relevant to the situation that might occur should the sediments be dredged, excavated, or eroded as part of a fish passage improvement project.

Implications for Downstream Mercury Transport

Because elemental mercury has a strong propensity to flour, agitating and disturbing contaminated sediments cause it to break down into continuously smaller particles. The grain size of elemental mercury observed in this study was 6 µm and less (*fig. 18*). Larger particles of mercury are commonly observed in close proximity to hydraulic mines (Hunerlach and others, 1999), and the grain size is reduced during fluvial transport downstream. If sediments from Daguerre Point Dam were released downstream, further breakdown of elemental mercury particles would lead to increased surface area, which could lead to a higher degree of reactivity and potential for oxidation and methylation.

Concentrations of MeHg in the sediments behind Daguerre Point Dam are relatively low; therefore, MeHg alone probably would not be a significant risk if the sediments were released in conjunction with a fish passage improvement project. However, inorganic mercury associated with these sediments, especially the finer grained fractions, could transform to MeHg after it is released. The relatively high levels of reduced-S buried in these sediments could stimulate Hg methylation should the environment of these currently buried sediments be changed from reducing to oxidizing. The extent of increased Hg(II)-methylation would depend on the reactivity of the inorganic Hg(II) fraction associated with these sediments, which is currently unknown. It is also unknown how long this stimulation would last; it likely depends on the extent of reoxidation of reduced-S pools, the amount and depth of sediment removed, the characteristics of downstream depositional areas, the amount of microbially available Hg(II), and the final disposition of the dredged material.

Implications for Geomorphology and Hydrogeology

Data from historical exploration drill holes to the east and southeast of Daguerre Point, made available to the USGS by Cal Sierra Development Incorporated, made it possible to construct bedrock elevation contours (*fig. 3*, *plate 1*). Drill-hole depth and bedrock elevation data were interpreted by the USGS and plotted to create a contour map showing the elevation of the top of bedrock. The resulting map was then compared with a 1941 bedrock contour map from the Yuba Consolidated Goldfield records and a historical map (Weatherbe, 1907) of the Yuba River channel near Daguerre Point. Both maps confirm a bifurcation of the deeper and older channel of the Yuba River Channel upstream of the Daguerre Point Dam and a pre-dam flow path to the south south-west around the outcrop of Daguerre Point (*fig. 3*, *plate 1*).

Bedrock elevation at Daguerre Point Dam is about 30 feet above the lowest elevation of deposited hydraulic mine tailings, indicating that the gravel bed of the Yuba River was lower before being inundated with debris. An estimated 300,000,000 cubic yards of hydraulic mining debris was deposited in the bed of the Yuba River, which varied from 12 to 30 feet in depth (Weatherbe, 1907). Historical cross-sectional data generated in the 1940s by the Yuba Consolidated Goldfield show that tailings from hydraulic mine debris ranged in thickness from 16 to 82 feet, almost 50 feet greater than previously reported (Gilbert, 1917). Free elemental mercury (that has not been fully absorbed into gold grains found within tailings) may be available for dispersion through abrasion when disturbed.

The range in elevation from the crest of Daguerre Point Dam to the lowest bedrock south of the dam varies from 200 to 225 feet (*plate 1*). If Daguerre Point Dam is removed to improve fish passage, the Yuba River could attempt to reestablish its original channel course to the south of Daguerre Point, eroding hydraulic mine debris and dredge tailings. The northern abutment of Daguerre Dam is anchored in an excavated portion of an older natural levee along the right bank of the Yuba River. Prior to construction of Daguerre Point Dam, the older channel turned south and flowed around the more resistant topographic high point of Daguerre Point. During flood stage in 1997, the Yuba River flowed both over and around Daguerre Point Dam and through the Yuba Goldfields following the older channel. About one mile south of Daguerre Point, the ancestral Yuba River flowed southwest to west, through a deep narrow gorge (*plate 1*, *fig. 3*). Reconstruction of the contour lines for the bedrock surface using the historical drill-hole data, together with results of this study, shows a geologically controlled bend to the southwest that has apparently contributed to the deep incision of the older channel during its early history.

Downstream of Daguerre Point Dam, coarse gravels and cobbles are found within the training walls, and in buried lenses upstream of the dam and throughout the dredged portion of the goldfields. The coarse, unconsolidated gravel deposits typically have a high hydraulic conductivity, which allows rapid seepage of ground water. Ground-water seepage through the training walls may affect flow in the main channel of the Yuba River. One possibility is that subsurface flow occurs along the bedrock-gravel contact and (or) through coarse gravel lenses in a deeper channel (the former river channel) to the south of the present channel. The flow in the deeper channel re-enters the main channel of the lower Yuba River approximately 1 to 1.5 miles downstream of Daguerre Point Dam.

Comparing drill-hole data from this USGS report with historical drill-hole data and bedrock contour maps indicates a wide range of distribution in the types of previously mined sediments stored upstream of the Daguerre Point Dam. Hydraulic mine tailings contain the highest concentration of mercury and gold-amalgam and, therefore, should be of greatest concern for downstream transport. Fine-grained lenses of hydraulic mine sediments buried by dredge tailings may be remobilized if the relatively coarse-grained dredge tailings are eroded due to river degradation in response to dam removal

We observed subsurface flows through the previously mined, coarse-grained dredge tailings (such as training walls and other cobble-rich berms) upstream of the Daguerre Point Dam. In response to topographic gradients, subsurface flows increase toward the deeper bedrock depression of the ancestral Yuba River channel and toward lower-elevation wetlands ponds throughout the Yuba Goldfields. The topographic gradient in the bedrock elevation surface to the south indicates that the Yuba River near and upstream of Daguerre Point Dam may be a losing stream. A recent water-balance analysis (ENTRIX, 2003) concluded that some loss of flow may occur from the Yuba River channel between Englebright Dam and Marysville, but total flow from the river channel could not be fully addressed with available data. The ENTRIX (2003) analysis also concluded that additional flow enters the Yuba River (either as ungaged surface flow or ground-water flow), resulting in higher flows at Marysville than water balance calculations indicated.

Our recent observations indicate that a substantial portion of the fine-grained material has been eroded from the base of the training walls used to stabilize the Yuba River channel; the fine-grained material has been deposited in isolated ponds within the dredged rows of tailings. Removal of Daguerre Point Dam may allow velocities to increase and cause the Yuba River to scour and migrate back to its original channel in the south by undercutting both the training walls and rows of dredge tailings. If a new flow path is established, large quantities of debris and tailings would be available for the Yuba River to transport downstream, which could either enhance or degrade fish habitat, depending on the fish species and the sediment transport characteristics.

It is interesting to note that, from October 1905 to October 1906, the total detrital load (mostly hydraulic tailings) of the Yuba River near the Daguerre Point Dam location was calculated to be 7,200,000 cubic yards and consisted of 31 percent silt, 26 percent sand, and 43 percent gravel (Gilbert, 1917). The average grain-size distribution from the six USGS drill holes (residual sandy fraction plus gravel, *table 2*) is 6 percent silt and clay, 49 percent sand, and 45 percent gravel. The decrease in silt and increase in sand may be attributed to concentration of fines caused by dredging, to stratification of sand-silt lenses in settling ponds, and, to a lesser extent, to the loss of fine material (silty and clay-silt fractions) during drilling.

Particle-size distribution varies greatly and depends on the type of mining and the amount of reworking of hydraulic debris and earlier dredge tailings. About 55 percent of the sediment stored behind Daguerre Point Dam is sand-size and smaller. Because the stratigraphy and particle-size distribution is highly variable, there may be a larger proportion of silt and clay in sediments throughout the Yuba Goldfields. In general, these finer particle sizes contain more mercury and are widely distributed in the fluvial tailings upstream of Daguerre Point Dam.

Summary

The Daguerre Point Dam was built in the early 1900s to retain mining debris from the hydraulic placer-gold mines in the upper Yuba River watershed. The current position of the Yuba River behind the Daguerre Point Dam is north of its original pre-mining channel and above its prior stream bed elevation. At present, the lower Yuba River below Daguerre Point Dam has abandoned the training walls constructed in the early 1900s and has assumed a meandering course through the fluvial tailings. Hydraulic mine tailings from the upper Yuba River watershed and local sources, as well as previously unmined gravels upstream of the Daguerre Point Dam, were dredged almost continually between 1904 and 1968; some areas were dredged multiple times to progressively increasing depth. Mercury and gold-amalgam lost from previous hydraulic mining operations have been recovered since 1904 by dredging, which has been the principal method of mining in the Yuba Goldfields. More than 1 billion cubic yards of gold-bearing gravel have been dredged in the Yuba Goldfields. Dredging was active until 2003, when this activity stopped because of a sunken dredge.

Drill-hole data from this study compared with historical drill-hole data and bedrock elevation contour maps indicate a wide range of distribution in the types of previously mined sediments stored behind Daguerre Point Dam. About 55 percent of sediment presently stored upstream of Daguerre Point Dam is sand size or smaller. The highest concentrations of mercury are associated with the finer particle sizes, especially in the residual (undredged) hydraulic mine tailings. These tailings are thickest closest to the dam and attenuate with depth upstream from USGS drill-hole DPD-2 to DPD-3.

Typically, the surface of the exposed gravel bars and the bed of the Yuba River upstream of Daguerre Point Dam are well armored with coarse gravel to a depth of several feet. Hydraulic mine tailings stored upstream of the dam can be transported during flood stage. Although most of the fine particles pass over the dam, some consisting of the heaviest minerals, including gold and gold-mercury amalgam, can become trapped in the interstices of the gravel. The remnant portions of the training walls upstream of the dam contain some of the earliest dredged material and continue to supply fine-grained sediment to the river bed as they erode.

Concentrations of mercury and several other trace elements in the fine-grained sediment trapped behind Daguerre

Point Dam are of potential environmental concern. Median concentration values of arsenic, chromium, copper, and nickel in clay-silt separates (less than 0.060 millimeter) were higher than consensus threshold effects levels for ecological toxicity; maximum concentrations of lead, mercury, and zinc were also above the threshold effects levels. Total mercury concentrations were 3 to 30 times higher in fine-grained fraction than in the sandy fraction. Although concentrations of methylmercury are relatively low in sediments trapped behind Daguerre Point Dam, there is a potential for converting a significant portion of inorganic mercury to methylmercury if these sediments are released to the lower Yuba River below Daguerre Point as a consequence of fish passage improvement projects. Oxidation of reduced sulfur in the sediments would produce aqueous sulfate; given the right environmental conditions, the additional sulfate could stimulate sulfate-reducing bacteria, which are thought to be the principal microbes that methylate mercury. Additional testing is needed to make more quantitative predictions of the consequences of sediment remobilization in this system.

References Cited

Alpers, C.N., and Hunerlach, M.P., 2000, Mercury contamination from historic gold mining in California: U.S. Geological Survey Fact Sheet 061-00, 6 p., also available at *http://ca.water.usgs.gov/mercury/fs06100.html*.

Alpers, C.N., Taylor, H.E., and Domagalski, J.L. eds., 2000, Metals transport in the Sacramento River, California, 1996–97. Volume 1. Methods and Data: U.S. Geological Survey Water-Resources Investigations Report 99-4286, 429 p., also available at *http://water.usgs.gov/pubs/wri/wrir_994286/*.

American Public Health Association, 1981, Section 209G: Volatile and fixed matter in nonfilterable residue and in solid and semisolid samples, *in* Franson, M.A.H., ed., Standard Methods form the Examination of Water and Wastewater (15th ed): Washington, D.C., American Water Works.

Ashley, R.P., Rytuba, J.J., Rogers, Ronald, Kotlyar, B.B., and Lawler, David, 2002, Preliminary report on mercury geochemistry of placer gold dredge tailings, sediments, bedrock, and waters in the Clear Creek Restoration Area, Shasta County, California. U.S. Geological Survey Open-File Report 02-401, 47 p.

Aubrey, L.E., 1910, Gold dredging in California: California State Mining Bureau, Bulletin 57, 312 p.

Bureau of Land Management, 2001, Land status map of the Yuba Goldfields: Bureau of Land Management, Folsom Field Office, 63 Natoma Street, Folsom, Calif.

California Department of Water Resources, 2003, Daguerre Point Dam – Yuba River, in Fish passage improvement: An element of CALFED's Ecosystem Restoration Program: Bulletin 250-2002, Public Review Draft, v. 2, p. 4-15 to 4-16, also available at *http://www.isi.water.ca.gov/fish/ChapterFront/Front%20Matter.pdf*.

California State Water Resources Control Board, 2003, Order vacating Water Right Decision 1644 and adopting revised Water Right Decision 1644 following consideration of additional evidence specified by Yuba County Superior Court, Order WR 2003-0016, 57 p., also available at *http://www.waterrights.ca.gov/hearings/WaterRightOrders/WRO2003-16.pdf*.

Churchill, R.K., 2000, Contributions of mercury to California's environment from mercury and gold mining activities: Insights from the historical record, *in* Extended abstracts for the U.S. EPA sponsored meeting, Assessing and managing mercury from historic and current mining activities, November 28-30, 2000, San Francisco, Calif. p. 33-36 and S35-S48.

Compeau, G.C., and Bartha, R., 1985, Sulfate-reducing bacteria: Principal methylators of mercury in anoxic estuarine sediment: Applied and Environmental Microbiology, v. 50, no. 2, p. 498-502.

De Wild, J.F., Olson, M.L., and Olund, S.D., 2002, Determination of methyl mercury by aqueous phase ethylation, followed by gas chromatographic separation with cold vapor atomic fluorescence detection: U.S. Geological Survey Open-File Report 01-455, 14 p., also available at *http://wi.water.usgs.gov/pubs/ofr-01-445/ofr-01-445.pdf*.

ENTRIX, 2003, Daguerre Point Dam Fish Passage Improvement Project, 2002 Water Resources Studies, prepared for California Department of Water Resources and U.S. Army Corps of Engineers, Stakeholder Review Draft, June 2003, 47 p.

Farrar, J.W. 1998, Results of the U.S. Geological Survey's analytical evaluation program for standard reference water samples: T-153 (trace constituents), M-146 (major constituents), N-57 (nutrient constituents), N-58 (nutrient constituents), P-30 (low ionic strength constituents), GWT-3 (ground -water major constituents), and Hg-26 (mercury) distributed in April 1998: U.S. Geological Survey Open-File Report 98-391, 160 p.

Gilbert, G.K., 1917, Hydraulic-mining debris in the Sierra Nevada: U.S. Geological Survey Professional Paper 105, 154 p.

Gilmour, C.C., Henry, E.A., and Mitchell, R., 1992, Sulfate stimulation of mercury methylation in freshwater sediments: Environmental Science and Technology, v. 26, p. 2281-2287.

Hagwood, J.J., 1981, The California Debris Commission: A history of the hydraulic mining industry in the western Sierra Nevada of California, and of the government agency charged with its regulation: Prepared for the U.S. Army Corps of Engineers, Sacramento, Calif., 102 p.

Hintelmann, H., 1999, Comparison of different extraction techniques used for methylmercury analysis with respect to accidental formation of methylmercury during sample preparation: Chemosphere, v. 39, p. 1093-1105.

Hintelmann, H., Falter, R., Ilgen, G., and Evans, R.D., 1997, Determination of artifactual formation of monomethylmercury in environmental samples using stable Hg^{2+} isotopes with ICP-MS detection-calculation of contents applying species specific isotope addition: Fresenius' Journal of Analytic Chemistry, v. 358, p. 363-370.

Hunerlach, M.P., Rytuba, J.J., and Alpers, C.N., 1999, Mercury contamination from hydraulic placer-gold mining in the Dutch Flat mining district, California, *in* Morganwalp, D.W., and Buxton, H.T., eds., U.S. Geological Survey Toxic Substances Hydrology Program – Proceedings of the Technical Meeting, Charleston, South Carolina, March 8-12, 1999: U.S. Geological Survey Water-Resources Investigations Report 99-4018B, v. 2, p. 179-190.

Janin, Charles, 1918, Gold dredging in the United States: U. S. Bureau of Mines Bulletin 36, 120 p.

Klasing, Susan, and Brodberg, Robert, 2003, Evaluation of potential health effects of eating fish from selected water bodies in the northern Sierra Nevada foothills (Nevada, Placer, and Yuba Counties): Guidelines for sport fish consumption: California Environmental Protection Agency, Office of Environmental Health Hazard Assessment, 48 p., also available at *http://www.oehha.ca.gov/fish/pdf/SierraLakesAdvisoryfinal.pdf*.

Lindgren, W., 1911, The Tertiary gravels of the Sierra Nevada of California: U.S. Geological Survey Professional Paper 73, 226 p.

MacDonald, D.D., Ingersoll, C.G., and Berger, T.A. 2000, Development and evaluation of consensus-based sediment quality guidelines for freshwater ecosystems: Archives of Environmental Contamination and Toxicology, v. 39, p. 20-31.

Marvin-DiPasquale, M., Agee, J., Bouse, R., and Jaffe, B., 2003, Microbial cycling of mercury in contaminated pelagic and wetland sediments of San Pablo Bay, California: Environmental Geology, v. 43, no. 3, p. 260-267.

Marvin-DiPasquale, M., Agee, J., McGowan, C., Oremland, R.S., Thomas, M., Krabbenhoft, D., and Gilmour, C., 2000, Methylmercury degradation pathways: A comparison among three mercury-impacted ecosystems: Environmental Science and Technology, v. 34, no. 23, p. 4908-4916.

Marvin-DiPasquale, M.C., and Capone, D.G., 1998, Benthic sulfate reduction along the Chesapeake Bay central channel. I. Spatial trends and controls: Marine Ecology Progress Series, v. 168, p. 213-228.

Marvin-DiPasquale, M.C., and Oremland, R.S., 1998, Bacterial methylmercury degradation in Florida Everglades peat sediment: Environmental Science and Technology, v. 32, no. 17, p. 2556-2563.

May, J.T., Hothem, R.L., Alpers, C.N., and Law, M.A., 2000, Mercury bioaccumulation in fish in a region affected by historic gold mining: The South Yuba River, Deer Creek, and Bear River Watersheds, California, 1999: U.S. Geological Survey Open File Report 00-367, 30 p., also available at *http://ca.water.usgs.gov/archive/reports/ofr00367/index.html*.

Mining and Scientific Press, 1905, Control of hydraulic mining debris in California by the Federal Government, September 2, 1905, p. 152-155

Olson, M.L., and De Wild, J.F., 1999, Low-level collection techniques and species-specific analytical methods for mercury in water, sediment, and biota, *in* Morganwalp, D.W., and Buxton, H.T., eds., U.S. Geological Survey Toxic Substances Hydrology Program—Proceedings of the Technical Meeting, Charleston, South Carolina, March 8-12, 1999: U.S. Geological Survey Water-Resources Investigations Report 99-4018B, v. 2, 11 p., also available at *http://wi.water.usgs.gov/pubs/WRIR-99-4018-B/*.

Oremland, R.S., Culbertson, C.W., and Winfrey, M.R., 1991, Methylmercury decomposition in sediments and bacterial cultures: Involvement of methanogens and sulfate reducers in oxidative demethylation: Applied and Environmental Microbiology, v. 57, no. 1, p. 130-137.

Oremland, R.S., Miller, L.G., Dowdle, P., Connell, T., and Barkey, T., 1995, Methylmercury oxidative degradation potentials in contaminated and pristine sediments of the Carson River, Nevada: Applied and Environmental Microbiology, v. 61, p. 2745-2753.

Peart, D.B., Antweiler, R.C., Taylor, H.E., Roth, D.A., and Brinton, T.I., 1998, Re-evaluation and extension of the scope of elements in US Geological Survey Standard Reference Water Samples: Analyst, v. 123, p. 455-476.

Qian, J., and Mopper, K., 1996, Automated high-performance, high-temperature combustion total organic carbon analyzer: Analytical Chemistry, v. 68, no. 18, p. 3090-3097.

Robinson, J.B., and Tuovinen, O.H., 1984, Mechanisms of microbial resistance and detoxification of mercury and organomercury compounds: Physiological, biochemical, and genetic analyses: Microbiology Reviews, v. 48, no. 2, p. 95-124.

Slotton, D. G., Ayers, S.M., Reuter, J.E., and Goldman, C.R., 1997, Gold mining impacts on food chain mercury in northwestern Sierra Nevada streams (1997 revision), Appendix B in Larry Walker Associates, Sacramento River watershed mercury control planning project-report for the Sacramento Regional County Sanitation District: Sacramento, Calif., Larry Walker Associates, 74 p.

Taylor, H.E., 2001, Inductively coupled plasma-mass spectromity: Practices and techniques: Academic Press, San Diego, Calif., 294 p.

Ulrich, G.A., Krumholz, L.R., and Suflita, J.M., 1997, A rapid and simple method for estimating sulfate reduction activity and quantifying inorganic sulfides: Applied and Environmental Microbiology, v. 63, no. 4, p. 1627-1630.

Weatherbe, D'Arcy, 1907, Dredging for gold in California: Mining and Scientific Press, 217 p.

Wells, John, 1973, Placer examination—Principles and practice: Bureau of Land Management Technical Bulletin 4, 209 p.

Yeend, W.E., 1974, Gold-bearing gravel of the ancestral Yuba River, Sierra Nevada, California: U.S. Geological Survey Professional Paper 772, 44 p.

Appendixes

Appendix A. Description of Drill Sites, Daguerre Point Dam, California

Table A1. Drill hole lithology, Daguerre Point Dam, California.

[ft, foot; DPD, Daguerre Point Dam]

Drill hole/Depth (ft)	Date	Time	Lithology
			DPD-1
0–5	8/14/01	1200	sandy gravel with light brown, quartz-rich silt
5–10	8/14/01	1200	sandy gravel with medium brown, quartz-rich silt
10–15	8/14/01	1200	dark brown silty clay with some gravel and increasing black sands; VG observed in fines
15–17.5	8/14/01	1500	reddish brown silty clay and angular greenstone rock, bedrock
			DPD-2
0–5	8/15/01	1200	very coarse sand-rich gravel with cobbles
5–10	8/15/01	1400	up to 50 per cent quartz-rich sandy gravel with light brown silty clay
10–13.5	8/15/01	1600	greenstone boulder
13.5–15	8/16/01	1030	quartz-rich sand with abundant pebbles
15–20	8/16/01	1200	large cobbles with sub-rounded sand and pebbles; some angular fractured gravel
20–25	8/16/01	1330	80 per cent fine-grained silty sand and increasing silt with depth
25–30	8/16/01	1500	silty sand with some gravel and increase in reddish clay
30–35	8/16/01	1700	quartz-rich sand
			DPD-3
0–5	8/20/01	1030	large cobble and gravel with quartz-rich sand
5–10	8/20/01	1100	gravel and quartz-rich sand; some sandy silt
10–15	8/20/01	1330	gravel and sand with reddish brown silty clay
15–20	8/20/01	1500	70-80 per cent sandy silt with some gravel
			DPD-4
0–10	8/21/01	1300	compacted quartz-rich sandy gravel with large greenstone fragments
10–15	8/21/01	1530	quartz-rich sandy gravel with iron-stained pebbles; wood at 14.5 feet
15–20	8/22/01	900	20 per cent quartz sand and reddish brown to light brown silt
20–25	8/22/01	1100	sand-rich gravel with 20 per cent sandy silt
25–30	8/22/01	1230	dark reddish brown silty clay with large pebbles; “hardpack” at 28 feet; increase in greenish sand
			DPD-5
0–5	8/24/01	1030	gravelly sand
5–10	8/24/01	1130	40 per cent quartz-rich pebbly sand with light brown silty clay
10–15	8/24/01	1430	increasing sand with medium brown silty clay
15–20	8/24/01	1530	quartz-rich sandy silt with increasing greenstone fragments; broke cable at 20 feet
			DPD-6
0–5	8/27/01	1530	quartz-rich pebbly sand; light brown silty clay
5–10	8/28/01	930	reddish brown silty clay with quartz pebbles and sand
10–15	8/28/01	1130	20 per cent quartz pebbles; sand, and reddish brown silty clay
15–20	8/28/01	1330	quartz pebbles, sand, and reddish brown silty clay
20–25	8/28/01	1430	25 per cent sand with pebbles and cobbles; reddish brown silty clay with greenstone rocks
25–30	8/28/01	1530	pebbly sand, increasing dark brown silty clay

Table A2. Physical description of sediments used to determine mercury methylation and demethylation potentials, Daguerre Point Dam, California.

[ft, foot; °C, degrees Celsius; DPD, Daguerre Point Dam]

Site	Depth interval (ft)	Collection date	Subsampling date	Sample description	Sediment temperature (°C)	Incubation temperature (°C)
DPD-1	0-5	8/14/01	8/30/01	About a 50–60 percent sandy silt with a gray/white color	18	19
DPD-1	10-15	8/14/01	8/30/01	A silty clay with a high percentage of decomposed greenstone; sample was a reddish brown color and represents the gravel/bedrock interface.	18	19
DPD-3	3-5	8/20/01	8/30/01	60-70 percent quartz-rich sandy silt with a gray/white color; some pea-gravel and small cobbles.	18	19
DPD-3	15-20	8/20/01	8/30/01	70-80 percent sandy silts with a dark reddish brown color.	18	19
DPD-5	3-5	8/24/01	8/30/01	Pebbly sand with light brown silts and clays of which about 40 percent is a quartz-rich sand.	20	19
DPD-5	15-20	8/24/01	8/30/01	Sandy silt with small pebbles and a high percentage of greenstone; at about 17.5 ft, large angular boulders of greenstone were encountered (probably bedrock of the Daguerre Point outcrop near the drill hole).	20	19
DPD-6	25-30	8/27/01	8/30/01	Pebbly sand with reddish brown silty clays and lots of broken greenstone rock.	unknown	19

Appendix B. Particle-Size Distribution of Sediments, Daguerre Point Dam, California

Table B1. Particle-size distribution of the sandy fraction plus gravel for sizes ranging from 75 millimeters to 0.075 millimeter, Daguerre Point Dam, California.

[DPD, Daguerre Point Dam; ft, foot; mm, millimeter; g, gram; —, no data]

Drill-hole/Depth (ft)	Percentage of particles passing through sieve										Sample mass (g)
Screen opening size (mm)	75	50	25	4.75	2.36	1.18	0.60	0.30	0.15	0.075	
DPD-1											
0–5	—	—	95.4	53.1	40.4	31.5	24.5	17.5	9.3	3.8	2,330.9
5–10	—	—	78.1	53.4	45.7	40.3	34.3	25.2	17.1	9.3	1,329.5
10–15	—	72.0	67.9	58.8	56.7	54.2	49.9	43.4	34.2	12.9	2,253.6
15–17.5	—	—	—	97.5	96.8	90.2	82.7	68.9	58.9	29.2	808.2
DPD-2											
0–5	—	96.8	89.2	55.9	45.0	37.3	29.3	20.1	13.1	7.5	963.8
5–10	—	97.2	87.1	53.9	37.6	25.2	14.2	6.7	4.1	2.5	1,443.2
10–13.5	94.6	92.8	80.9	55.3	44.2	35.1	21.6	8.3	4.4	2.6	1,535.7
13.5–15	96.7	92.7	90.6	50.3	39	30.7	18.4	6.4	3.2	1.7	1,917.4
15–20	—	99.2	93.1	59.2	43	28.7	14.8	6.2	2.9	1.5	1,476.8
20–25	—	98.0	81.4	35.1	23.5	14.2	7.1	3.6	2.1	1.2	1,448.8
25–30	99.7	99.1	86.8	77.0	71.8	65.3	54.4	37.4	18.3	7.9	1,047.6
30–35	—	—	—	—	99.9	99.6	97.9	82.5	45.9	18.7	573.1
DPD-3											
0–5	97.8	90.9	80.8	42.9	30.3	20.5	10.8	5.3	3.0	1.5	1,294.1
5–10	98.0	94.6	84.2	46.8	36.4	27.5	15.3	7.6	4.5	2.5	1,849.8
10–15	97.1	89.6	71.0	50.1	47.5	44.7	36.2	14.6	6.2	2.5	1,761.2
15–20	99.6	97.5	92.7	85.4	81.7	75.8	61.9	22.9	7.8	3.5	1,488.9
DPD-4											
0–10	—	93.4	81.5	45.1	33.8	25.9	17.2	9.9	6.2	3.5	2,319.5
10–15	—	99.0	88.1	45.7	36.6	32.3	25.1	8.8	4.1	2.1	2,107.9
15–20	—	95.0	94.0	58.6	50.0	45.9	39	16.2	8.5	3.7	2,028.9
20–25	—	98.1	95.1	15.1	6.6	4.0	3.2	2.5	1.7	1.0	2,527.9
25–30	—	98.9	97.7	75.1	65.9	55.1	45.3	30.6	17.9	8.8	2,571.2
DPD-5											
0–5	—	—	98.96	61.53	43.49	33.13	25.21	16.56	10.51	5.94	1,516.5
5–10	—	99.26	95.5	47.92	36.49	29.82	23.55	15.02	9.26	5.28	1,058.7
10–15	—	—	86.49	65.76	55.99	49.03	40.53	27.16	18.52	11.81	1,192.5
15–20	—	—	—	34.01	8.83	1.57	1.29	1.03	.78	.59	282.8
DPD-6											
0–5	—	99.55	98.19	52.52	39.55	32.05	26.74	21.05	16.07	10.63	1,942.4
5–10	—	15.84	89.6	51.97	39.37	30.22	22.2	13.39	7.04	2.65	1,490.7
10–15	—	99.6	94.55	54.49	46.48	38.49	27.08	12.85	6.53	3.05	2,037.4
15–20	—	99.09	85.92	46.16	36.94	28.67	19.24	9.52	5.32	2.67	1,718.3
20–25	—	—	88.06	41.81	30.59	24.22	17.98	11.57	7.13	3.45	2,363.1
25–30	—	95.71	76.88	27.07	20.98	15.42	8.51	3.06	1.45	.79	1,826.0

Table B2. Particle-size distribution of the sandy fraction from 4 millimeters to 0.00025 millimeter, Daguerre Point Dam, California.

[DPD, Daguerre Point Dam; ft, foot; mm, millimeter]

Drill-hole/ Depth (ft)	Percentage of particles passing through sieve and sedigraph																			
Screen opening size (mm)	Sieve							Sedigraph												
	4	2	1	0.5	0.25	0.125	0.063	0.045	0.032	0.024	0.016	0.012	0.008	0.006	0.004	0.003	0.002	0.001	0.0005	0.00025
DPD-1																				
0–5	100	99.8	82.0	63.6	44.9	27.4	13.9	1.5	1.0	0.7	0.5	0.4	0.3	0.2	0.2	0.1	0.1	0.0	0.0	0.0
5–10	100	99.9	85.3	65.6	44.3	30.2	18.6	2.6	1.9	1.5	1.1	.9	.6	.5	.5	.4	.3	.2	.1	.0
10–15	100	99.9	87.1	72.4	57.9	45.0	28.1	5.9	3.9	2.8	1.9	1.6	1.3	1.1	1.0	.9	.8	.6	.5	.3
15–17.5	100	99.9	96.8	89.8	77.9	59.7	35.5	10.6	8.6	7.3	5.9	5.3	4.5	3.9	3.4	3.1	2.6	1.9	1.4	1.1
DPD-2																				
0–5	100	99.8	81.7	57.2	32.6	18.0	8.0	0.5	0.4	0.3	0.2	0.2	0.1	0.1	0.1	0.0	0.0	0.0	0.0	0.0
5–10	100	99.8	70.6	37.0	16.9	10.4	6.3	.3	0.3	.2	.2	.1	.1	.1	.1	.0	.0	.0	.0	.0
10–13.5	100	99.9	82.5	44.8	16.0	7.6	4.0	.1	0.1	.1	.1	.1	.0	.0	.0	.0	.0	.0	.0	.0
13.5–15	100	99.6	80.5	41.1	13.3	7.4	4.8	.2	0.2	.2	.1	.1	.1	.1	.1	.0	.0	.0	.0	.0
15–20	100	99.4	68.8	29.4	9.1	4.1	2.6	.1	0.1	.1	.0	.0	.0	.0	.0	.0	.0	.0	.0	.0
25–30	100	99.9	91.0	77.0	50.3	20.0	5.8	.3	0.2	.2	.1	.1	.1	.1	.1	.1	.0	.0	.0	.0
30–35	100	100.0	99.6	96.8	78.6	49.8	26.7	6.1	4.5	3.5	2.6	2.2	1.6	1.4	1.1	.9	.7	.4	.2	.2
DPD-3																				
0–5	100	99.4	70.4	36.1	18.2	10.0	4.4	0.2	0.1	0.1	0.1	0.0	0.0	0.0	0.0	0.0	0.0	0.0	0.0	0.0
5–10	100	99.8	75.3	35.9	17.1	10.3	5.7	.3	0.2	.2	.1	.1	.1	.1	.1	.0	.0	.0	.0	.0
10–15	100	99.9	90.1	61.3	23.0	13.3	7.3	.5	0.4	.3	.2	.2	.2	.1	.1	.1	.1	.1	.0	.0
15–20	100	100.0	94.3	76.6	31.7	14.9	8.7	.7	0.6	.5	.4	.4	.3	.2	.2	.1	.1	.1	.0	.0
DPD-4																				
0–10	100	99.7	78.0	40.9	16.9	8.3	3.3	0.1	0.1	0.1	0.0	0.0	0.0	0.0	0.0	0.0	0.0	0.0	0.0	0.0
10–15	100	99.9	86.9	58.4	13.6	5.9	2.4	.1	0.0	.0	.0	.0	.0	.0	.0	.0	.0	.0	.0	.0
15–20	100	100.0	93.2	75.7	29.7	13.1	4.2	.1	0.1	.1	.1	.0	.0	.0	.0	.0	.0	.0	.0	.0
20–25	100	99.7	62.5	36.4	18.8	8.9	4.1	.1	0.1	.1	.1	.1	.0	.0	.0	.0	.0	.0	.0	.0
25–30	100	99.8	82.4	59.3	33.0	16.6	8.4	.6	0.4	.3	.3	.2	.2	.2	.1	.1	.1	.0	.0	.0
DPD-5																				
0–5	100	99.9	76.9	49.3	24.0	11.4	5.9	0.3	0.2	0.2	0.1	0.1	0.1	0.1	0.0	0.0	0.0	0.0	0.0	0.0
5–10	100	99.9	80.9	52.9	23.6	11.2	6.2	.3	0.3	.2	.2	.2	.1	.1	.1	.1	.0	.0	.0	.0
10–15	100	99.9	86.4	59.7	28.3	16.1	8.4	.6	0.4	.3	.2	.2	.1	.1	.1	.1	.0	.0	.0	.0
15–20	100	99.8	94.6	78.7	48.7	24.5	4.7	.2	0.1	.1	.1	.0	.0	.0	.0	.0	.0	.0	.0	.0
DPD-6																				
0–5	100	99.6	79.5	56.8	34.7	19.3	8.9	0.6	0.4	0.3	0.2	0.1	0.1	0.1	0.1	0.1	0.0	0.0	0.0	0.0
5–10	100	99.7	82.1	58.7	34.4	17.5	6.2	.3	0.2	.1	.1	.1	.0	.0	.0	.0	.0	.0	.0	.0
10–15	100	99.7	78.5	45.8	14.6	5.7	2.7	.1	0.0	.0	.0	.0	.0	.0	.0	.0	.0	.0	.0	.0
15–20	100	100.0	79.2	50.8	25.2	14.9	7.8	.5	0.4	.3	.2	.2	.2	.1	.1	.1	.1	.0	.0	.0
20–25	100	99.9	80.7	57.9	36.4	22.3	10.8	1.0	0.8	.6	.5	.5	.4	.3	.3	.2	.2	.1	.1	.1
25–30	100	99.9	75.1	37.9	18.9	15.3	13.6	1.8	1.7	1.6	1.5	1.3	1.1	1.0	.8	.7	.6	.4	.3	.2

Table B3. Particle-size distribution of the silty fraction from 2 millimeters to 0.00025 millimeter, Daguerre Point Dam, California.

[Initial sample from suspended-sediment overflow (SSO). DPD, Daguerre Point Dam; ft, foot; mm, millimeter]

Drill hole/ Depth (ft)	Percentage of particles passing through sieve and sedigraph																		
Screen opening size (mm)	Sieve						Sedigraph												
	2	1	0.5	0.25	0.125	0.063	0.045	0.032	0.024	0.016	0.012	0.008	0.007	0.004	0.003	0.002	0.001	0.0005	0.00025
DPD-2																			
0–5	100	100	100	100	100	100	100	98	97	94	89	79	70	56	47	35	21	12	6
5–10	100	100	100	100	100	100	100	99	98	93	88	79	70	57	47	36	21	11	5
15–20	100	100	100	100	100	99	99	98	97	94	90	83	75	64	56	45	32	22	12
20–25	100	100	100	100	100	98	95	94	92	86	81	73	66	58	52	45	33	23	13
25–30	100	100	100	100	99	95	94	92	87	76	66	52	44	35	29	24	17	12	8
30–35	100	100	100	100	100	98	98	98	96	88	78	62	52	39	33	26	18	13	9
DPD-3																			
15–20	100	100	100	100	100	98	99	99	98	98	98	96	94	91	88	85	80	77	75
DPD-4																			
10–15	100	100	100	100	99	96	95	91	88	84	77	69	62	52	44	38	26	18	13
15–20	100	100	100	100	99	94	91	87	82	74	70	60	54	46	42	36	28	19	11
DPD-5																			
0–5	100	100	100	100	100	100	99	99	98	98	98	96	94	91	88	85	80	77	75
5–10	100	100	100	100	100	99	100	100	100	100	99	94	87	74	64	51	33	21	9
10–15	100	100	100	100	100	98	98	97	93	85	77	65	55	41	32	23	13	9	3
15–20	100	100	100	100	100	98	100	100	100	99	99	94	88	76	66	53	33	17	2
DPD-6																			
0–5	100	100	100	100	100	99	98	97	93	85	77	65	55	41	32	23	13	9	3
5–10	100	100	100	99	97	94	100	100	100	99	99	94	88	76	66	53	33	17	2
10–15	100	100	100	100	99	96	100	100	100	99	98	93	85	74	65	53	36	24	12
15–20	100	100	100	100	100	99	100	100	99	96	93	88	82	71	62	50	34	21	12
20–25	100	100	100	100	100	98	98	96	94	89	82	71	63	51	44	36	25	18	12
25–30	100	100	100	99	94	89	100	99	98	95	91	83	74	61	52	41	25	15	7

Table B4. Particle-size distribution of the clay-silt fraction from 2 millimeters to 0.00025 millimeter, Daguerre Point Dam, California.

[Initial 2-millimeter separation from SWECO stainless steel vibratory separator. DPD, Daguerre Point Dam; ft, foot; mm, millimeter]

Drill hole/ Depth (ft)	Percentage of particles passing through sieve and sedigraph																		
Screen opening size (mm)	Sieve						Sedigraph												
	2	1	0.5	0.25	0.125	0.063	0.045	0.032	0.024	0.016	0.012	0.008	0.006	0.004	0.003	0.002	0.001	0.0005	0.00025
DPD-2																			
20–25	100	100	100	100	100	100	100	100	99	99	98	96	93	90	84	75	54	36	20
25–30	100	100	99	96	84	71	70	67	63	54	47	38	32	26	22	17	12	9	6
30–35	100	100	100	100	99	95	95	93	88	79	73	66	62	58	56	54	51	49	47
DPD-3																			
0–5	100	100	100	100	100	100	99	99	98	98	98	96	94	91	88	85	80	77	75
5–10	100	100	100	100	100	100	100	100	100	99	99	97	90	78	67	53	34	20	9
10–15	100	100	100	100	100	100	100	100	100	100	99	94	87	74	64	51	33	21	9
15–20	100	100	100	100	100	99	98	93	86	75	64	51	41	28	23	16	8	3	0
DPD-4																			
10–15	100	100	100	100	100	100	100	100	100	99	99	94	88	76	66	53	33	17	2
15–20	100	100	100	100	100	100	100	100	100	99	98	93	85	74	65	53	36	24	12
20–25	100	100	100	100	100	100	100	100	99	98	98	94	87	74	64	50	35	23	13
25–30	100	100	100	100	100	100	100	100	99	96	93	88	82	71	62	50	34	21	12
DPD-5																			
0–5	100	100	100	100	100	100	100	99	99	97	91	75	63	49	40	30	20	12	6
5–10	100	100	100	100	100	100	100	100	100	99	99	95	90	80	72	59	41	25	13
10–15	100	100	100	100	100	100	99	100	99	99	96	91	84	72	64	52	35	21	11
15–20	100	100	100	100	100	100	100	100	99	94	88	78	71	61	56	49	41	34	26
DPD-6																			
0–5	100	100	100	100	100	100	98	97	93	83	74	61	51	39	32	23	13	7	4
5–10	100	100	100	100	100	100	100	99	97	92	87	74	65	52	43	33	20	12	6
10–15	100	100	100	100	100	100	100	99	98	95	91	84	76	65	56	45	31	20	13
15–20	100	100	100	100	100	100	100	99	96	90	83	71	62	50	43	34	24	16	10
20–25	100	100	100	100	100	99	99	97	95	88	81	69	60	49	42	33	24	17	11
25–30	100	100	99	95	89	82	82	80	77	71	65	56	48	39	34	27	20	14	9

Table B5. Silty fraction suspended-sediment concentrations, Daguerre Point Dam, California.

[ft, foot; mg/L, milligram per liter; DPD, Daguerre Point Dam]

Drill hole/Depth (ft)	Sediment concentration (mg/L)
DPD-2	
20–25	2,400
25–30	116,000
30–35	79,500
DPD-3	
0–5	2,400
5–10	5,000
10–15	12,400
15–20	147,600
DPD-4	
0–10	6,100
10–15	7,200
15– 20	6,100
20–25	7,100
25–30	19,300
DPD-5	
0–5	10,800
5–10	10,400
10–15	18,600
15–20	40,000
DPD-6	
0–5	30,400
5–10	9,400
10–15	13,800
15–20	33,400
20–25	100,500
25–30	254,400

Appendix C. Particle-Size Distribution and Microscopic Observations of Heavy Minerals, Daguerre Point Dam, California

Table C1. Particle-size distribution and gold tenor of heavy mineral concentrates, Daguerre Point Dam, California.

[DPD, Daguerre Point Dam. ft, foot; g, gram; mm, millimeter; mg, milligram; mg/yd^3, milligram per cubic yard. <, less than]

Drill Hole/ Depth (ft)	Total weight (g)	Particle sizes (mm)					Number of gold grains observed	Estimated gold weight (mg)	Gold grade/ tenor (mg/yd^3)
		1 to 2 (percent)	0.5 to 1.0 (percent)	0.25 to 0.50 (percent)	0.063 to 0.25 (percent)	< 0.063 (percent)			
DPD-1									
0–5	6.7	0.0	0.0	10.0	85.0	5.0	1	Trace	[1]1
5–10	11.2	.0	.0	7.0	91.0	2.0	23	2.1	120
10–15	31.7	.0	2.0	4.0	90.0	4.0	115	4.4	170
15–17.5	11.3	.0	.0	1.0	94.0	5.0	17	1.9	160
DPD-2									
0–5	15.5	0.0	2.0	15.0	81.0	2.0	17	1.1	76
5–10	46.8	.2	1.0	35.0	63.0	1.0	7	.1	2
10–13.5	28.3	.0	1.0	29.0	69.0	1.0	10	1	40
13.5–15	38.2	.3	1.0	22.0	76.0	1.0	12	1	16
15–20	64.6	.0	1.0	22.0	76.0	1.0	25	3.2	75
20–25	50.1	.0	1.0	24.0	74.0	1.0	19	1.8	45
25–30	666.9	.0	.0	25.0	74.0	1.0	43	1.9	19
30–35	81.5	.0	.0	3.0	95.0	2.0	1	.3	7
DPD-3									
0–5	17	1.0	1.0	33.0	64.0	1.0	8	0.2	11
5–10	61.1	1.0	2.0	34.0	62.0	1.0	16	2.1	44
10–15	129.4	.0	.0	7.0	91.0	2.0	15	1.4	31
15–20	367.3	.0	.0	52.0	47.0	1.0	15	.8	9
DPD-4									
0–10	42.5	0.0	1.0	33.0	65.0	1.0	8	0.5	16
10–15	44.3	.0	1.0	21.0	77.0	1.0	15	1	20
15–20	28	.0	2.0	2.0	95.0	1.0	25	2.3	90
20–25	4	.0	.0	3.0	94.0	3.0	6	.1	3
25–30	109.9	1.0	1.0	33.0	64.0	1.0	6	Trace	[1]1
DPD-5									
0–5	17.6	0.0	0.6	12.5	82.4	1.1	15	0.8	80
5–10	61.4	.2	.5	14.5	81.3	2.0	23	1.1	60
10–15	25.2	.4	.4	4.8	90.9	2.8	14	1	72
15–20	0	0	0	0	0	0	0	0	0
DPD-6									
0–5	27.1	0.0	0.7	5.2	91.5	1.5	6	0.2	[1]4
5–10	23.5	.0	.4	3.8	94.9	.9	4	Trace	[1]1
10–15	69.2	.0	.3	36.3	62.3	.4	3	Trace	[1]1
15–20	52.1	.0	.2	52.4	45.9	.4	5	.2	4
20–25	18.7	.0	.5	17.1	80.7	.5	3	.1	6
25–30	16.8	.0	.6	44.0	55.4	.6	6	Trace	[1]1

[1] Assigned a value of 1.

Table C2. Microscopic observations of heavy mineral concentrates, Daguerre Point Dam, California.

[DPD, Daguerre Point Dam. Observations: X, trace; XX, abundant; XXX, very abundant; C, coarse; F, fine; VF, very fine; UF, ultra fine. mg, milligram, mm, millimeter; —, not observed]

Drill Hole/ Depth (ft)	Number of gold grains observed	Estimated gold weight (mg)	Gold	Mercury	Amalgam (gold-mercury)	Pyrite	Magnetite	Garnets (0.5-1 mm)	Chromite	Other (ilmenite, zircon, sphene)
					DPD-1					
0–5	1	Trace	F	—	x	xxx	x	x	x	x
5–10	23	2.1	F-UF	—	—	x	x	x	x	x
10–15	115	4.4	1-C, F-UF	—	—	x	xx	x	x	xx
15–17.5	17	1.9	F-UF	—	—	x	x	xx	x	xxx
					DPD-2					
0–5	17	1.1	VF	—	—	x	x	x	x	x
5–10	7	.1	VF	—	—	x	xx	x	x	x
10–13.5	10	1	F-VF	—	—	xx	x	x	x	x
13.5–15	12	1	F-UF	—	—	xx	xx	x	x	x
15–20	25	3.2	C-UF	—	x	xxx	xx	x	x	x
20–25	19	1.8	F-UF	—	—	x	xx	xx	xx	x
25–30	43	1.9	F-UF	x	xxx	x	xxx	x	xxx	x
30–35	1	.3	C	—	x	xx	xx	—	xx	—
					DPD-3					
0–5	8	0.2	F-VF	—	—	xx	x	xx	x	x
5–10	16	2.1	F-VF	—	x	xx	xx	xxx	xx	x
10–15	15	1.4	C-VF	—	x	x	xxx	—	xxx	x
15–20	15	.8	F-VF	—	xx	x	xxx	x	xxx	xx
					DPD-4					
0–10	8	0.5	F-VF	—	—	xxx	xx	xx	x	x
10–15	15	1	F-VF	—	—	xx	xx	x	x	x
15–20	25	2.3	F-VF	—	—	x	x	—	x	x
20–25	6	.1	VF	—	—	xxx	x	—	x	x
25–30	6	Trace	VF	—	—	x	xxx	x	xxx	x
					DPD-5					
0–5	15	0.8	F-UF	—	—	xx	x	x	x	x
5–10	23	1.1	F-VF	—	—	x	xx	x	x	x
10–15	14	1	F-VF	—	—	x	x	x	x	xxx
15–20	0	0								
					DPD-6					
0–5	6	0.2	VF	—	—	x	x	—	x	x
5–10	4	Trace	VF	—	—	x	x	—	x	x
10–15	3	Trace	UF	—	—	x	xx	x	x	x
15–20	5	.2	UF	—	—	x	xx	—	x	x
20–25	3	.1	F-UF	—	—	xx	x	x	x	x
25–30	6	Trace	VF	—	—	xx	x	—	x	x

Appendix D. Quality Assurance and Quality Control Data for USGS Laboratories, Daguerre Point Dam, California

Table D1. Chemistry of Yuba River water used during drilling near Daguerre Point Dam, California, August 24, 2001.

[Laboratory location: CO, Colorado; WI, Wisconsin. µS/cm, microSiemens per centimeter; mg/L, milligram per liter; °C, degrees Celsius; SD, standard deviation of triplicate analyses; ng/L, nanogram per liter; n.d., not determined; <, less than]

Field measurements									
Site	Time	pH	Specific conductance (µS/cm)	Dissolved oxygen (mg/L)	Temperature (°C)				
Yuba River at Daguerre Point Dam	15:00	6.7	72	11.2	18				
Laboratory measurements									
Site	Time	Replicate	Total mercury, filtered (ng/L) CO	SD (ng/L)	Total mercury, unfiltered (ng/L) CO	SD (ng/L)	Methyl-mercury, filtered (ng/L) WI	Methyl-mercury, unfiltered (ng/L) WI	
Yuba River at Daguerre Point Dam	15:00	1 of 2	0.5	0.1	1.0	0.2	<0.04	<0.04	
Yuba River at Daguerre Point Dam	15:00	2 of 2	.7	.1	1.1	.1	n.d.	n.d.	
Method detection limit			.4		.4		.04	.04	

Table D2. Mercury concentrations of blanks taken during drilling, August 28, 2001, Daguerre Point Dam, California.

[Analyses done at U.S. Geological Survey laboratory in Boulder, Colorado. SD, standard deviation of triplicate analyses; SWECO, manufacturer of vibratory separator; ng/L, nanogram per liter; <, less than; —, not applicable]

	Time	Total mercury unfiltered (ng/L)	SD (ng/L)	Total mercury, filtered (ng/L)	SD (mg/L)
Equipment blank–stainless steel trough	16:00	2.3	0.1	—	—
Equipment blank–5-gallon plastic bucket	16:02	<.4	.2	—	—
Equipment blank–25-gallon plastic tub	16:04	.4	.3	—	—
Equipment blank–SWECO vibratory screen	16:06	2.1	.1	—	—
Process blank	16:08	—	—	1.3	.0

Table D3. Mercury concentrations in standard reference water samples, blanks, and spikes, Daguerre Point Dam, California.

[Analyzed at U.S. Geological Survey research laboratory in Boulder, Colorado. SD, standard deviation; ng/L, nanogram per liter; na, not available]

	Number of observations	Analyzed		Most probable value		Reference or comment
		Total mercury (ng/L)	SD (ng/L)	Total mercury (ng/L)	SD (ng/L)	
Standard reference water sample						
Hg-7	25	237	23	240	na	Peart and others (1998)
Hg-15	32	388	20	390	na	Peart and others (1998)
Hg-26	29	698	27	700	90	Farrar (1998)
Laboratory blanks						
		1.2	0.2			
		.7	.1			
		.6	.1			
		.2	.1			
Spike						
5-ng/L spike of laboratory blank		5.14				recovery = 103 percent

Table D4. Results for trace and major elements in standard reference material, Daguerre Point Dam, California.

[Avg, average of three replicate analyses; SD, standard deviation; Wt%, weight percent; µg/g, microgram per gram; na, not applicable]

Field ID	Al Aluminum Wt%		As Arsenic µg/g		Au Gold µg/g		B Boron µg/g		Ba Barium µg/g		Be Beryllium µg/g		Bi Bismuth µg/g		Ca Calcium Wt%	
	Avg	SD	Avg	SD	Avg	SD	Avg	SD	Avg	SD	Avg	SD	Avg	SD	Avg	SD
Buffalo River Sediment 2704	5.6	0.1	24	0	0.019	0.002	128	1	304	3	2.0	0.1	0.65	0.04	1.6	0.1
Buffalo River Sediment 2704	4.7	.2	22	1	.012	.003	233	10	353	1	1.6	.1	.64	.05	2.0	.0
Buffalo River Sediment 2704	5.3	.2	23	1	.012	.000	215	6	363	2	1.9	.1	.67	.03	1.9	.1
Buffalo River Sediment 2704	3.5	.1	21	1	.015	.005	183	10	313	6	2.0	.1	.78	.02	1.7	.1
Buffalo River Sediment 2704	3.1	.1	22	0	.011	.002	135	15	224	10	1.7	.1	.58	.01	2.3	.0
Buffalo River Sediment 2704	5.3	.2	21	0	.011	.000	212	5	387	12	1.7	.0	.62	.02	2.4	.1
Average	4.6	1.0	22	1.2	.013	.0	184	44	324	58	1.8	.2	.66	.07	2.0	.3
Buffalo River Sediment (Bold numbers, certified)	**6.11**	**.16**	**23.4**	**.8**	na	na	na	na	**414**	**12**	na	na	na	na	**2.60**	**.03**

Field ID	Cd Cadmium µg/g		Ce Cerium µg/g		Co Cobalt µg/g		Cr Chromium µg/g		Cs Cesium µg/g		Cu Copper µg/g		Dy Dysprosium µg/g		Er Erbium µg/g	
	Avg	SD	Avg	SD	Avg	SD	Avg	SD	Avg	SD	Avg	SD	Avg	SD	Avg	SD
Buffalo River Sediment 2704	3.9	0.1	43	1	15	0	139	3	5.9	0.1	105	1	2.0	0.1	1.1	0.0
Buffalo River Sediment 2704	3.7	.1	25	1	14	1	132	1	4.7	.0	101	1	2.8	.0	1.5	.0
Buffalo River Sediment 2704	3.6	.0	38	0	14	0	133	2	4.3	.0	100	3	2.5	.1	1.3	.0
Buffalo River Sediment 2704	3.5	.0	18	0	13	0	126	5	4.1	.1	98	3	2.1	.1	1.2	.0
Buffalo River Sediment 2704	3.5	.2	27	1	13	1	129	7	2.9	.0	102	0	3.0	.1	1.7	.1
Buffalo River Sediment 2704	3.4	.0	37	0	13	0	121	2	3.3	.0	99	1	2.6	.0	1.4	.0
Average	3.6	.2	31	10	14	1	130	6	4.2	1.1	101	3	2.5	.4	1.4	.2
Buffalo River Sediment (Bold numbers, certified)	**3.45**	**.22**	72	na	**14.0**	**.6**	**135**	**5**	6	na	**99**	**5**	6	na	na	na

Field ID	Eu Europium µg/g		Fe Iron Wt%		Ga Gallium µg/g		Gd Gadolinium µg/g		Ho Holmium µg/g		K Potassium Wt%		La Lanthanum µg/g		Li Lithium µg/g	
	Avg	SD	Avg	SD	Avg	SD	Avg	SD	Avg	SD	Avg	SD	Avg	SD	Avg	SD
Buffalo River Sediment 2704	0.52	0.03	4.3	0.3	15	0	2.0	0.2	0.39	0.01	2.0	0.1	14	0	46	1
Buffalo River Sediment 2704	.74	.02	3.9	.2	14	1	3.1	.2	.54	.01	2.0	.0	14	0	41	2
Buffalo River Sediment 2704	.70	.03	4.1	.0	14	0	2.7	.1	.46	.00	2.0	.1	16	0	42	0
Buffalo River Sediment 2704	.55	.03	3.9	.2	13	0	2.3	.0	.40	.01	1.8	.1	9.0	.2	41	0
Buffalo River Sediment 2704	.73	.00	4.1	.2	13	0	2.9	.0	.60	.03	1.2	.1	11	0	39	1
Buffalo River Sediment 2704	.77	.02	4.2	.1	13	0	2.8	.0	.53	.01	1.9	.0	16	0	36	1
Average	.67	.11	4.1	.2	14	1	2.6	.4	.49	.08	1.8	.3	13	3	41	3
Buffalo River Sediment (Bold numbers, certified)	1.3	na	**4.11**	**0.10**	15	na	na	na	na	na	**2.00**	.04	29	na	**47.5**	**4.1**

Field ID	Lu Lutetium µg/g		Mg Magnesium Wt%		Mn Manganese µg/g		Mo Molybde-num µg/g		Na Sodium Wt%		Nd Neodymium µg/g		Ni Nickel µg/g		P Phospho-rous µg/g	
	Avg	SD	Avg	SD	Avg	SD	Avg	SD	Avg	SD	Avg	SD	Avg	SD	Avg	SD
Buffalo River Sediment 2704	0.17	0.00	0.91	0.02	597	36	4.6	0.6	0.52	0.04	12	0	59	1	1,050	34
Buffalo River Sediment 2704	.24	.02	.51	.00	530	31	3.9	.3	.46	.04	16	1	45	3	969	59
Buffalo River Sediment 2704	.21	.01	.62	.01	562	6	4.0	.3	.41	.00	16	0	44	1	1,030	8
Buffalo River Sediment 2704	.19	.00	.16	.01	521	22	3.9	.6	.45	.02	11	0	43	1	964	30
Buffalo River Sediment 2704	.26	.00	.49	.02	550	29	3.9	.6	.55	.02	14	1	42	0	1,050	12
Buffalo River Sediment 2704	.21	.00	1.1	.0	560	11	4.0	.0	.47	.00	18	0	41	1	1,010	9
Average	.21	.03	.62	.32	553	27	4.1	.3	.48	.05	15	3	46	7	1,012	38
Buffalo River Sediment (Bold numbers, certified)	.6	na	**1.20**	**.02**	**555**	**19**	na	na	**.547**	**.014**	na	na	**44.1**	**3.0**	**998**	**28**

Table D4. Results for trace and major elements in standard reference material, Daguerre Point Dam, California.—Continued

[Avg, average of three replicate analyses; SD, standard deviation; Wt%, weight percent; µg/g, microgram per gram; na, not applicable]

Field ID	Pb Lead µg/g		Pr Praseo-dymium µg/g		Rb Rubidium µg/g		Re Rhenium µg/g		S Sulfur Wt%		Sb Antimony µg/g		Sc Scandium µg/g		Se Selenium µg/g	
	Avg	SD	Avg	SD	Avg	SD	Avg	SD	Avg	SD	Avg	SD	Avg	SD	Avg	SD
Buffalo River Sediment 2704	161	4	3.4	0.1	104	0	0.003	0.001	0.47	0.00	4.2	0.1	6.6	1.1	1.3	0.1
Buffalo River Sediment 2704	178	1	4.1	.0	61	3	<.003	.001	.45	.01	4.1	.2	7.2	.1	1.1	.1
Buffalo River Sediment 2704	167	0	4.3	.0	79	1	.003	.000	.48	.01	3.7	.0	6.9	.6	1.4	.6
Buffalo River Sediment 2704	150	4	2.8	.0	49	2	.004	.001	.43	.00	3.8	.1	4.9	.1	.8	.6
Buffalo River Sediment 2704	147	8	3.4	.1	8.6	.7	.003	.002	.46	.00	3.6	.1	8	0	1.4	.0
Buffalo River Sediment 2704	141	0	4.5	.0	60	0	.002	.002	.45	.02	3.7	.0	11	0	1.8	.1
Average	157	14	3.7	.7	60	32	.002	.002	.46	.02	3.9	.2	7.4	2.0	1.3	.3
Buffalo River Sediment (Bold numbers, certified)	**161**	**17**	na	na	100	na	na	na	**.397**	**.004**	**3.79**	**.15**	12	na	**1.12**	**.05**

Field ID	Sm Samarium µg/g		Sr Strontium µg/g		Tb Terbium µg/g		Te Tellurium µg/g		Th Thorium µg/g		Ti Titanium Wt%		Tl Thalium µg/g		Tm Thulium µg/g	
	Avg	SD	Avg	SD	Avg	SD	Avg	SD	Avg	SD	Avg	SD	Avg	SD	Avg	SD
Buffalo River Sediment 2704	2.5	0.0	121	2	0.34	0.01	0.14	0.02	6.5	0.1	0.46	0.00	0.88	0.07	0.17	0.00
Buffalo River Sediment 2704	3.5	.2	103	5	.47	.02	.21	.02	7.1	.3	.42	.02	.89	.02	.24	.01
Buffalo River Sediment 2704	3.3	.1	112	3	.42	.01	.18	.01	7.1	.1	.43	.00	.86	.03	.20	.01
Buffalo River Sediment 2704	2.6	.1	106	4	.36	.01	.13	.01	4.6	.0	.42	.02	.81	.00	.18	.00
Buffalo River Sediment 2704	3.2	.0	90	1	.50	.00	.14	.01	4.7	.3	.43	.00	.79	.06	.26	.00
Buffalo River Sediment 2704	3.7	.0	130	1	.45	.02	.18	.05	4.9	.1	.38	.01	.77	.12	.20	.00
Average	3.1	.5	111	14	.42	.06	.16	.03	5.8	1.2	.42	.03	.83	.05	.21	.03
Buffalo River Sediment (Bold numbers, certified)	6.7	na	130	na	na	na	na	na	9.2	na	**.457**	**.018**	**1.06**	**.07**	na	na

Field ID	U Uranium µg/g		V Vanadium µg/g		W Tungsten µg/g		Y Yttrium µg/g		Yb Ytterbium µg/g		Zn Zinc µg/g		Zr Zirconium µg/g	
	Avg	SD	Avg	SD	Avg	SD	Avg	SD	Avg	SD	Avg	SD	Avg	SD
Buffalo River Sediment 2704	3.1	0.0	103	2	1.7	0.1	9.8	0.2	1.1	0.0	457	9	163	2
Buffalo River Sediment 2704	3.0	.0	96	5	1.5	.0	12	1	1.5	.1	438	6	138	8
Buffalo River Sediment 2704	3.0	.1	97	2	2.5	.0	11	0	1.3	.1	438	12	132	3
Buffalo River Sediment 2704	2.9	.1	91	2	1.5	.1	10	0	1.2	.0	432	14	153	4
Buffalo River Sediment 2704	2.8	.1	91	4	1.6	.1	15	0	1.8	.1	415	8	824	279
Buffalo River Sediment 2704	2.7	.1	90	4	1.4	.1	10	0	1.4	.0	424	3	531	217
Average	2.9	.2	95	5	1.7	.4	11	2	1.4	.3	434	14	323	290
Buffalo River Sediment (Bold numbers, certified)	**3.13**	**.13**	**95**	**4**	na	na	na	na	2.8	na	**438**	**12**	300	na

Table D5. Digestion blanks for trace elements and major elements, Daguerre Point Dam, California.

[Avg, average of three replicate analyses; SD, standard deviation; µg/L, microgram per liter; mg/L, milligram per liter; <, less than]

Field ID	Al Aluminum µg/L		As Arsenic µg/L		Au Gold µg/L		B Boron µg/L		Ba Barium µg/L		Be Beryllium µg/L		Bi Bismuth µg/L		Ca Calcium mg/L	
	Avg	SD	Avg	SD	Avg	SD	Avg	SD	Avg	SD	Avg	SD	Avg	SD	Avg	SD
Digestion Blank	12	1	<0.1	0.1	<0.004	0.002	<6	4	0.1	0.0	0.04	0.04	0.10	0.03	0.02	0.02
Digestion Blank	13	2	<.1	.1	<.004	.002	<6	0	.1	.0	<.03	.03	.07	.03	<.02	.01
Digestion Blank	<8	19	.1	.0	<.004	.005	6	3	.3	.5	<.03	.03	.29	.20	.03	.03
Digestion Blank	<8	3	<.1	.1	<.004	.001	6	6	<.1	.1	<.03	.01	<.02	.002	<.02	.02
Digestion Blank	311	12	<.1	.1	<.004	.001	<6	5	2.2	.0	<.03	.02	<.02	.005	.06	.03

Field ID	Cd Cadmium µg/L		Ce Cerium µg/L		Co Cobalt µg/L		Cr Chromium µg/L		Cs Cesium µg/L		Cu Copper µg/L		Dy Dysprosium µg/L		Er Erbium µg/L	
	Avg	SD	Avg	SD	Avg	SD	Avg	SD	Avg	SD	Avg	SD	Avg	SD	Avg	SD
Digestion Blank	<0.02	0.03	0.033	0.002	<0.02	0.02	<2	1	0.14	0.03	0.36	0.29	<0.004	0.002	<0.008	0.004
Digestion Blank	<.02	.01	.029	.001	<.02	.01	<2	2	.12	.04	.16	.07	<.004	.003	<.008	.002
Digestion Blank	.14	.10	.012	.002	.03	.01	<2	1	.10	.15	1.8	2.1	<.004	.006	<.008	.004
Digestion Blank	.04	.02	.021	.002	<.02	.006	<2	2	<.04	.05	.21	.15	<.004	.004	<.008	.003
Digestion Blank	.03	.01	.20	.01	<.02	.009	<2	2	.19	.00	.09	.05	.009	.003	<.008	.001

Field ID	Eu Europium µg/L		Fe Iron µg/L		Ga Gallium µg/L		Gd Gadolinium µg/L		Ho Holmium µg/L		K Potassium mg/L		La Lanthanum µg/L		Li Lithium µg/L	
	Avg	SD	Avg	SD	Avg	SD	Avg	SD	Avg	SD	Avg	SD	Avg	SD	Avg	SD
Digestion Blank	<0.004	0.003	22	39	<0.01	0.00	<0.005	0.002	<0.002	0.001	<0.04	0.01	0.010	0.002	<0.1	0.1
Digestion Blank	<.004	.001	<20	8	<.01	.01	<.005	.006	<.002	.000	<.04	.02	.014	.001	<.1	.2
Digestion Blank	<.004	.001	<20	7	<.01	.00	<.005	.009	<.002	.001	.18	.10	.008	.002	.2	.3
Digestion Blank	<.004	.000	<20	13	<.01	.003	<.005	.002	<.002	.001	<.04	.02	.008	.001	<.1	.08
Digestion Blank	<.004	.002	37	5	<.01	.006	.009	.002	<.002	.001	<.04	.02	.069	.003	<.1	.09

Field ID	Lu Lutetium µg/L		Mg Magnesium mg/L		Mn Manganese µg/L		Mo Molybde-num µg/L		Na Sodium mg/L		Nd Neodymium µg/L		Ni Nickel µg/L		P Phosphorous µg/L	
	Avg	SD	Avg	SD	Avg	SD	Avg	SD	Avg	SD	Avg	SD	Avg	SD	Avg	SD
Digestion Blank	<0.002	0.000	<0.005	0.002	0.2	0.2	<0.5	1.0	<0.1	0.1	0.01	0.01	0.85	0.09	<20	10
Digestion Blank	<.002	.000	<.005	.000	<.2	.0	<.5	.6	<.1	.0	<.01	.01	.85	.07	<20	8
Digestion Blank	<.002	.001	.014	.015	.3	.5	<.5	.5	.1	.2	<.01	.00	2.3	1.3	29	12
Digestion Blank	<.002	.001	<.005	.000	<.2	.1	<.5	.5	<.1	.0	<.01	.01	1.7	.2	21	14
Digestion Blank	<.002	.000	.032	.010	.7	.3	<.5	.1	<.1	.1	.07	.02	.32	.05	<20	8

Field ID	Pb Lead µg/L		Pr Praseodymium µg/L		Rb Rubidium µg/L		Re Rhenium µg/L		S Sulfur mg/L		Sb Antimony µg/L		Sc Scandium µg/L		Se Selenium µg/L	
	Avg	SD	Avg	SD	Avg	SD	Avg	SD	Avg	SD	Avg	SD	Avg	SD	Avg	SD
Digestion Blank	0.25	0.20	0.005	0.001	<0.03	0.02	<0.003	0.001	<0.2	0.1	<0.04	0.01	<1.0	0.1	<0.8	0.7
Digestion Blank	.20	.05	.003	.001	<.03	.01	<.003	.002	<.2	.1	<.04	.06	<1.0	.8	<.8	.2
Digestion Blank	1.1	.9	<.002	.001	.31	.39	<.003	.001	<.2	.2	.25	.11	<1.0	.4	<.8	.4
Digestion Blank	.13	.02	<.002	.001	<.03	.01	<.003	.001	<.2	.1	<.04	.04	<1.0	.4	<.8	.4
Digestion Blank	.09	.02	.018	.001	.29	.03	<.003	.001	<.2	.1	<.04	.02	<1.0	.2	<.8	.5

Table D5. Digestion blanks for trace elements and major elements, Daguerre Point Dam, California.—Continued

[Avg, average of three replicate analyses; SD, standard deviation; µg/L, microgram per liter; mg/L, milligram per liter; <, less than]

Field ID	Sm Samarium µg/L		Sr Strontium µg/L		Tb Terbium µg/L		Te Tellurium µg/L		Th Thorium µg/L		Ti Titanium µg/L		Tl Thalium µg/L		Tm Thulium µg/L	
	Avg	SD	Avg	SD	Avg	SD	Avg	SD	Avg	SD	Avg	SD	Avg	SD	Avg	SD
Digestion Blank	<0.01	0.01	<0.2	0.2	<0.001	0.000	<0.06	0.04	0.004	0.004	<4	6	<0.04	0.07	<0.002	0.001
Digestion Blank	<.01	.00	<.2	.0	<.001	.001	<.06	.01	.003	0.002	<4	3	<.04	.02	<.002	.001
Digestion Blank	<.01	.01	.2	.3	<.001	.001	<.06	.05	.005	0.005	<4	3	<.04	.00	<.002	.001
Digestion Blank	<.01	.01	<.2	.0	<.001	.001	<.06	.03	.003	0.002	<4	3	<.04	.06	<.002	.001
Digestion Blank	.01	.01	1.2	.4	.003	.000	<.06	.02	.024	0.005	<4	3	<.04	.04	<.002	.000

Field ID	U Uranium µg/L		V Vanadium µg/L		W Tungsten µg/L		Y Yttrium µg/L		Yb Ytterbium µg/L		Zn Zinc µg/L		Zr Zirconium µg/L	
	Avg	SD	Avg	SD	Avg	SD	Avg	SD	Avg	SD	Avg	SD	Avg	SD
Digestion Blank	0.006	0.010	<0.3	0.1	0.02	0.02	0.014	0.003	<0.004	0.002	<0.9	0.3	0.07	0.02
Digestion Blank	.005	.001	<.3	.4	<.02	.01	.009	.004	<.004	.003	<.9	.4	<.05	.01
Digestion Blank	.005	.001	.3	.2	<.02	.02	.007	.008	<.004	.004	13	14	.06	.02
Digestion Blank	.005	.004	<.3	.1	<.02	.01	.006	.003	<.004	.003	2.1	1.0	.09	.08
Digestion Blank	.005	.002	<.3	.2	<.02	.01	.024	.004	<.004	.002	1.2	.0	.17	.08

Table D6. Spike recoveries for trace elements, Daguerre Point Dam, California.

Date	As Arsenic	Ca Calcium	Cd Cadmium	Cu Copper	Fe Iron	Mg Magnesium	Pb Lead	Zn Zinc
	Percentage recovery							
11/7/2003	112	105	100	102	102	101	99	104
11/21/2003	99	102	104	102	106	101	107	101
12/16/2003	109	102	107	106	102	92	106	110

Table D7. Comparison of replicate analyses of trace and major elements in digested sediments, Daguerre Point Dam, California.

[Avg, average of three replicate analyses; Wt%, weight percent; SD, standard deviation; µg/L, microgram per liter; ft, foot; dup., duplicate; <, less than; RPD, relative percent difference; na, not applicable]

Drill hole	Depth (ft)	Al Aluminum Wt%		As Arsenic µg/g		Au Gold µg/g		B Boron µg/g		Ba Barium µg/g		Be Beryllium µg/g		Bi Bismuth µg/g	
		Avg	SD	Avg	SD	Avg	SD	Avg	SD	Avg	SD	Avg	SD	Avg	SD
DPD-4	10-15	5.1	0.1	32	2	0.008	0.004	128	1	591	0	1.01	0.13	<0.04	0.03
DPD-4, dup.	10-15	6.6	.2	32	1	.011	.003	146	20	673	6	1.12	.14	<.05	.06
DPD-4	15-20	5.6	.2	20	1	.012	.002	96	3	755	5	1.02	.05	<.04	.01
DPD-4, dup.	15-20	5.0	.2	19	1	.008	.001	116	1	689	4	1.03	.03	<.04	.09
DPD-5	5-10	5.6	.1	22	0	.017	.003	167	2	488	9	1.07	.04	<.04	.07
DPD-5, dup.	5-10	5.4	.2	23	0	.012	.003	134	1	451	3	1.1	.1	<.04	.05
		RPD		RPD		RPD		RPD		RPD		RPD		RPD	
DPD-4	10-15	27.1		0.2		35.2		13.0		13.0		10.8		20.9	
DPD-4	15-20	10.2		7.4		39.3		18.1		9.2		1.0		1.2	
DPD-5	5-10	4.3		4.9		38.1		22.0		7.9		6.2		.0	

Drill hole	Ca Calcium Wt%		Cd Cadmium µg/g		Ce Cerium µg/g		Co Cobalt µg/g		Cr Chromium µg/g		Cs Cesium µg/g		Cu Copper µg/g		Dy Dysprosium µg/g	
	Avg	SD	Avg	SD	Avg	SD	Avg	SD	Avg	SD	Avg	SD	Avg	SD	Avg	SD
DPD-4	1.76	0.07	0.28	0.10	19	1	38	1	195	2	1.5	0.3	98	4	1.5	0.1
DPD-4, dup.	3.27	.03	.31	.05	25	0	37	1	148	1	1.5	.1	95	3	2.6	.0
DPD-4	1.69	.06	.31	.01	16	1	31	0	172	1	1.2	.1	103	2	1.5	.1
DPD-4, dup.	1.48	.03	.17	.08	13	0	31	1	154	1	1.0	.1	98	3	1.4	.0
DPD-5	1.90	.09	.40	.06	21	1	33	1	190	8	1.0	.0	106	3	1.6	.0
DPD-5, dup.	1.57	.04	.43	.05	18	0	34	1	186	7	1.3	.1	111	2	1.3	.1
	RPD		RPD		RPD		RPD		RPD		RPD		RPD		RPD	
DPD-4	59.9		9.3		28.5		1.8		27.8		0.6		2.4		55.6	
DPD-4	13.3		57.9		20.8		1.0		10.9		17.4		4.4		4.7	
DPD-5	19.0		7.0		13.5		1.7		2.0		27.5		4.2		20.4	

Drill hole	Er Erbium µg/g		Eu Europium µg/g		Fe Iron Wt%		Ga Gallium µg/g		Gd Gadolinium µg/g		Ho Holmium µg/g		K Potassium Wt%		La Lanthanum µg/g	
	Avg	SD	Avg	SD	Avg	SD	Avg	SD	Avg	SD	Avg	SD	Avg	SD	Avg	SD
DPD-4	0.85	0.06	0.42	0.04	7.7	0.0	15	0	1.5	0.0	0.30	0.01	0.78	0.02	7.9	0.5
DPD-4, dup.	1.45	.05	.75	.02	6.9	.1	14	0	2.5	.0	0.51	.00	0.83	.03	11.8	.0
DPD-4	.90	.00	.45	.02	7.1	.2	16	0	1.6	.0	0.32	.00	0.81	.02	6.4	.0
DPD-4, dup.	.80	.04	.42	.03	5.9	.1	15	0	1.3	.0	0.27	.01	0.80	.03	5.1	.2
DPD-5	.93	.03	.53	.02	6.8	.3	16	0	1.8	.0	0.33	.01	0.90	.03	8.7	.2
DPD-5, dup.	.74	.02	.40	.06	7.2	.2	17	0	1.3	.1	0.27	.01	0.92	.03	7.1	.0
	RPD		RPD		RPD		RPD		RPD		RPD		RPD		RPD	
DPD-4	52.0		57.2		11.2		1.8		51.3		52.9		5.8		39.8	
DPD-4	11.3		8.4		18.2		9.7		16.9		18.9		1.5		21.8	
DPD-5	22.8		27.7		5.2		3.9		31.1		19.6		2.0		20.4	

Drill hole	Li Lithium µg/g		Lu Lutetium µg/g		Mg Magnesium Wt%		Mn Manganese µg/g		Mo Molybdenum µg/L		Na Sodium Wt%		Nd Neodymium µg/g		Ni Nickel µg/g	
	Avg	SD	Avg	SD	Avg	SD	Avg	SD	Avg	SD	Avg	SD	Avg	SD	Avg	SD
DPD-4	14	1	0.12	0.00	1.6	0.0	960	25	51	2	1.09	0.00	8.0	0.1	121	0
DPD-4, dup.	17	1	.22	.00	1.7	.0	976	121	57	7	1.51	.03	12.3	.1	120	4
DPD-4	16	1	.14	.00	1.5	.0	972	46	9.9	.5	1.14	.06	7.5	.0	100	1
DPD-4, dup.	15	1	.12	.00	1.2	.0	931	28	9.6	.8	1.03	.05	6.5	.0	98	2
DPD-5	15	1	.14	.00	1.5	.1	1,750	101	9.1	.5	1.17	.07	9.0	.0	112	3
DPD-5, dup.	17	0	.11	.00	1.5	.0	1,780	17	8.8	.1	1.14	.04	7.3	.0	112	3
	RPD		RPD		RPD		RPD		RPD		RPD		RPD		RPD	
DPD-4	16.2		60.5		8.5		1.7		9.5		32.4		41.7		1.1	
DPD-4	9.1		13.2		21.5		4.4		3.6		10.4		14.9		1.4	
DPD-5	13.5		22.4		1.5		1.7		3.4		2.8		20.8		.2	

Table D7. Comparison of replicate analyses of trace and major elements in digested sediments, Daguerre Point Dam, California.—Continued

[Avg, average of three replicate analyses; Wt%, weight percent; SD, standard deviation; µg/L, microgram per liter; ft, foot; dup., duplicate; <, less than; RPD, relative percent difference; na, not applicable]

Drill hole	P Phosphorus µg/g		Pb Lead µg/g		Pr Praseodymium µg/g		Rb Rubidium µg/g		Re Rhenium µg/g		S Sulfur Wt%		Sb Antimony µg/g		Sc Scandium µg/g	
	Avg	SD	Avg	SD	Avg	SD	Avg	SD	Avg	SD	Avg	SD	Avg	SD	Avg	SD
DPD-4	1,010	16	17	1	2.1	0.0	23	1	<0.004	0.006	1.16	0.01	2.7	0.4	12	1
DPD-4, dup.	866	28	17	0	3.2	.1	30	1	<.004	.002	.31	.02	3.0	.4	6	0
DPD-4	732	52	20	1	1.8	.0	23	1	.004	.002	.37	.02	1.8	.1	16	0
DPD-4, dup.	644	16	20	1	1.5	.1	18	1	<.004	.002	.37	.01	1.9	.2	12	0
DPD-5	787	21	16	1	2.3	.1	22	1	<.004	.003	.04	.01	1.3	.2	14	1
DPD-5, dup.	832	19	17	1	1.9	.1	23	0	<.004	.002	.04	.01	1.4	.2	13	0
	RPD		RPD		RPD		RPD		RPD		RPD		RPD		RPD	
DPD-4	15.4		0.2		41.5		27.2		na		115.0		10.2		70.1	
DPD-4	12.9		2.7		17.0		21.4		na		.1		5.0		30.0	
DPD-5	5.5		5.2		18.7		5.8		na		12.9		7.2		11.3	

Drill hole	Se Selenium µg/g		Sm Samarium µg/g		Sr Strontium µg/g		Tb Terbium µg/g		Te Tellurium µg/g		Th Thorium µg/g		Ti Titanium Wt%		Tl Thallium µg/g	
	Avg	SD	Avg	SD	Avg	SD	Avg	SD	Avg	SD	Avg	SD	Avg	SD	Avg	SD
DPD-4	1.4	0.4	1.7	0.1	206	2	0.24	0.02	0.07	0.04	2.8	0.1	0.44	0.02	0.19	0.03
DPD-4, dup.	1.8	.8	2.8	.0	205	5	.44	.00	.07	.02	4.1	.1	.30	.00	.35	.00
DPD-4	<.9	1.3	1.7	.1	196	14	.26	.01	.10	.03	2.5	.1	.55	.02	.21	.03
DPD-4, dup.	<.9	.7	1.5	.0	171	2	.23	.01	.12	.07	2.2	.1	.50	.01	.19	.00
DPD-5	<.9	.3	1.8	.0	203	14	.27	.00	.13	.04	3.0	.1	.54	.03	.30	.05
DPD-5, dup.	1.0	.1	1.5	.1	196	7	.21	.00	.11	.02	2.4	.1	.53	.01	.24	.04
	RPD		RPD		RPD		RPD		RPD		RPD		RPD		RPD	
DPD-4	25.8		49.4		0.1		57.7		1.5		38.7		37.9		60.2	
DPD-4	na		6.7		13.5		13.9		14.7		12.4		9.6		10.4	
DPD-5	na		18.8		3.6		22.6		16.0		22.5		1.4		22.4	

Drill hole	Tm Thulium µg/g		U Uranium µg/g		V Vanadium µg/g		W Tungsten µg/g		Y Yttrium µg/g		Yb Ytterbium µg/g		Zn Zinc µg/g		Zr Zirconium µg/g	
	Avg	SD	Avg	SD	Avg	SD	Avg	SD	Avg	SD	Avg	SD	Avg	SD	Avg	SD
DPD-4	0.13	0.01	1.9	0.1	221	4	1.1	0.0	7.1	0.3	0.88	0.02	138	14	50	1
DPD-4, dup.	.22	.01	1.9	.0	223	4	1.1	.0	13.0	.1	1.45	.05	135	5	50	2
DPD-4	.13	.01	1.6	.1	257	1	1.1	.0	7.0	.0	.85	.05	114	5	53	0
DPD-4, dup.	.11	.00	1.6	.1	241	7	.98	.03	6.5	.2	.83	.01	113	10	48	2
DPD-5	.13	.00	1.8	.0	225	7	1.2	.0	7.9	.2	.90	.01	109	9	54	1
DPD-5, dup.	.104	.006	1.7	.1	225	5	1.2	.0	6.3	.2	.74	.03	132	17	54	1
	RPD		RPD		RPD		RPD		RPD		RPD		RPD		RPD	
DPD-4	49.8		1.1		0.7		0.1		59.0		49.3		2.0		0.2	
DPD-4	15.8		1.2		6.3		8.6		7.3		1.7		1.3		9.6	
DPD-5	25.1		3.6		.3		1.7		22.8		19.7		19.3		.5	

Table D8. Replicate analyses of total mercury and methylmercury by the U.S. Geological Survey Wisconsin District Mercury Laboratory, Daguerre Point Dam, California.

[All replicates are laboratory replicates unless otherwise noted. DPD, Daguerre Point Dam; RPD, relative percent difference; r1, replicate 1; r2, replicate 2; r3, replicate 3; E, estimated value. ft, foot; ng/g, nanogram per gram; <less than; —, no data]

Drill hole	Depth (ft)	Replicates						Laboratory replicates Total mercury	Field replicates Total mercury	
		Methylmercury, wet			Total mercury, wet					
		r1 (ng/g)	r2 (ng/g)	r3 (ng/g)	r1 (ng/g)	r2 (ng/g)	r3 (ng/g)	RPD (r1, r2) (percent)	RPD (r1, r3) (percent)	RPD (r2, r3) (percent)
Clay-silt fraction (Centrifuge tubes)										
DPD-1	5-10	<0.012	0.165	<0.01	33.3	22.7	—	38.1	—	—
DPD-1	15-17.5	<.05	<.05	—	17.9	24.0	—	29.4	—	—
DPD-2	25-30	<.006	<.007	<.07	247	240	[1]244	2.6	1.3	1.4
DPD-6	25-30	<.06	<.08	.05E	204	208	[1]196	1.7	4.1	5.9

Drill hole	Depth (ft)	Replicates						Laboratory replicates Total mercury	Field replicates Total mercury
		Methylmercury, dry			Total mercury, dry				
		r1 (ng/g)	r2 (ng/g)	r3 (ng/g)	r1 (ng/g)	r2 (ng/g)	r3 (ng/g)	RPD (r1, r2) (percent)	RPD (r1, r2) (percent)
Sandy fraction									
DPD-2	0-5	<0.001	<0.001	<0.001	10.1	11.0	—	8.3	—
DPD-2	15-20	<.001	<.001	—	13.2	[1]20.6	—	—	43.6
DPD-2	20-25	<.001	<.001	—	20.3	15.0	—	30.4	—
DPD-4	15-20	<.001	<.001	<.001	21.3	21.6	—	1.5	—
DPD-5	15-20	<.001	<.001	—	12.1	11.9	—	1.1	—

[1] Field replicate

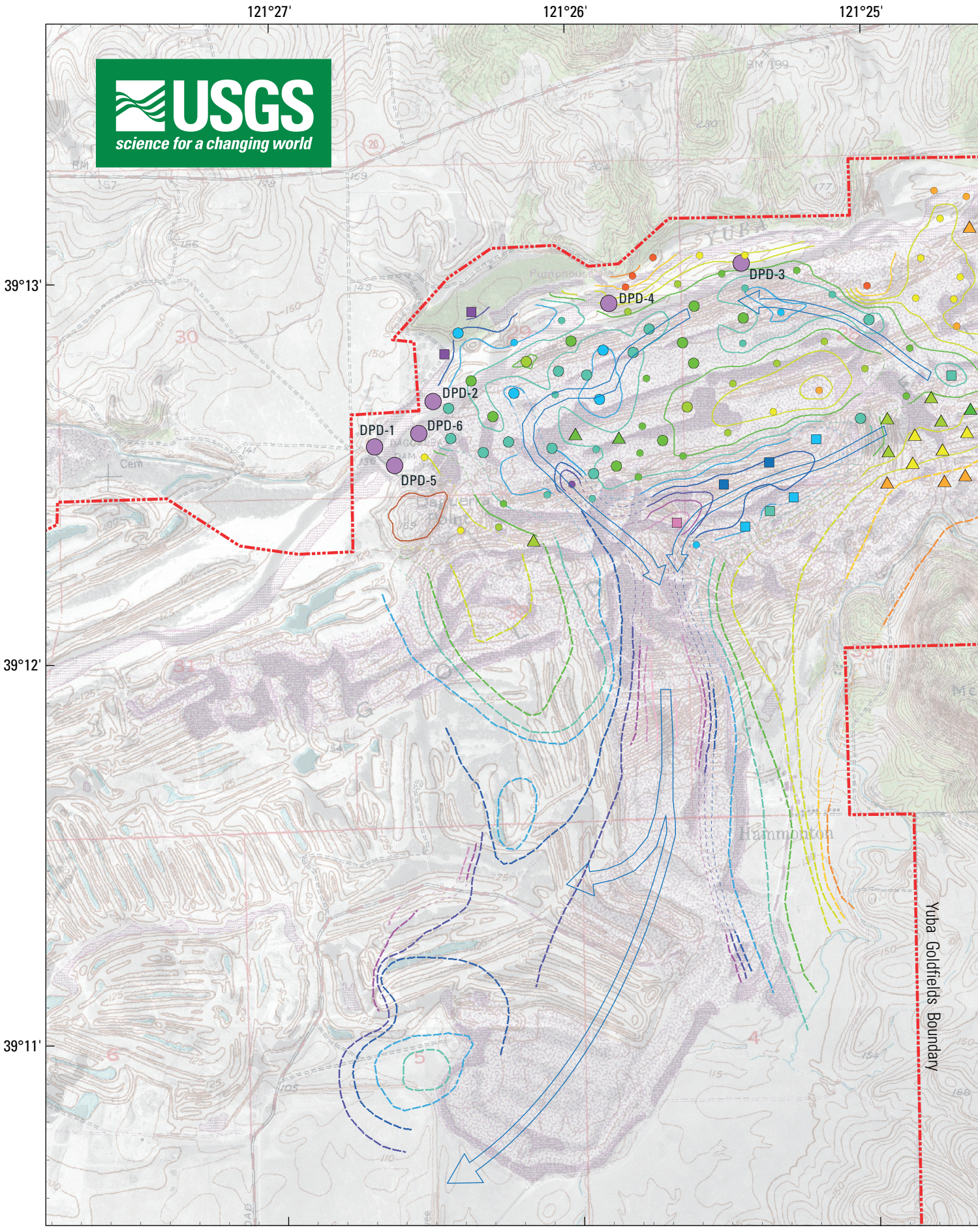

Appendix E. Plate 1. Map of Bedrock Elevation Contours, Daguerre Point Dam, California.

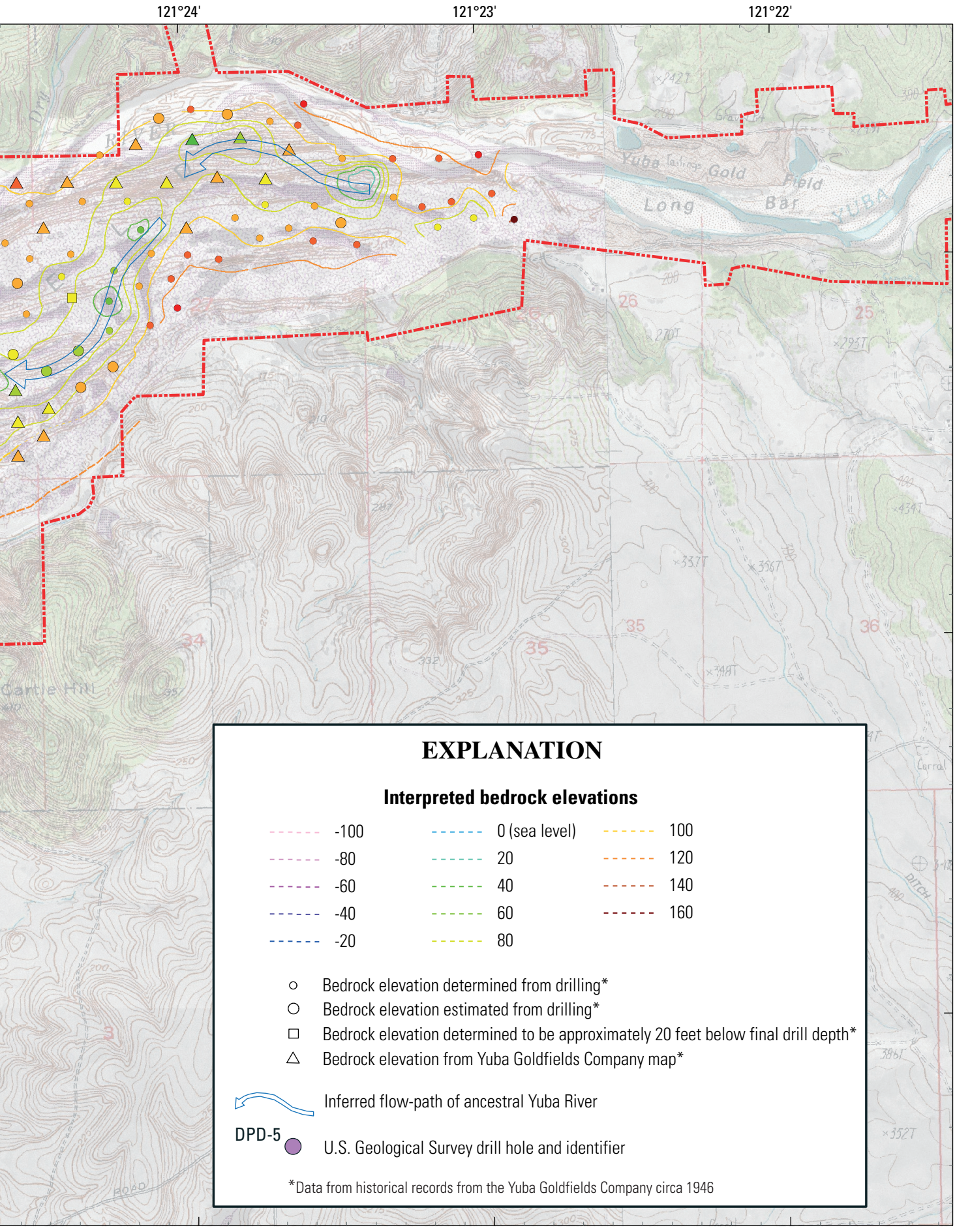

EXPLANATION

Interpreted bedrock elevations

-100	0 (sea level)	100
-80	20	120
-60	40	140
-40	60	160
-20	80	

- Bedrock elevation determined from drilling*
- Bedrock elevation estimated from drilling*
- Bedrock elevation determined to be approximately 20 feet below final drill depth*
- Bedrock elevation from Yuba Goldfields Company map*

Inferred flow-path of ancestral Yuba River

DPD-5 U.S. Geological Survey drill hole and identifier

*Data from historical records from the Yuba Goldfields Company circa 1946

0 2,000 4,000 Feet

CONTOUR INTERVAL 20 FEET

Glossary of Placer Terms

(adapted from Wells, 1973)

Alluvial. Deposited by a stream.

Alluvial Gold. Gold found in association with water-worn material.

Amalgam. An alloy of mercury with gold or another metal. In the case of placer gold, a gold amalgam will contain nearly equal proportions of gold and mercury. Mercury placed in the riffles of a sluice box forms a gold amalgam as a result of its chemical affinity for gold.

Auriferous. Containing gold.

Bedrock. The solid rock underlying auriferous gravel, sand, clay, and other sediments, and upon which the alluvial gold rests. Bedrock may be composed of igneous, metamorphic, or sedimentary rock.

Black Sand. Heavy grains of various minerals which have a dark color and usually accompany gold in alluvial deposits. The heavy minerals may consist mostly of magnetite, ilmenite, and hematite associated with other minerals such as garnet, rutile, zircon, chromite, amphiboles, and pyroxenes. In Western gold placers, the black sand content is commonly between 5 and 20 pounds per cubic yard of gravel.

Bucket-Line Dredge. A dredge in which the material excavated is lifted by an circular chain of buckets. The type of bucket-line dredge generally employed in placer mining is a self-contained digging, washing, and disposal unit, operating in a pond and capable of digging more than 100 feet below water. The dredge backfills its working pit (pond) as it advances.

Channel. A stream-eroded depression in the bedrock, ordinarily filled with gravel. See – *Tertiary Channel*.

Churn Drill. A portable drilling machine arranged to successively raise and drop a heavy string of tools suspended from a drill line. By means of successive blows, the formation is chopped up and the hole deepened.

Color. A particle of metallic gold found in the pan or on a gravity-concentrator table after a sample has been washed.

Debris. The *tailings* from hydraulic mines.

Flood Gold. Fine-size gold flakes carried or redistributed by flood waters and deposited on gravel bars as the flood waters recede. Flood gold sometimes forms superficial concentrations near the upstream end of accretion bars.

Floodplain. That portion of a river valley adjacent to the river channel which is built of sediments during the present regimen of the stream and which is covered with water when the river overflows its banks at flood stages.

Floured Mercury (*Quicksilver*). The finely granulated condition of quicksilver, produced by its agitation during the amalgamation process. A thin film of oxide coating on small globules of quicksilver prevents them from reuniting once they are separated.

Fluvial. Of, or pertaining to rivers; produced by river action, as a fluvial plain.

Heavy Minerals. The accessory detrital minerals of high specific gravity. The *black sand* concentrate commonly referred to in the mining of placer deposits would more properly be called a "heavy-mineral" concentrate.

Hydraulic Mining. A method of mining in which a bank of gold-bearing earth or gravel is washed away by a powerful jet of water and carried into sluices where the gold is separated from the earth or gravel by its specific gravity.

Jig. A machine in which heavy minerals are separated from sand on a screen in water by imparting a reciprocating motion to the screen or by water pulsing through the screen. Where the heavy mineral is larger than the screen openings, a concentrate bed will form on top of the screen. Where the heavy mineral particles are smaller than the screen openings, a fine-size concentrate will fall through and be collected in a trap beneath the screen.

Nugget effect. Anomalously high precious metal assays resulting from the analysis of samples that may not adequately represent the composition of bulk material tested due to non-uniform distribution of nuggets in the material sampled.

Placer. A place where gold is obtained by washing; an alluvial or glacial deposit, as of sand or gravel, containing particles of gold or other valuable minerals.

Placer mining. The form of mining in which the surficial detritus is washed for gold or other valuable minerals. When water under pressure is employed to break down the gravel, the term *Hydraulic Mining* is generally employed.

Quicksilver. Elemental mercury, a liquid at room temperature.

River Mining. The mining of part or all of a river bed after by-passing the stream by means of flumes or tunnels or by use of wing dams to divert the river from the working area.

Riffle. A groove in the bottom of an inclined trough or sluice, for arresting gold contained in sands or gravels.

Tailings. The washed material which issues from the end of a sluice or other recovery device in a *placer mining* operation. The tailings from hydraulic mines are generally referred to as *debris* in legislative documents.

Tenor. The percentage or average content of an ore. As commonly used, it is synonymous with an approximate or a general value rather than a precisely known value.

Tertiary Channel. Ancient gravel deposits, often auriferous, composed of stream alluvium of Tertiary age. Tertiary gravel deposits are abundant in the Sierra Nevada gold belt of California; many have been covered by extensive volcanic eruptions and subsequently elevated by mountain uplifts. They are now found as deeply-buried channels, high above the present stream beds.

Trace. A very small quantity of gold, usually a speck too small to weigh.

USGS

125 years of science for America

1879–2004